1992

Surface properites of coal and their effects on the selective oil agglomeration process

Xiaoping Qiu
Iowa State University

Order Number 9220981

Surface properties of coal and their effects on the selective oil agglomeration process

Qiu, Xiaoping, Ph.D.

Iowa State University, 1992

U·M·I
300 N. Zeeb Rd.
Ann Arbor, MI 48106

Surface properties of coal and their effects on the selective oil agglomeration process

by

Xiaoping Qiu

A Dissertation Submitted to the
Graduate Faculty in Partial Fulfillment of the
Requirements for the Degree of
DOCTOR OF PHILOSOPHY

Major: Chemical Engineering

Approved:

Signature was redacted for privacy.

In Charge of Major Work

Signature was redacted for privacy.

For the Major Department

Signature was redacted for privacy.

For the Graduate College

Iowa State University
Ames, Iowa
1992

TABLE OF CONTENTS

LIST OF TABLES

LIST OF FIGURES

ACKNOWLEDGEMENTS

The author would like to acknowledge the sources of funding for this project. This work was performed at Ames Laboratory under contract no. W-7405-Eng-82 with the U. S. Department of Energy. The United States government has assigned the DOE Report number IS-T-1592 to this thesis. This work was also supported (in part) by the Iowa State Mining and Mineral Resources Research Institute through the Department of the Interior's Mineral Institutes program administered by the U. S. Bureau of Mines under Allotment Grant Nos. G1104119, G1114119, and G1194119.

The author would also like to acknowledge Dr. John McClelland, Prof. Siquan Lou, Prof. Y. C. Hu, Dr. R. W. Allen and Mr. Jeff Fabian for their colaboration and assistance. The author also wishes to thank Dr. Robert S. Hansen, Dr. John Eggebrecht and Dr. Jan Drzymala for discussions about this project. The author wishes to recognize and acknowledge her Committee: Dr. Carol L. Kilgour, Dr. Robert S. Hansen, Dr. Charles E. Glatz and Dr. William H. Abraham. The author also wishes to thank Dr. Richard Markuszewski and Dr. John W. Patterson for temporarily serving on her committee. Finally, the author wishes to thank her major professor Dr. Thomas D. Wheelock for his guidance, patience and support throughout this project and her program of study.

CHAPTER 1. INTRODUCTION

Background

With the decrease of the world's oil reserves, coal is becoming increasingly important as an alternative energy source. Coal is the most abundant fossil fuel in the United States. The mineable coal deposits are estimated to last for 500 years at current consumption levels [1].

Most of the coal produced in the United States is used in electricity generation. In 1988 approximately 80 percent of the 862 million tons of coal produced in the United States was burned in power plants [2]. However, many problems are associated with burning coal due to the presence of sulfur and ash-forming minerals. The heat content of the coal is reduced due to the mineral matter, thereby decreasing the quality of the coal as a fuel [3]. The sulfur, which is present in the form of iron pyrite (FeS_2), can cause equipment wear and it can oxidize to form acids which cause boiler corrosion. In addition, the generated gaseous sulfur dioxide in the flue gas may cause acid rain. Excessive amounts of ash will cause slagging, fouling and erosion of various parts of a boiler, plug the air preheaters, and overload the electrostatic precipitators. Disposing of large amounts of ash from boilers is also a problem at power plants. At the same time, the environmental regulations are more restrictive. The solution of these problems requires more study of present and future economically feasible

methods of coal beneficiation or cleaning.

Coal beneficiation or cleaning is the process of removing the mineral matter from the carbonaceous material to prepare a material with certain characteristics required for coal conversion and utilization technologies. Coal cleaning methods can be classified into three main categories: conventional physical cleaning by washing, nonconventional physical cleaning, and chemical cleaning.

Although most of the coal cleaning methods currently practiced belong to conventional physical cleaning, their big disadvantage is that they are not effective for dealing with fine coal. Almost 20 % of the coal produced in the United States is lost as fines [4]. If cleaning is limited to coarse particles, much of the mineral matter is not liberated. Hence, the removal of mineral matter is limited. To avoid this problem, nonconventional methods which will clean fine coal are required. Froth flotation, oil agglomeration and selective flocculation are among the most promising physical separation processes for treating fine particles [5]. The surface properties of fine coal particles play an important role in these coal cleaning processes.

Selective Oil Agglomeration and Surface Properties

In an oil agglomeration process, an immiscible liquid (oil) is added to an aqueous suspension of fine coal and mineral matter. The suspension is agitated so the oil will be emulsified and contacted with the fine coal and mineral particles. Ideally, the oil will preferentially attach to the hydrophobic (carbonaceous) particles. The oil-attached particles will stick together upon collision to form agglomerates. The hydrophilic (mineral matter) particles, on the other hand, will not be wetted by the oil and will not agglomerate upon collision. The oil will promote the growth of

coal agglomerates which can be separated by screening to leave tailings containing most of the suspended free mineral matter and any unrecovered fine coal. This process can treat particles ranging from a few angstroms to 2-3 mm in size. The process is simple, and, in energy terms, an attractive alternative to or supplement for thermal drying or steam assisted filtration. The agglomerates cause minimal materials handling problems. The process can provide a low cost method for solving environmental problems associated with tailings lagoons of "black water" produced by coal washeries. The water used for oil agglomeration can be recycled. Because of these advantages, selective oil agglomeration has been attracting much attention.

Figure 1.1 shows the idealized stages for spherical agglomeration. For oil agglomeration to take place, the oil must attach to the coal particles. That is, the interfacial force for oil to spread on the coal surface in a water environment must be large in order to displace the water and to prevent the oil from being detached because of hydrodynamic forces. Usually, the more hydrophobic the coal surface, the more likely the oil droplets will displace the water and attach to the coal particles. Therefore, the interfacial tensions among coal, oil and water in the three-phase system are very important in controlling the process. The binding forces determine the efficiency of oil agglomeration, the oil dosage, and the strength and sizes of agglomerates.

Although coal is usually naturally hydrophobic compared to most of the mineral matter, the hydrophobicity of the coal surface varies with coal rank. In some cases the coal itself is rather hydrophilic so that it doesn't respond well to oil agglomeration. Also the surface properties suffer changes during coal handling encountered in mining and preparation. The surface of coal is exposed to air and will undergo oxidation. Usually the surface hydrophobicity decreases with oxidation, and the ability

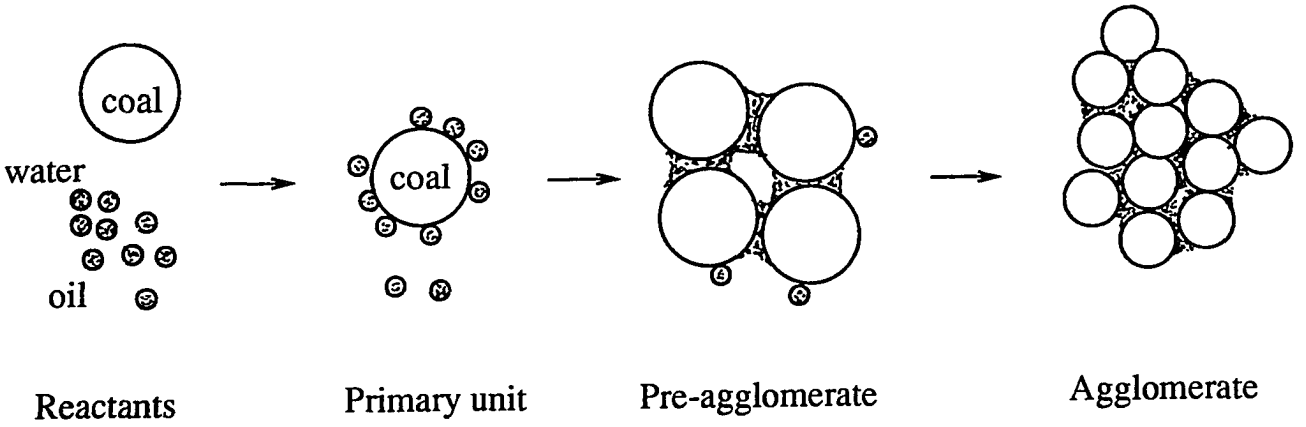

Figure 1.1: Schematic representation of idealized stages in spherical agglomeration, after Healy[6]

to respond to oil agglomeration decreases. Furthermore, the binding forces between oil and coal may vary with oil type. These challenges demand a fundamental study of how the oil agglomeration process is controlled by interfacial properties. This in turn requires proper characterization of the interfacial properties. Such a study is essential to optimize and to commercialize the selective oil agglomeration process.

Generally, surface hydrophobicity is expressed in terms of the contact angle formed when a water drop is placed on a flat solid surface [8]. A larger contact angle indicates strongly hydrophobic behavior, while a smaller contact angle represents weakly hydrophobic behavior. When the contact angle is zero, the liquid completely spreads on the solid. If a liquid drop is hydrocarbon oil, a small contact angle indicates strongly oleophilic behavior of the solid.

Another indicator of hydrophobicity is the heat of wetting. Former studies [8] have shown that when a polar solid is immersed in a polar liquid, the heat of wetting is large, while the contact angle is small. When the same solid is immersed in a non-polar liquid, the heat of wetting is small, while the contact angle is large.

Since the measurement of the contact angle is considered to be less objective than the measurement of the heat of wetting, it would be advantageous to determine the hydrophobicity of solids in liquid by measuring the heat of wetting. On the other hand, the three-phase contact angle can provide direct information about the interactions among oil, water and coal surfaces which may be useful for understanding the mechanism of the oil agglomeration process. Therefore, determining the three-phase contact angle is also of interest.

Research Purpose and Objectives

The overall purposes of this study were to establish practical methods for characterizing the surface hydrophobicity of coal and and for measuring other interfacial properties involved in the oil agglomeration process, and to determine how these properties control the oil agglomeration process. It was hoped that this study would provide a better understanding of the mechanism of the oil agglomeration process in order to aid process optimization. Specific objectives of this study were as follows:

1. Determine whether the heat of immersion is a proper method for characterizing the surface of coal used in an oil agglomeration process.

2. Determine the factors which affect the heat of immersion measurement, such as coal moisture content, liquid type, coal rank, and coal particle size, and also establish standard conditions for the heat of immersion measurement.

3. Determine how the coal surface hydrophobicity is affected by the concentration of oxygen functional groups introduced when coal is oxidized by air at 150° C.

4. Determine whether oil agglomeration test results for oxidized coal samples correlate with heat of immersion. Extend this work to two coals, one hydrophobic and one hydrophilic.

5. Determine the feasibility of measuring agglomeration performance by observing the change in turbidity of a particle suspension as it is agglomerated.

6. Determine the feasibility of measuring the three-phase contact angle by using the suction potential method. Determine the factors which affect the measurement of the three-phase contact angle by this method.

7. Measure the three-phase contact angle of coals of various ranks and different particle sizes, using various oil types.

8. Determine the spreading of oil on a coal surface for the oil-water-coal system by determining the three-phase contact angle. Correlate the spreading coefficient with oil agglomeration response if possible. This study is aimed at providing useful information about how to choose a proper oil as the bridging liquid to get optimal oil agglomeration performance for various coals.

9. Determine whether and how the presence of air bubbles or an air film affect the spreading of oil on a coal surface immersed in water and consequently how it will affect the oil agglomeration process.

It was thought that coals of different surface hydrophobicity would respond differently to oil agglomeration. Therefore, the operating parameters required to achieve the best recovery of coals of different rank would be different. Hence this study would provide guidance for choosing proper operating conditions such as oil type, oil dosage, and other parameters.

CHAPTER 2. THE CONTACT ANGLE AND THE HEAT OF IMMERSION

Three-phase Contact Angle and the Heat of Immersion

Generally, surface hydrophobicity is expressed in terms of a contact angle [8]. The conventional concept of a contact angle is shown in Figure 2.1.

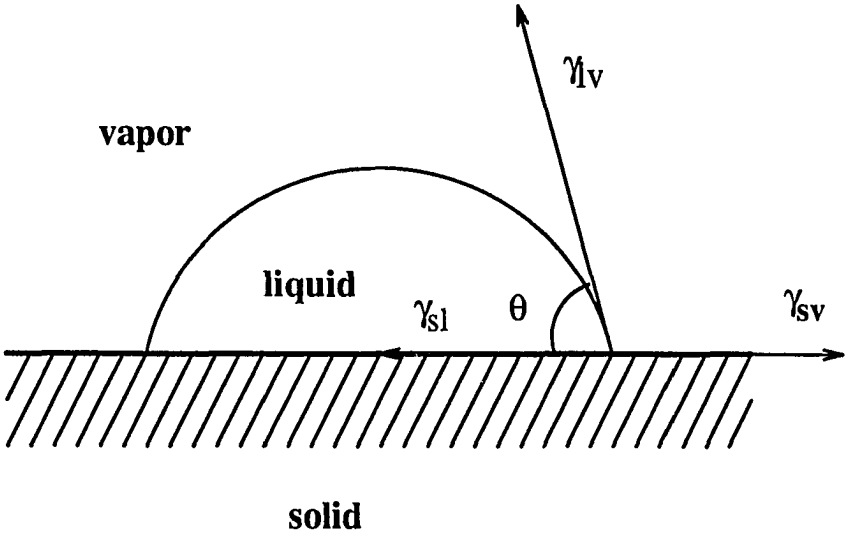

Figure 2.1: Contact angle for a sessile drop in a liquid-vapor-solid system. After Zisman[9]

In this diagram γ_{sl} is the interfacial tension at the solid-liquid interface, γ_{sv} the

surface tension of solid in contact with the liquid vapor, γ_{lv} the surface tension of the liquid in contact with its vapor, and θ is the contact angle of the liquid with the solid surface. Generally, when the liquid is water, a larger contact angle indicates strongly hydrophobic behavior, while a smaller contact angle represents weakly hydrophobic behavior. When the contact angle is zero, the liquid spreads completely on the solid. Then the solid is said to be wet by the liquid.

Since oil agglomeration of coal involves the oil-water-coal, three-phase system, the contact angle between an oil-water interface and a coal surface under water is of special interest. This contact angle, θ, is shownin Figure 2.2.

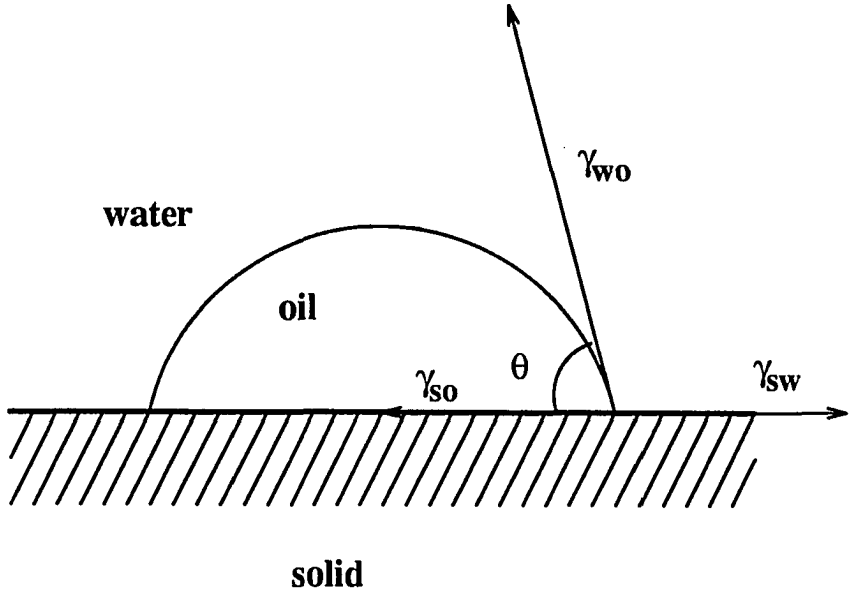

Figure 2.2: The three-phase contact angle for the oil-water-solid system

Oil in this system is largely immiscible with water. The contact angle in the oil-water-solid system has been expressed in two different ways in the literature. One

way is the angle measured through the oil phase, θ, as shown in Figure 2.2. The other way is the angle measured through the water phase which is $180 - \theta$. Yang and Drzymala[7] advocated the convention of always expressing the three-phase contact angle as the angle measured through the oil phase as shown in Figure 2.2. In this way, the general rule for a gas-liquid-solid system (the smaller the angle, the better the liquid can wet the solid) can be applied to an oil-water-solid system as follows: the smaller the angle, the better the oil will displace the water from the solid surface and spread on the solid surface. On the other hand, if the angle is measured through the water phase, the above rule can be stated as follows: the larger the angle, the better the oil will displace the water from the solid surface.

The heat of immersion is usually regarded as an exothermic quantity of energy released when a solid is immersed in a liquid. It can provide information about the energy of interaction between the solid and liquid. It has been found that the heat of immersion can be related to hydrophobicity of a solid surface. Former studies [8] have shown that when a polar solid is immersed in a polar liquid, the heat of wetting is large, while the contact angle is small. When the same solid is immersed in a non-polar liquid, the heat of wetting is small, while the contact angle is large. Ideally, when the heat of immersion is used as an indicator of surface hydrophobicity, no chemical or physical interactions other than wetting of the solid by the liquid should be involved.

Since measuring the contact angle may be less objective than measuring the heat of wetting, it may be advantageous to determine the hydrophobicity of a solid by measuring its heat of wetting in a liquid. Although there have been a number of publications about the thermodynamics of interfacial phenomena, only a few reports

have been concerned with correlating the heat of wetting with the contact angle. No publications concerned with the measurement of heat effects in oil-water-coal systems have been found. For an oil agglomeration process, what is needed is the three-phase contact angle and the heat of wetting for an oil-water-solid system. Of interest is the thermodynamic relationship between the heat of wetting and the contact angle and the application of their relationship to calculate the contact angle from heat of immersion data for both a solid-liquid-vapor system and an oil-water-solid system.

Thermodynamic Relationship Between the Heat of Immersion and the Contact Angle

1. Liquid-Vapor-Solid System

The heat of immersion can be related to the contact angle for a liquid-vapor-solid system by the following expression (see Appendix C):

$$-\Delta H = \left[\gamma_{lv} - T\left(\frac{\partial \gamma_{lv}}{\partial T}\right)_p\right] cos\ \theta_{slv} - \gamma_{lv} T \left(\frac{\partial cos\ \theta_{slv}}{\partial T}\right)_p . \qquad (2.1)$$

In this equation, ΔH is the heat of immersion of a clean solid surface in one liquid, and the contact angle is that determined when a liquid drop is placed on a clean solid surface.

2. Liquid-Liquid-Solid System

A similar relationship to that for a liquid-vapor-solid system can be expressed as follows for a liquid-liquid-solid system (see Appendix C):

$$-\Delta H = \left[\gamma_{l_1 l_2} - T\left(\frac{\partial \gamma_{l_1 l_2}}{\partial T}\right)_p\right] cos\ \theta_{sl_1 l_2} - \gamma_{l_1 l_2} T\left(\frac{\partial cos\ \theta_{sl_1 l_2}}{\partial T}\right)_p . \quad (2.2)$$

In this expression, θ_{sl1l2} is the three-phase contact angle which can be determined for a liquid-liquid-solid system. However, ΔH, which involves two liquids, can not be directly determined by conventional calorimetry. Therefore, in this study the heat of immersion in one liquid and the three-phase contact angle for a liquid-liquid-solid system were determined empirically. The thermodynamic relationship between these two surface properties is discussed in Appendix C.

CHAPTER 3. EXPERIMENTAL STUDY OF THE HEAT OF IMMERSION OF COAL

Review of Previous Work

The heat of immersion has been found to be a sensitive indicator of surface hydrophilicity. Furthermore, the heat of immersion measurement can be applied very easily to fine particles for which contact angle measurement is usually difficult. For these reasons, the heat of immersion is a very promising method for determining the hydrophilicity of solid particles in various liquid systems. However, the heat of immersion of solid particles has been found to depend on particle size, liquid type, and moisture content of the solids. To standardize the measurement, it is necessary to determine how these factors affect the heat of immersion.

As mentioned in Chapter 2, the previous analysis is based on the assumption that no other heat effect, due to either chemical or physical changes, is involved in the immersing process. However, the process of immersion can be more complicated as many other changes can occur, especially for a complex material such as coal. There have been some reports [13][15] which have discussed this problem and have suggested that mineral oxides or organic contaminants on the surface of the solids may react with the liquid, and the heat of reaction would contribute to the integral heat measured. Besides this, omnipresent water will tenaciously hold onto the high-

energy solids, and at high temperature chemisorption may occur and contribute to the measured heat effect. Also swelling may cause breakage of C-C bonds on the solid surface, absorbing some of the heat of wetting.

To solve this problem, some investigators have tried to remove the impurities [15], and others have suggested that new techniques are needed to separate the "pure" heat of wetting and the heat contributed by other chemical or physical changes.

To improve our understanding of the immersing process, it would be necessary to distinguish between different heat effects. However, it may not be necessary to physically or chemically treat the surface of a real solid before measuring the heat of wetting in order to deduce other heat effects. Since these chemical or physical changes happen at the solid-liquid interface, they may change the surface tension, and, hence, the surface enthalpies H_{sv} and H_{sl}. Thus, the heat observed during the immersion process may represent only the real hydrophobicity of the solid-liquid system. Of course, if the immersion process involves physical or chemical changes beyond the solid-liquid interface, the associated heat effects should not be included in the heat of wetting.

Everett [16] carried out a detailed thermodynamic analysis of interfacial phenomena, but did not consider certain physical or chemical changes in a real system. A further thermodynamic analysis of interfacial phenomena, taking account of such changes, will provide a breakdown of all possible heat-producing interactions.

Another important factor which will affect the heat of wetting is the adsorption of H^+/OH^- ions. Wierer and Dobias [17] obtained experimental data for the exchange enthalpy of H^+/OH^- ion adsorption on minerals. The exchange enthalpy includes the heat of adsorption of H^+/OH^- ions on oxides and the heat of dissolution released

during dissolution of the lattice ions from the oxide surface. The experimental data for the exchange enthalpy ΔH_{ex} of H^+/OH^- ions on oxides at different pH show that the exchange enthalpy decreases with increasing pH in the low pH range. Then after reaching a minimum value it starts to increase with increasing pH in the high pH range. One possible interpretation of this result is that the surface tension does not change at the points of equal adsorption density (EAPs). When the pH is increased beyond the EAPs, the surface tension of the solid-liquid interface is changed, due to the adsorption of H^+/OH^- ions. Therefore, it may be concluded that the heat of wetting would be a minimum at the EAPs, whereas the contact angle would reach a maximum at the EAPs. Beyond the EAPs, the heat of wetting would increase with increasing concentrations of H^+ or OH^- ions, which would cause the contact angle to decrease.

It is most important when using Equation C.8 and Equation C.20 that the heat of wetting and contact angle are measured under the same conditions. In other words, if the hydrophobicity or contact angle of a given system is needed under certain conditions, the heat of wetting for the system must be measured under the same conditions. The initial condition of the solid sample must therefore be known or controlled.

To measure the heat of wetting for the process described in Chapter 2, the sample should be equilibrated with the liquid vapor at a certain T, P, and Pg before taking the measurement. If the solid is not pretreated by saturating it with the liquid vapor, the solid will absorb the vapor before the immersion process occurs. The measured heat will contain a contribution due to the heat of adsorption. Hollenbeck [12] described

the enthalpy change relationship by the following equation:

$$\Delta H_{s/l} = n1 \cdot \lambda + \Delta H_{ads} + \Delta H_{sfl}$$

where n1 is the number of moles of liquid adsorbed per unit surface area of solids, λ is the heat of vaporization of the liquid, ΔH_{ads} is the heat of adsorption, and ΔH_{sfl} and $\Delta H_{s/l}$ are, respectively, the heat of wetting with and the heat of wetting without presaturation by the liquid vapor.

Hollenbeck [12] pretreated the solid samples by putting them into relative humidity chambers for several days. The humidity varied from 5% to 100%. The samples were equilibrated with the water vapor, then the heat of immersion of the samples in water was measured. The results show that as the moisture content of the solid increased from 0 to 5%, the heat of wetting decreased sharply. As the moisture content continued to increase, the heat of wetting decreased slowly. Other investigators including Nordon [13] have obtained similar results for a bituminous coal-water system.

The generally accepted explanation was given by Zettlemoyer et al. [14]. The heat of wetting appears to depend primarily on the amount of bare surface present. This suggests that the surface of the solid is covered with energy sites with varying energy levels. As the high energy sites preferentially adsorb the vapor molecules, the heat of wetting depends on which sites are occupied by the vapor molecules.

We therefore can conclude that for measuring the heat of wetting, it is very important to control the moisture of the sample before measurement, as even small quantities of moisture can affect the heat of wetting greatly.

Basically, if we want to determine the hydrophobicity of a solid in a given liquid under certain conditions by measuring the heat of wetting, the measurement must

be conducted under the same conditions. If the experiment starts with a dry solid sample, the heat of adsorption should be determined experimentally or by theoretical calculation. A number of publications[15] have presented the thermodynamic equation from which the heat of adsorption can be calculated.

Overall, when determining the heat of wetting, all the physical and chemical changes need to be considered. The heat involved with the change should be included in the heat of wetting only if the change happens at an interface which would change the hydrophobicity of the solid surface in the liquid. If the change happens beyond the interface, the associated heat effect should not be included. Unfortunately, it is not easy to identify such changes and the associated heat effects.

In the 1940's, the heat of immersion was used to determine the surface area of coal particles [18]- [20]. For these measurements, it was assumed that there was no chemical interaction between the coal and the liquid, so the heat of immersion was directly proportional to the wetted surface area $\bar{S}$. $\bar{S}$ was calculated by assuming that the heat of wetting was 1 cal/10 m^2. This value for the heat of wetting was established by measuring the heat of wetting of carbon black, the surface area of which was determined by electron microscopy. The surface area measured by electron microscopy was also comparable to that measured by sorption techniques. Other measurements indicated that 1 cal/10 m^2 applied to all carbonaceous solids and that it was substantially independent of the nature of the wetting liquid. Bond and Spencer [21] measured the heat of wetting of a carbon black (with $\bar{S} = 230 m^2/g$) in 16 different liquids and found an average value of 1 cal/9 m^2, with a maximum deviation of $\pm 25\%$, and with most values within $\pm 10\%$ of this average. However, later measurements with a Bruceton, Pennsylvania, coal in some 30 different liquids

indicated a much greater variation [22]. Great caution must be exercised in using a universal value for the heat of wetting as Berkowitz [22] pointed out. Heat released by some other interactions may be involved. For example, the heat of immersion in methanol is now known to be grossly distorted by imbibition and/or polar interaction of methanol with oxygen-bearing functional groups (notably -OH) at the coal surface [23] - [26]. Imbibition would tend to create new surfaces (through associated swelling of the coal), and the interaction of methanol with functional groups is an exothermic process. In either case, a fictitiously high value of heat of immersion or the calculated wetted surface area would be observed. Also the effects may depend on how deeply the methanol penetrates into the internal pores of the coal. The heat of immersion also depends on the respective molar volumes of liquids in which it is immersed.

The surface area obtained by these methods is calculated by assuming that the fluid completely penetrates all pore spaces. However, this is not true because fluid molecules having different molar volume will penetrate the internal pores to a different extent. Although it is possible to estimate the relative values of the surface area accessible to different adsorbates, the absolute surface area of coal is still an uncertain quantity. Bond and Spencer[21] studied the heat of wetting of graphite in various liquids with different molar volumes and found that the heat of wetting decreases with increasing molar volume. They thought this phenomenon indicated that smaller molecules can penetrate into micropores while larger molecules can only penetrate into macropores. Spencer and Bond [27] later pointed out that different methods used during the last 30 years to measure the specific surface area of coal, including gas and vapor adsorption and the heat of immersion, had given

contradictory results and had led to considerable confusion. The specific surface area obtained for a given coal can vary according to both the method and the conditions of measurement(e.g., adsorption at different temperatures, etc.). Hence, they pointed out that growing evidence suggested that the concept of "specific surface" when applied to sorbents containing pores having a diameter less than 1 Angstrom had no physical meaning. They also suggested that great attention should be paid to directly characterizing the large pores by mercury penetration porosimetry and other methods. Furthermore, they believed that the heat of immersion should not be used to estimate the specific surface area of coal.

Partyka et al. [28] examined the "absolute" calorimetric determination method originally suggested by Harkins and Jura [29]. In the measurements by Partyka et al. [28], the outgassed powder was brought into equilibrium with the saturation pressure of a liquid in order to be covered with a "duplex" adsorbed film, which was thick enough (for instance 1.5 to 2 nm of water, i.e., five to seven molecular layers) to present an external surface identical in nature with that of the bulk liquid. The wetted powder was then immersed in the liquid. The heat released by the loss of the liquid/vapor interface was related by Harkins [30] to its area A through the following basic relationship:

$$|\Delta_{imm}H| = A(\gamma^{l,g} - T\frac{\partial\gamma^{l,g}}{\partial T}) \tag{3.1}$$

where $\gamma^{l,g}$ is the surface tension of the liquid/vapor interface and T is the absolute temperature of the system. From an evaluation of $\Delta_{imm}H$ and from an independent knowledge of $\gamma^{l,g}$ and $\frac{\partial\gamma^{l,g}}{\partial T}$ it was possible to determine A without any assumption concerning the molecular cross-section of the liquid used for measurement. However,

this method was used successfully for only a very limited number of samples (pure and alumina coated anatase and pure graphite). Yet the validity of this method has been questioned. Firstly, in a saturated vapor it is impossible to avoid capillary condensation which lowers the extent of the available liquid/vapor interface; secondly, the calculated surface area must be corrected for the thickness of the preadsorbed film.

Glanville et al. [31] studied the heat of immersion of a subbituminous Wyodak No. 3 coal in water as a function of coal moisture content. The heat of immersion was found to decrease with increasing moisture content over a range from 1% to 15%. Samples were equilibrated for no less than 8 days at different relative humidities (R.H.) over aqueous sulfuric acid solutions of varying concentration, and subsequently subjected to gravimetric analysis and Karl-Fischer (K-F) titration to determine the moisture content. The samples were then maintained for two hours at less than 10^{-4} torr at the desired temperature. After this treatment, the samples were exposed to water vapor in a volumetric adsorption apparatus. The moisture content of the coal samples was varied by exposing the samples to water vapor for varying lengths of time. The glass ampules containing the coal samples were then sealed off under vacuum and subjected to a heat of immersion measurement. The results showed that the heat of immersion of this coal decreased dramatically with increasing moisture content. It was also found that the specific surface area measured by water vapor adsorption at room temperature was almost five times that measured by Krypton adsorption at low temperature.

Starzewski and Grillet [32] measured the enthalpy of immersion of four French coals of various ranks in water, methanol and tetralin at 20, 30, and 50 °C. They

believed that the enthalpy of immersion in methanol and tetralin resulted from at least two phenomena, a rapid wetting of the solid, followed by a slow dissolution of the coal in the solvent. Hence, they tried to measure the "true" enthalpy of immersion by pretreating the coals. The coal surfaces were saturated by the solvent, then dried and degassed. Then the coal sample was immersed in the liquid which had been saturated with coal. However, the "true" enthalpy of immersion may not represent the true heat of wetting, for the extraction of coal also changes the surface properties of the original coal surface. In this case, the physical process of wetting and the dissolution process cannot be separated.

Experimental

1. Sample Preparation

Illinois No. 6 coal from Illinois and No. 2 Gas Seam coal from Raleigh County, West Virginia, were prepared for determining heat of immersion in various liquids. The coals were crushed, dry ground, and then separated into narrow particle size fractions. Separation involved screening with standard sieves using a mechanical shaker followed by further screening with a Sonic Sifter.

2. Particle Size Analysis and Determination of Specific Surface Area

Two techniques were used to determine the particle size distribution : Microtrac particle size analysis and automatic image analysis. Since the available Microtrac particle size analyzer could only determine the size of particles up to 176 μm, only the size fractions which were below 100 mesh (< 149 μm) were analyzed by the Microtrac particle size analyzer. The particle size distribution of each of the larger size fractions

Table 3.1: Composition of Illinois No. 6 coal used for heat of immersion measurements

Particle Size, mesh (U.S.Std.)	Mean Size, μm	Surface area,[a] $cm^2 \backslash cm^3$	$cm^2 \backslash g$	Ash,[b] wt. %	Total sulfur,[c] wt. %
-45/+70	241	275	212	4.99	3.39
-70/+100	158	428	330	5.24	3.48
-100/+200	110	728	560	6.80	3.32
-200/+270	82	856	659	6.94	3.41
-270/+400	63	1172	902	7.32	3.53

[a]Calculated external particle surface area.
[b]Dry basis.
[c]As received basis.

(-45/+70 mesh and -70/+100 mesh) was determined by automatic image analysis. The average particle size, d_p, of each of the distributions was then determined. The average specific external surface area S (area per unit volume of coal) was calculated by $S = 6/d_p$, assuming the coal particles to be spherical. The ash and total sulfur contents of each sample were also determined by standard methods. The analytical results are listed in Tables 3.1 and 3.2.

3. Controlling Moisture Content of Coal Samples

The moisture content of two coals of -100/+200 mesh size was adjusted either by vacuum drying at room temperature or by placing the samples in desiccators

Table 3.2: Composition of No. 2 Gas Seam coal used for heat of immersion measurements

Particle Size, mesh (U.S.Std.)	Mean Size, μm	Surface area,[a] $cm^2 \backslash cm^3$	$cm^2 \backslash g$	Ash,[b] wt. %	Total sulfur,[c] wt. %
-45/+70	284	191	146	3.40	0.76
-70/+100	181	428	327	3.08	0.76
-100/+200	113	888	679	3.66	0.82
-200/+400	71	1014	776	2.50	0.82

[a]Calculated external particle surface area.
[b]Dry basis.
[c]As received basis.

containing saturated solutions of different salts or NaOH solutions of various concentrations and allowing enough time for the samples to reach a constant weight. The purposes were to determine the dependence of the heat of immersion of coal on the coal moisture content and to establish a standard condition for controlling the moisture content of coal samples for heat of immersion measurement.

For vacuum drying, a thin layer of the coal sample was placed in a small glass jar. The uncovered glass jar was then placed in the vacuum desiccator with desiccant. Then the desiccator was evacuated for 8 hr every day for 7 days before determining the moisture content and the heat of immersion.

NaOH solutions of various concentration were used for adjusting the moisture content of Illinois No. 6 coal of -100/+200 mesh size. A predetermined amount of NaOH ws placed in a beaker, then 200 ml deionized water was slowly added while stirring. Then the solution was transferred to a clean desiccator. A small

glass jar containing a thin layer of the coal sample was placed in the desiccator and then the desiccator was evacuated for 30 min. The desiccator was closed and the sample was equilibrated for more than 3 days. After 3 days, the sample was weighed to determine if the weight of the glass jar had reached a constant. When the weight of the glass jar became constant, the moisture content of each coal sample was determined subsequently by drying a small portion of the sample in an oven at 110-120$^{\circ}C$ for 1.5 hr.

The moisture content of No. 2 Gas Seam coal (-100/+200 mesh size) was adjusted by saturated solutions of different salts. These salts were LiCl, $MgCl_2$, NaCl and KCl. About 150 g salt was placed in a 500 ml beaker, 200 ml deionized water was slowly added while stirring. Then the solution was stirred using a magnetic stirrer for 30 min. More salt was added if all the salt was dissolved. When saturated, the solution was then transferred to a clean vacuum desiccator. The subsequent procedure was the same as described above for using NaOH solutions.

Tables 3.3 and 3.4 list the moisture content of both Illinois No. 6 coal and No. 2 Gas Seam coal of -100/+200 mesh size for various drying conditions.

According to these tables, a saturated solution of LiCl produced coal with the lowest moisture content. Also since a saturated solution was employed, the drying condition was reproducible.

4. Measurement of The Heat of Immersion

The heat of immersion of coal in water or other organic liquids was measured by a TRONAC Model 450 Isoperibol Titration Calorimeter. A small amount of coal, weighing from 0.1 to 0.5 g, was placed in a glass ampule. The stem of the ampule

Table 3.3: The moisture content of Illinois No. 6 coal of -100/+200 mesh size at different conditions

Drying Conditions	Moisture Content of Coal, %
Vacuum Drying	1.97
100 g NaOH + 200 g H_2O	4.13
60 g NaOH + 200 g H_2O	5.52
Pure H_2O	9.45

Table 3.4: The moisture content of No. 2 Gas Seam coal of -100/+200 mesh size at different conditions

Drying Conditions	Relative Humidity in Desiccator, %	Moisture Content of Coal, %
Vacuum Drying		1.85
LiCl Saturated Solution	11	1.27
$MgCl_2$ Saturated Solution	33	2.47
NaCl Saturated Solution	75	3.32
KCl Saturated Solution	85	6.10

was sealed with a microflame torch. The ampule was then placed on the sample shelf in the Dewar cell. The Dewar cell contained 50 ml water or some other liquid. The temperature of the liquid inside the Dewar cell was adjusted to 25° C and 22 hr was allowed for the temperature of the coal sample to be stablized at 25° C. Then the ampule was broken by a mechanical breaker and the heat of immersion was recorded.

Results and Discussion

1. Heat of Immersion vs. Moisture Content of Coal

As shown in Figures 3.1 and 3.2, the heat of immersion of of both Illinois No. 6 coal and No. 2 Gas Seam coal in water decreased with increasing coal moisture content. Therefore, controlling the moisture content of coal samples used for heat of immersion measurement is important. It also suggested that heat of immersion of coals with different surface properties must be compared at the same moisture content. It is recommended that a LiCl saturated solution be used as the standard method of controlling moisture content of coal samples for heat of immersion measurements in this project.

2. Heat of Immersion vs. the Particle Size of Coal

Although the measured heat of immersion usually corresponds to the heat released per unit weight of solids, the heat of immersion per unit surface area is a better indicator of the surface properties of a solid material. A comparison of the hydrophobicity of different solids must be based on this value. It is usually assumed that the heat of immersion per unit surface area is a constant for a given coal immersed in a given liquid. Hence, a horizontal line would be expected when the heat

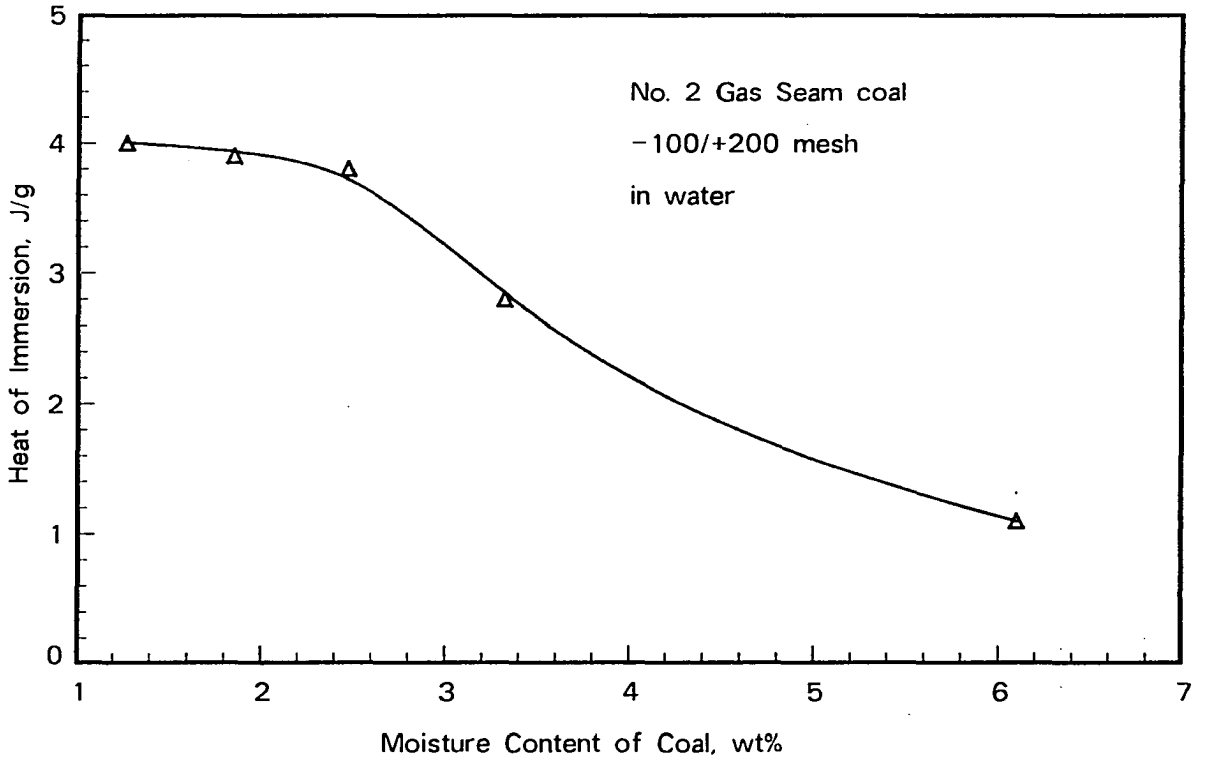

Figure 3.1: Correlation between the heat of immersion in water for Illinois No. 6 coal of the -100/+200 mesh size and the moisture content of the coal

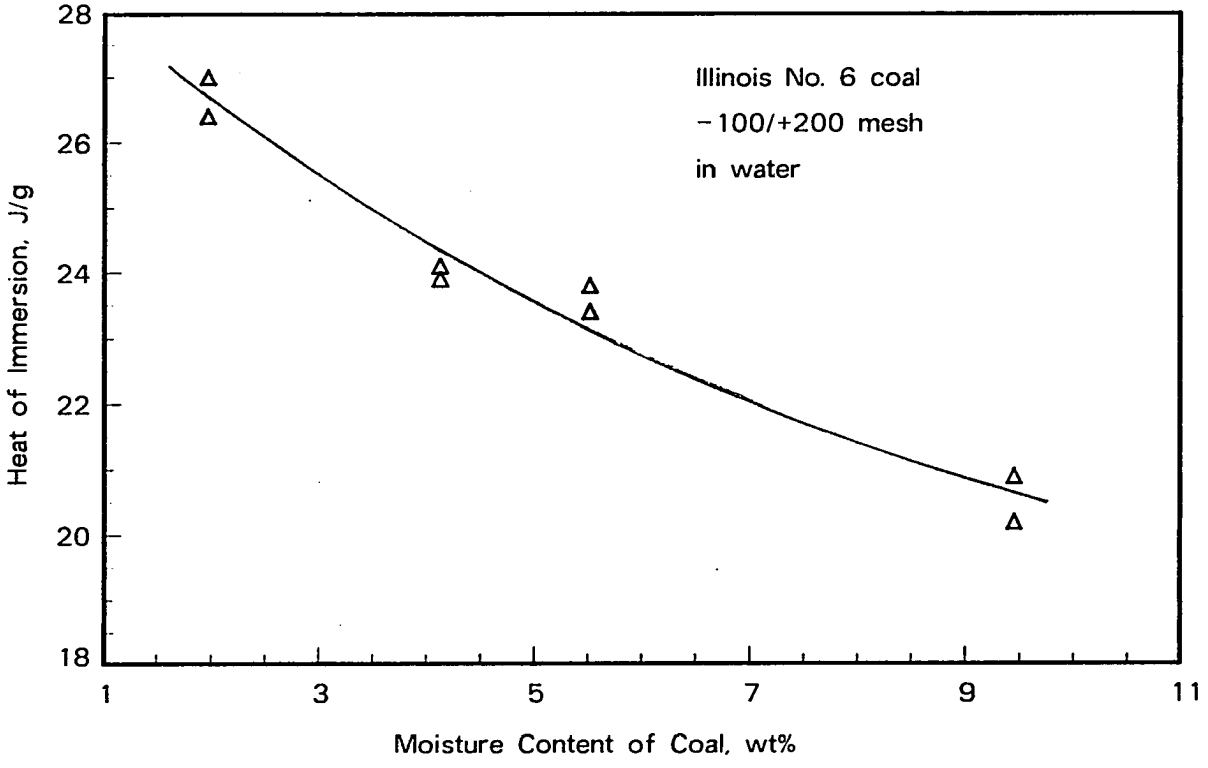

Figure 3.2: Correlation between the heat of immersion in water for No. 2 Gas Seam coal of the -100/+200 mesh size and the moisture content of the coal

of immersion per unit of external area is plotted against the specific external surface area of a series of coal samples which differ only in particle size, provided that only the external surface of the coal particles is wetted by the liquid. However, the results for both Illinois No. 6 coal and No. 2 Gas Seam coal show that the heat of immersion per unit of external surface area decreased with increasing external surface area (see Figures 3.3 and 3.4).

The surface composition and the mineral particle content of the coal samples were slightly different among different size fractions of a given coal. According to Tables 3.1 and 3.2, the sulfur and ash contents differed only slightly among the various size fractions. Since mineral particles are more hydrophilic than coal particles, the existence of more mineral particles and/or mineral components on the surface of coal particles would increase the total heat of immersion of a coal sample. Therefore, the apparent heat of immersion of coal particles would decrease with decreasing particle size.

If the heat of immersion per unit surface area is truly constant, two reasons may be responsible for the phenomena indicated in Figures 3.3 and 3.4. First, the surface characteristics of the larger particles may not be identical to those of the smaller particles. The surface roughness and surface composition may not be the same for different size fractions. If the surface roughness affects the heat of immersion, the smaller particles which have a smoother surface would have a lower heat of immersion.

Because the contact angle may increase with increasing surface roughness [8], the surface hydrophobicity may increase with increasing surface roughness. Therefore, this may lower the corresponding heat of immersion.

Secondly, the external surface of coal particles is not the true surface area wetted

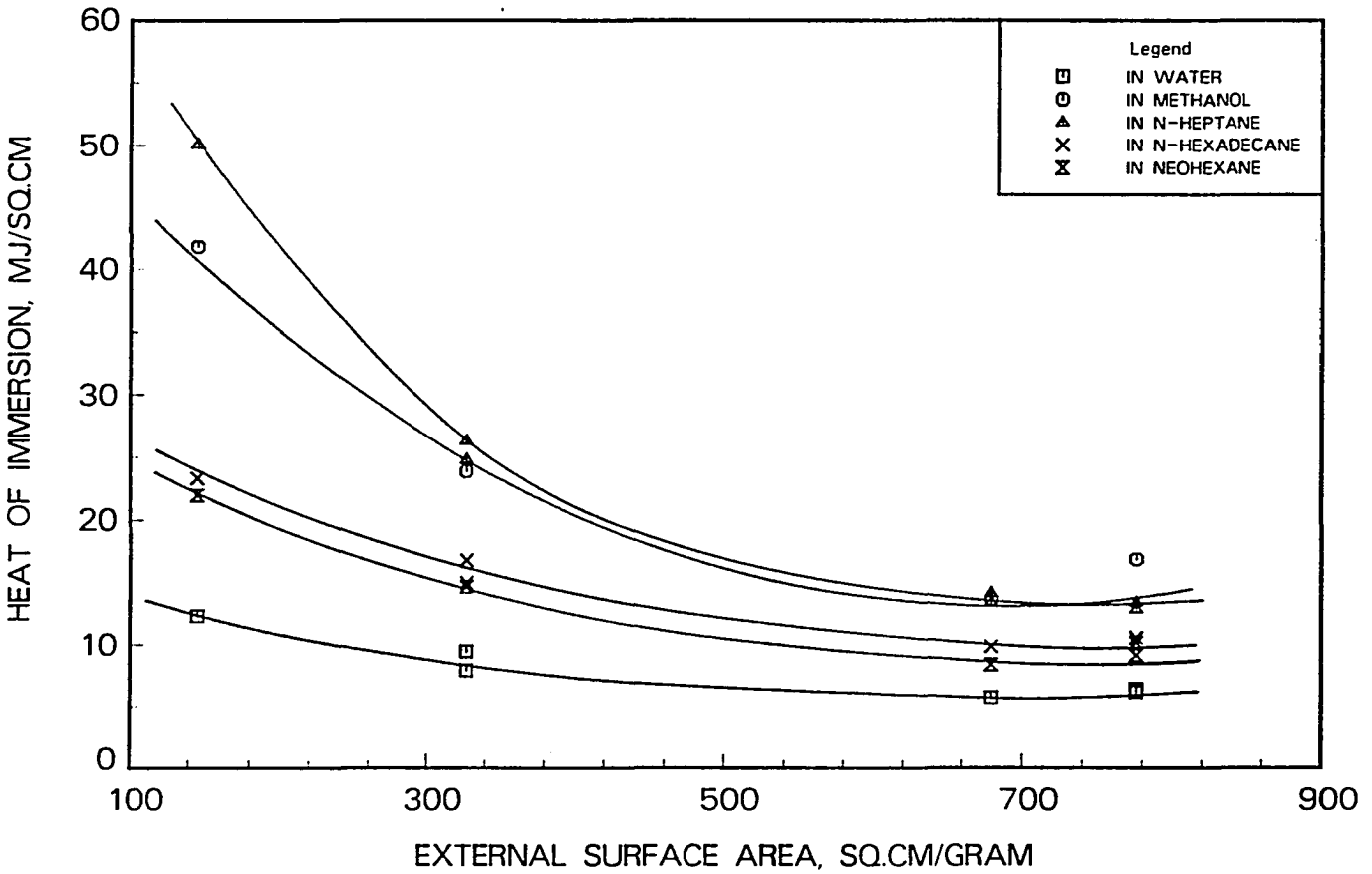

Figure 3.3: Correlation between the heat of immersion per unit of external surface area and specific external surface area for No. 2 Gas Seam coal

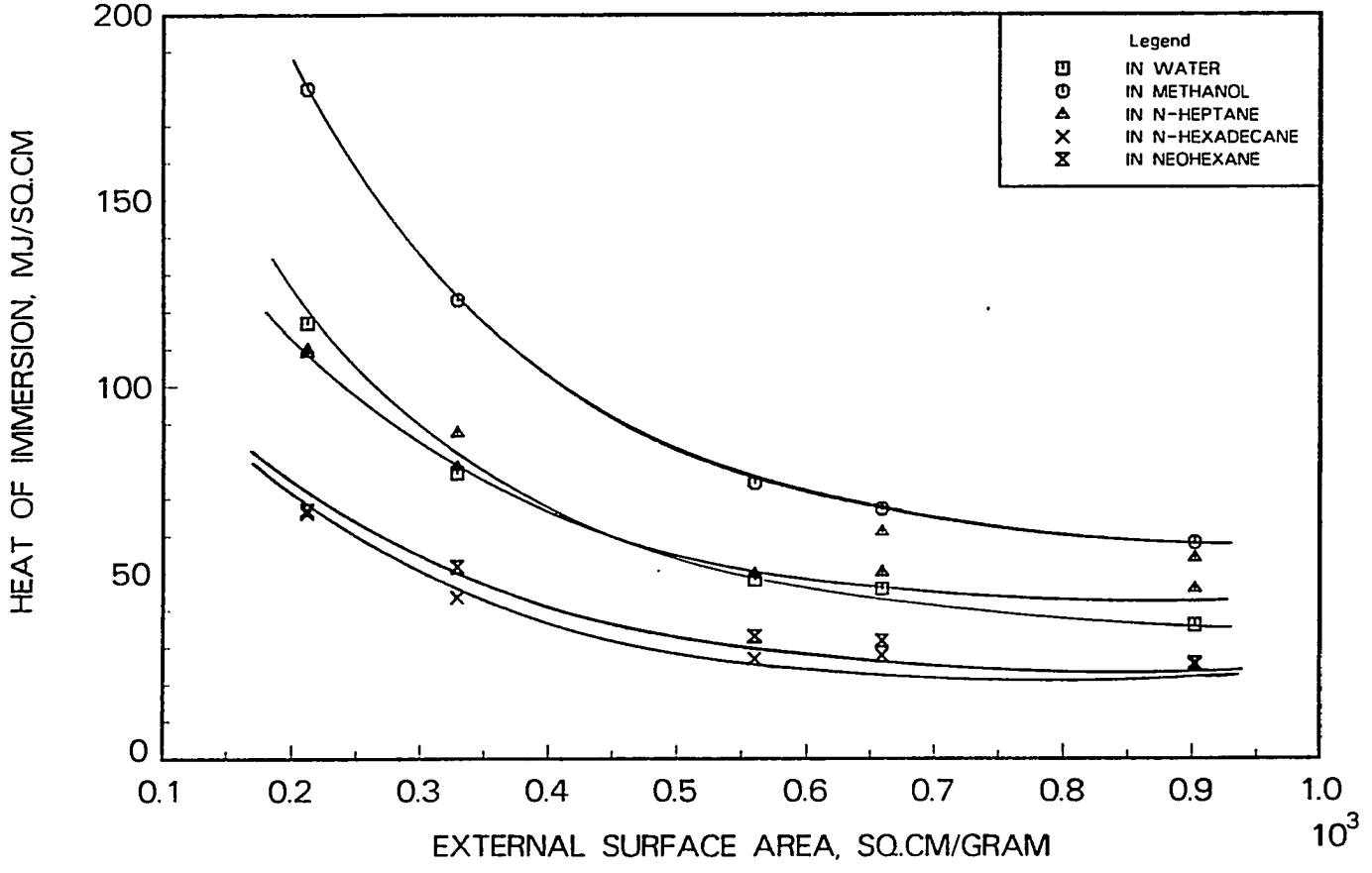

Figure 3.4: Correlation between the heat of immersion per unit of external surface area and specific external surface area for Illinois No. 6 coal

by the immersion process. Since coal is a porous material, liquid will penetrate into the pores of the coal and wet part of the internal surface. This portion of the surface area must be taken into account when calculating the heat of immersion per unit of wetted surface. However, it is extremely difficult to determine the total wetted surface area as has been discussed in the literature review. An alternative method must be used to calculate the heat of immersion, based on the actual wetted surface area. A simple model can be developed if it is assumed the heat of immersion per unit of actual wetted surface area is constant for a given solid in a given liquid, i.e.,

$$\frac{\Delta H\,(J/g)}{S_t\left(cm^2/g\right)} = h = constant \tag{3.2}$$

where

$$S_t = S_e + xS_i, \tag{3.3}$$

where $0 \leq x \leq 1$.

The total wetted surface area S_t consists of the external surface area S_e and a portion of the total internal surface area S_i. The fraction x, determined by the extent of penetration of the liquid into the internal pores, is an unknown factor. The internal pore surface area is a quantity which is very hard to determine as well. Nevertheless, the fraction of the pore surface area being wetted by the immersion process, x, can be assumed to be constant for different size fractions of the same coal under the same conditions of wetting.

This assumption is based on the pore radius distribution theory. Since the pore size distribution for a given coal should be the same regardless of particle size, the fraction of pores into which the liquid can penetrate will be the same also. Hence,

the penetration extent, x, will be the same for various size fractions. The value of x is mainly determined by the smallest pores that the wetting liquid can access under certain conditions. Under the same temperature, pressure, and mechanical conditions, the minimum radius, r_o, of the pores which the wetting liquid can penetrate mainly depends on the molar volume of the wetting liquid, and, therefore, so does the value of x. For large molecules r_o is large, so the fraction of pore surface area, x, is small, and vice versa. The hydrophobic interaction between coal and wetting liquid will also affect r_o and x to some extent.

By substituting Equation 3.3 for S_t in Equation 3.2, the following simple model of heat of immersion is obtained:

$$\Delta H = hS_e + xS_i h \tag{3.4}$$

According to Equation 3.4, a plot of the measured heat of immersion (J/g) versus the external surface area of various size fraction should yield a straight line having a slope of h, which is the normalized heat of immersion per unit of actual wetted surface area. Figures 3.5 and 3.6 indicate a good linear relationship for the experimental data obtained with the two coals. Also the regression coefficient R in Tables 3.5 and 3.6 indicates a good fit of the experimental data to Equation 3.4. The χ^2-test showed that the linear model could be accepted with 95% confidence.

Table 3.5 shows that the normalized heat of immersion, h, was almost the same for hexadecane and neohexane, which indicates a similar interaction for these two liquids with Illinois No. 6 coal. The value of h for water was slightly lower. The large value of h for methanol could have been due to imbibition and/or polar interaction of methanol with oxygen-bearing functional groups (notably -OH) at the

Table 3.5: Regression results for Illinois No. 6 coal

Liquid Type	x·$S_i \cdot h$, J/g	h, mJ/cm^2	$x \cdot S_i$, cm^2/g	x	r^2
Water	21.59	11.86	271.2	0.0389	0.972
Methanol	33.20	19.07	1741	0.0372	0.939
Heptane	16.24	30.62	530.4	0.0113	0.926
Hexadecane	10.21	12.53	814.8	0.0174	0.930
Neohexane	12.10	12.51	967.2	0.0206	0.989

coal surface [23] - [26]. Imbibition, which tended to create new surfaces (through associated swelling of the coal), and interaction of methanol with functional groups are exothermic processes. Either of these processes would have caused a high value of ΔH which resulted in a high value of h.

The exceptionally high value of h for heptane in Table 3.5 was probably caused by some interaction between coal and heptane other than wetting. Illinois No. 6 coal is a lower rank coal which may contain more waxes and resins. These materials may be dissolved by heptane. To study this aspect, heptane and hexadecane were used separately to extract fine particles of Illinois No. 6 coal for 4 hr at room temperature, and the extracts were analyzed by UV-Vis spectra. The difference spectra between the respective extracts and pure heptane and hexadecane were obtained. No significant difference between the hexadecane extract and pure hexadecane was found. However, strong absorbance peaks in the difference spectrum between heptane extract and pure heptane were found at 225 nm^{-1} and 250 nm^{-1}. The absorbance at 225 nm^{-1} could have been due to carbonyl groups, and that at 250 nm^{-1} could have been due to

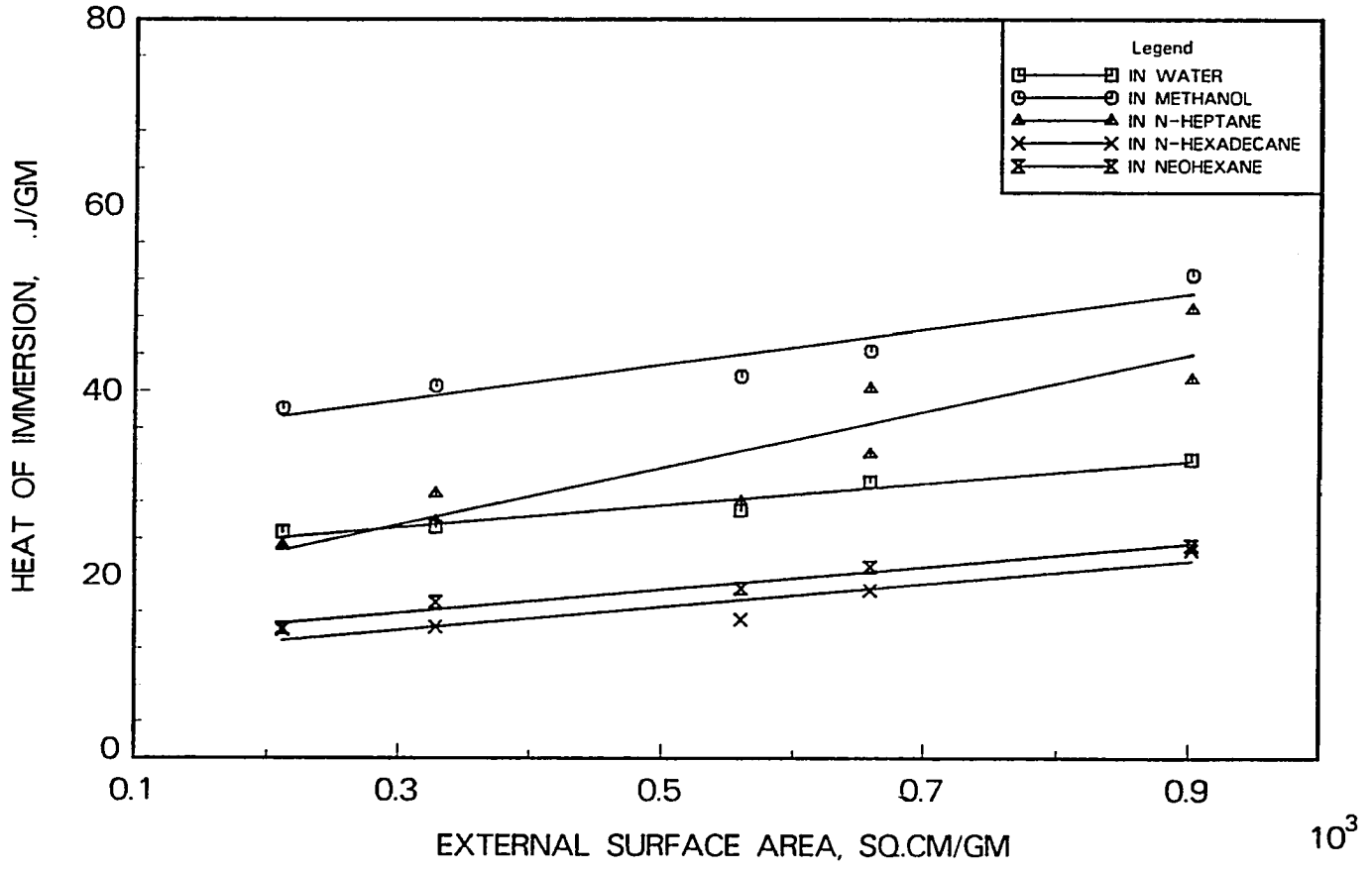

Figure 3.5: Correlation between the heat of immersion per unit of weight and specific external surface area for Illinois No. 6 coal

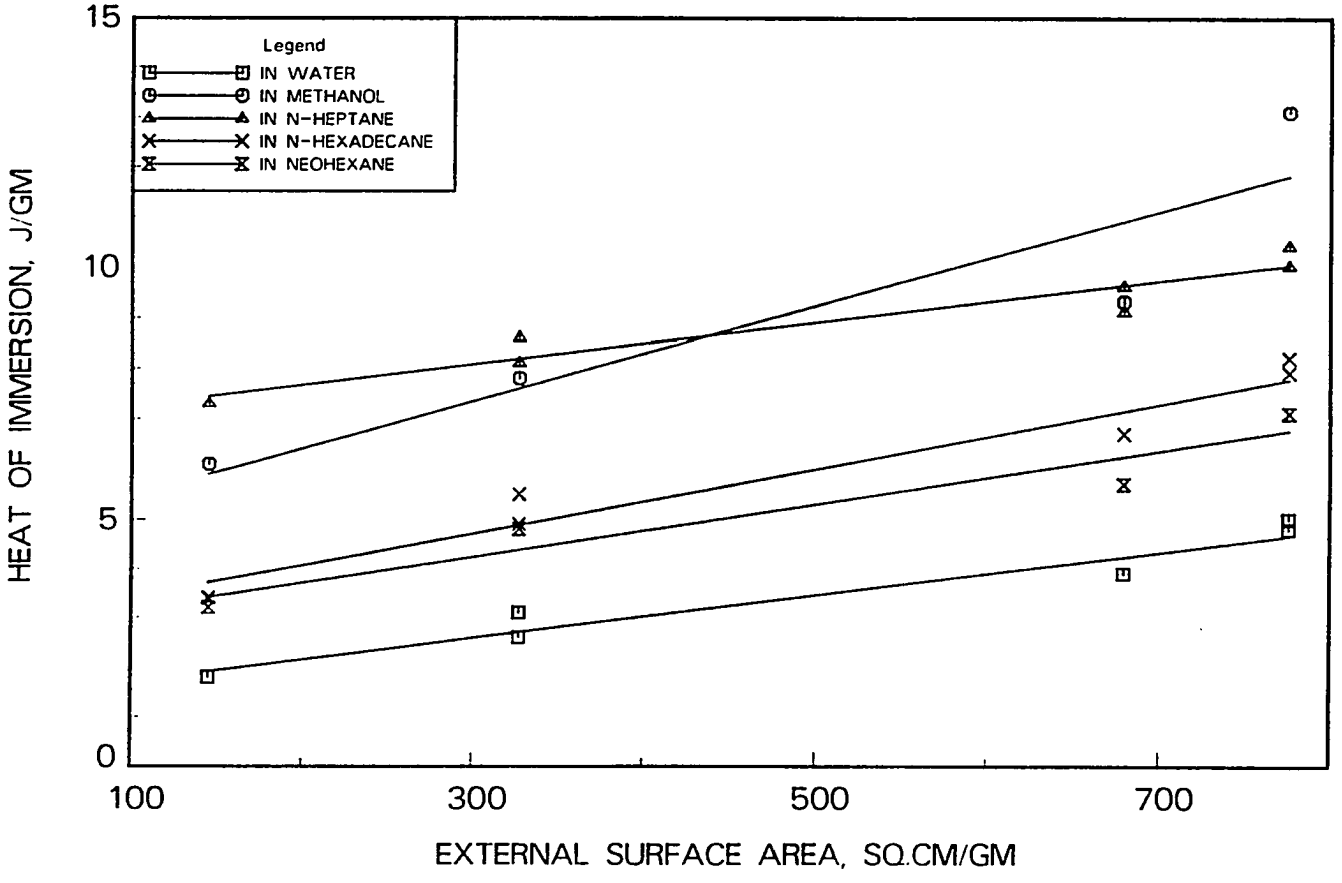

Figure 3.6: Correlation between the heat of immersion per unit of weight and specific external surface area for No. 2 Gas Seam coal

Table 3.6: Regression results for No. 2 Gas Seam coal

Liquid Type	x·$S_i \cdot h$, J/g	h, mJ/cm^2	$x \cdot S_i$, cm^2/g	x,	r^2
Water	1.250	4.520	276.5	0.0095	0.974
Methanol	4.619	9.243	499.7	0.0172	0.916
Heptane	6.854	4.075	1682	0.0577	0.956
Hexadecane	2.749	6.634	414.4	0.0142	0.975
Neohexane	2.643	5.304	498.3	0.0171	0.959

aromatic rings. These assignments suggested the presence of humic-like materials in the heptane extract from Illinois No. 6 coal.

After obtaining a value of h, the actual internal wetted surface area, $x \cdot S_i$, was calculated by dividing the intercept $h \cdot S_i \cdot h$, by the slope h. The value of x was calculated by dividing $x \cdot S_i$ by S_i which was determined to be 46.40 m^2/g for Illinois No. 6 coal by Quantachrome Autoscan Mercury Porosimetry. The results in Table 3.5 show similar values of x for hexadecane and neohexane for Illinois No. 6 coal, while the values of x for water and methanol are about the same. Based on molar volumes methanol should have penetrated the coal structure to a greater extent than water. However, the higher value of h for methanol due to imbibition and polar interaction other than wetting produced a smaller value of $x \cdot S_i$. For this very reason the value of x was much lower.

Table 3.6 shows that the normalized heat of immersion, h, of No. 2 Gas Seam coal was much smaller than that of Illinois No. 6 coal shown in Table 3.5. This means that the value of h for both coals indicates that Illinois No. 6 coal is much more

hydrophilic than No. 2 Gas Seam coal. Therefore, the normalized heat of immersion may be a very good indicator of surface hydrophilicity for comparing different types of coal without being affected by particle size. Again the values of x in Table 3.6 were calculated by the same method used for x in Table 3.5. S_i for No. 2 Gas Seam coal was determined to be 29.14 m^2/g by Quantachrome Autoscan Mercury Porosimetry. The value of x for water is much smaller than that for organic liquids, which may be because this coal is very hydrophobic; therefore, it is more difficult for water than organic liquids to penetrate into the internal pores of No. 2 Gas Seam coal.

CHAPTER 4. CHARACTERIZATION OF OXIDIZED COAL AND THE EFFECT OF COAL SURFACE PROPERTIES ON OIL AGGLOMERATION

Review of Previous Work

Ambient temperature surface oxidation of coal changes many physical and chemical properties important in direct utilization and conversion of coal. These properties include heating value, hydrophobicity, free-swelling index, liquid yield, coking quality and amenability to beneficiation. Characterization of the oxidation process is challenging in that surface phenomena are involved. Previous investigations utilizing a variety of methodologies to oxidize coal under controlled conditions have shown that acids, ketones, ethers, hydroxyl groups and other oxygenated compounds are produced on the surface [34].

The degree of oxidation of coal is usually determined by measuring the oxygen functional group content of the coal surface. A widely used method is an ion-exchange procedure proposed by Fuchs [41], and later modified by Brooks and Sternhell [42] and by Schafer [43][44]. This method can determine the concentration of surface carboxylic acid groups and phenolic groups by leaching the coal with sodium acetate and with barium oxide, respectively. Yet this method can only determine the leachable oxygen functional groups. During the last decade, better and more modern

techniques have been used to characterize coal oxidation while attempting to find the chemical changes on the coal surface. Hercules [34] used modern microprobe mass spectrometry methods including Laser Mass Spectrometry (LMS) and Secondary Ion Mass Spectrometry (SIMS) in combination with selected derivatization reduction to chemically characterize a complex matrix of coals. This study found that phenolic compounds were produced on the coal surface by oxidation. Fourier Transform Infrared Spectroscopy (FTIR) is becoming widely used for determining the oxygen functional groups on coal surfaces [45].

Ye et al. [40] measured the FTIR spectra of low rank coals which underwent thermal treatment at 130 C in air and used a hydrophilicity index calculated from FTIR spectra to describe the hydrophobic/hydrophilic character of the coals. The hydrophilicity index was defined as the ratio of the abundance of hydrophilic functional groups to the abundance of hydrophobic functional groups. Considering hydroxyl groups and carboxyl groups as the only hydrophilic groups and aliphatic and aromatic CH groups as hydrophobic functional groups, the hydrophilicity index was defined as follows:

$$Hydrophilicity \quad Index = \frac{(-COOM) + 2(-OH)}{(R-H) + (Ar-H)} \tag{4.1}$$

where (-COOM), (-OH), (R-H) and (Ar-H) are values of the absorption intensity for carboxyl, hydroxyl, aliphatic CH, and aromatic CH groups respectively. The hydroxyl group intensity was multiplied by 2 in Equation 4.1 because it was thought that the hydroxyl group has a dual functionality being able to act as both a hydrogen donor and hydrogen acceptor, whereas the carboxyl group acts only as a hydrogen acceptor. For this reason the contribution to the hydrophilic character of the surface by the hydroxyl group was expected to be twice that of the carboxyl group.

Numerous methods or techniques have been used to characterize the wetting properties of coal. These include contact angle measurement, immersion time measurement, mean critical wetting tension, heat of immersion, induction time for bubble-particle attachment, etc. [36]. Among these methods, the heat of immersion measurement is more objective, sensitive, and suitable for direct application to coal powders.

Fuerstenau et al. [36] characterized the wettability of as-received and oxidized coals by conducting film flotation experiments with a series of aqueous methanol solutions having different concentrations and levels of surface tension. It was found that the mean wetting surface tension, which serves as an index of wettability of coal, decreases with increasing extent of oxidation. This reflects the increase in hydrophilicity produced by oxidation. The flotation yield was found to decrease with the increase in oxidation extent. An increase in oxygen functional group content was also detected by using potentiometric titration.

Sadowski et al. [37] oxidized Upper Freeport coal at 150° C for up to 144 hr and conducted oil agglomeration tests at various pH values. It was found that with increased oxidation time, the surface concentrations of both carboxyl and hydroxyl groups were increased. The oil agglomeration recovery with a given oil dosage was reduced as well. The effects of oxidation on Zeta potential and contact angle were also studied and the results indicated that the relative oleophilic/hydrophilic nature of the coal surface is more important in the oil agglomeration process than the electrokinetic properties of the system.

The heat of immersion has been used to determine the wettability of coal and other surface properties such as pore structure and surface area. Phillips et al. [39] studied the effect of oxidation on the heat of immersion of coal in water, and observed

that the heat of immersion of Virginia-C coal increases with oxidation temperature. The increase in the heat of immersion can be correlated with the increase in surface oxygen-to-carbon ratio determined by Electron Spectroscopy for Chemical Analysis (ESCA). The ESCA technique, which involves measuring binding energies of electrons ejected by interaction of a molecule with a mono-energetic beam of soft X-rays, can yield information about the composition of the surface region of a particle.

Although a number of researchers have devoted much effort and applied various methods to understand the chemical oxidation of coal surfaces and its effect on the wetting behavior of coal and impact on surface controlled processes, this subject remains poorly understood and more work is still needed. Also more study of the relationship between oxygen functional group concentration and other indicators of hydrophilicity is needed.

Experimental

1. Sample Preparation and Oxidation

Two coals were selected for this study: No. 2 Gas Seam coal from Raleigh County, West Virginia, and Colchester Seam coal from Schuyler County, Illinois.

The No. 2 Gas Seam coal was selected because of its purity (4% ash, 0.2% pyritic sulfur, 0.6% organic sulfur) and good response to oil agglomeration. Previous experiments with this coal had shown that this coal is relatively hydrophobic and the surface properties of the coal are relatively stable. A portion of this coal was prepared by crushing, grinding, and screening. Grinding was accomplished with a high speed impact mill. The $-70/+100$ mesh ($-219/+149$ μm) size fraction was used for the first batch oxidation experiment. A relatively coarse size fraction was

chosen because a colleague planned to use some of the coal for the measurement of induction time which required relatively large particles. Later for a second batch oxidation experiment involving No. 2 Gas Seam coal, −200 mesh (- 75 μm) particles (i.e., particles which passed a 200 mesh screen) were selected. This size shift was made after realizing that the −70/ + 100 mesh particles were too large for good turbidity measurement.

The Colchester Seam coal is a high volatile C bituminous coal and is similar to Illinois No.6 coal. It was selected because of its inherently low ash content. A handpicked sample was obtained from the freshly exposed seam in the Cedar Creek Mine near Camden, Illinois, on June 13, 1990. This is a surface mine. The sample was immediately stored under argon. Later the coal was crushed, subdivided into smaller lots, and then again stored under argon. The ash content of the coal was found to be 4.5% and the total sulfur content 2.4%. A portion of Colchester coal was crushed, ground, and screened in the same manner as No. 2 Gas Seam coal had been treated. Particles which passed a 200 mesh screen were collected and divided into several portions for oxidation. One portion was oxidized as the first batch of Colchester coal had been treated, while the rest was stored under nitrogen for a second batch oxidation treatment.

For each coal, after collecting a sample of the untreated coal, the remaining material was spread in a very thin layer in two large aluminum pans which were placed in a convection oven set at 150° C. Samples of the treated coal were collected after 4, 8, 12, 24, 48 and 72 hr of treatment in the oven. A spinning riffle was used to obtain representative samples. After each sampling, the remaining material was mixed and respread. In addition, the material was mixed and respread after 2, 6,

and 10 hr of oxidation in the oven.

2. Characterization and Oil Agglomeration of Oxidized Coal

The samples of both treated and untreated coal were subsequently characterized by several different methods which included measurement of induction time, heat of immersion in water, and infrared absorption spectrum. In addition, the response of the coal to oil agglomeration was determined by monitoring the turbidity change of an agitated aqueous suspension treated with increasing amounts of heptane. Oil agglomeration recovery or yield was also determined at the end of the turbidity measurement. During an oxidation experiment 13 g coal was collected at each sampling. Of this amount 10 g was used for an oil agglomeration test, 1 g was given to a colleague for infrared absorption measurement, 1 g was given to another colleague for induction time measurement, and another 1 g was used for heat of immersion measurement.

3. Heat of Immersion Measurement

A 0.3 g sample of coal particles was placed in a glass ampule and sealed quickly for the heat of immersion measurement. The remainder of the 1 g sample was then placed in a desiccator containing a saturated solution of lithium chloride and stored for 7-8 days at room temperature for moisture equilibration. The procedure established in Chapter 3 for moisture equilibrium of coal particles was used in preparing the moisture-equilibrated samples. When moisture equilibrated, the coal samples were taken out from the desiccator and immediately sealed in glass ampules for the heat of immersion measurement. 50 ml deionized deionized water was used as immersion

liquid for each heat of immersion measurement at 25 °C by a TRONAC Model 450 Isoperibol Titration Calorimeter. The procedure for heat of immersion measurement was also described in Chapter 3.

4. FTIR Spectra

An FTIR photoacoustic analysis was made on each sample by collaborators S. Luo and J. F. McClelland to detect changes of oxygen functional groups on coal surface. The peak height of the oxidation differences of various oxygen functional groups was determined from the difference spectra of each oxidized coal sample relative to the unoxidized sample. The peak heights were determined for carboxyl group, hydroxyl group, aliphatic and aromatic C-H groups.

5. Oil Agglomeration Test and Turbidity Measurement

The oil agglomeration was conducted in the device shown in Figure 4.1. Ten grams of raw coal or oxidized coal were prewetted with deionized water. The coal suspension was transferred to the 480 ml glass jar which was fitted with an external loop of tubing through which the suspension passed to measure its turbidity. Sufficient deionized water was added to completely fill the vessel. After the suspension was conditioned for 2 to 3 min by stirring at 5500 rpm, turbidity monitoring was started. When agitation was applied, the suspension flowed through the external loop, and the turbidity of the suspension was measured with a photometric dispersion analyzer. Oil was added through the top of the glass jar in incremental doses until a certain predetermined dosage was attained. After the addition of oil, the suspension was screened with a 150 μm sieve to separate the agglomerates and the fines.

Both agglomerates and tailings were collected and dried overnight at 100-110°C and weighed to determine the agglomeration recovery.

Results and Discussion

The heat of immersion in water for both No. 2 Gas Seam coal and Colchester coal is shown in Figure 4.2. The difference in the heat of immersion between these two coals at zero oxidation time indicates that the raw Colchester coal was much more hydrophilic than No. 2 Gas seam coal. With increasing oxidation time, both coals showed a similar increasing trend in their heat of immersion which indicates that both coals became more hydrophilic with increasing oxidation no matter what their original rank was. The heat of immersion of both of these coals was shown to increase sharply during the first 24 hr and then slowly afterwards.

To compare the relative change in the heat of immersion of these two coals, the normalized heat of immersion was calculated by means of the expression

$$Normalized\ \ Heat\ \ of\ \ Immersion(\%) = \frac{(\Delta H)_t - (\Delta H)_o}{(\Delta H)_f - (\Delta H)_o} \times 100$$

and is shown in Figure 4.3. In above expression, $(\Delta H)_t$ is the heat of immersion of the coal which had undergone t hr of oxidation while $(\Delta H)_0$ and $(\Delta H)_f$ are the heats of immersion of nonoxidized coal and coal which had undergone 72 hr of oxidation, respectively.

Figure 4.3 shows a slight difference in the normalized heat of immersion for the two coals. The heat of immersion of No. 2 Gas seam coal increased faster than that of Colchester coal in the first 24 hr and then leveled off. The greater rate of increase in the heat of immersion during the initial period of oxidation was possibly

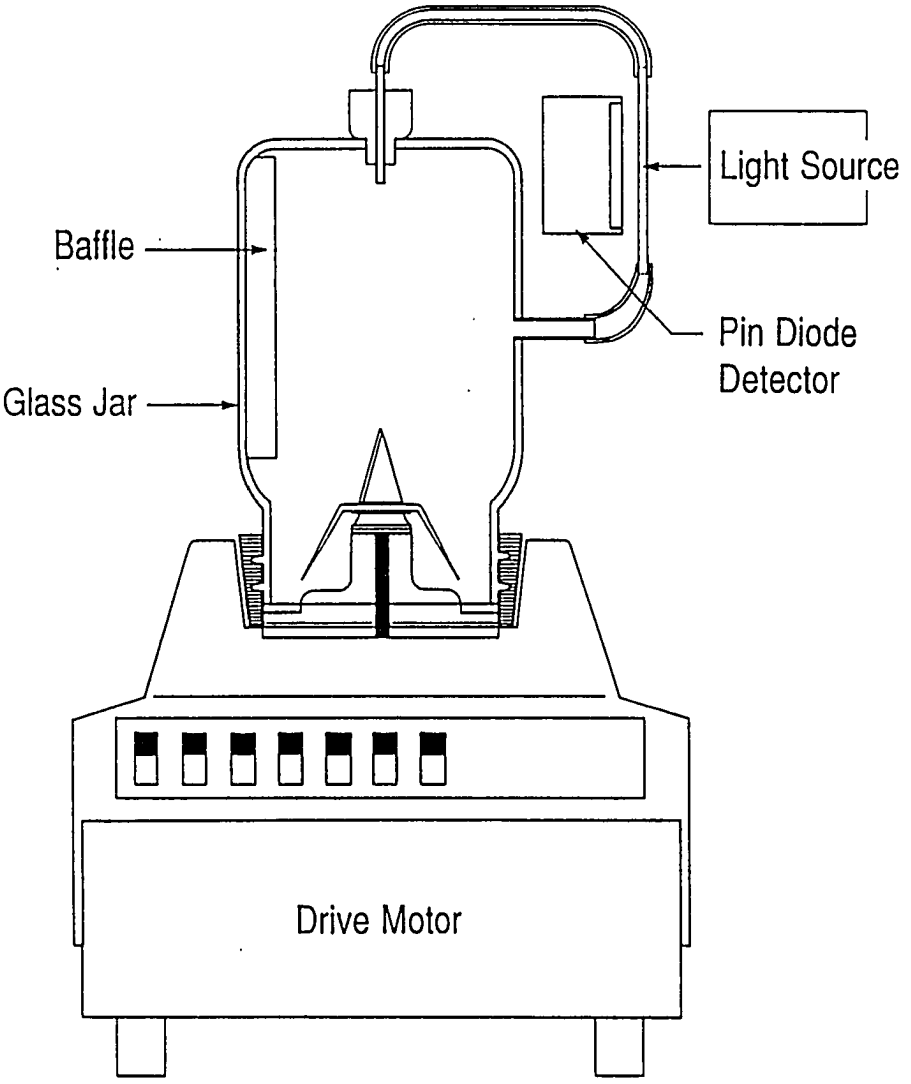

Figure 4.1: Oil agglomeration and turbidity monitering device

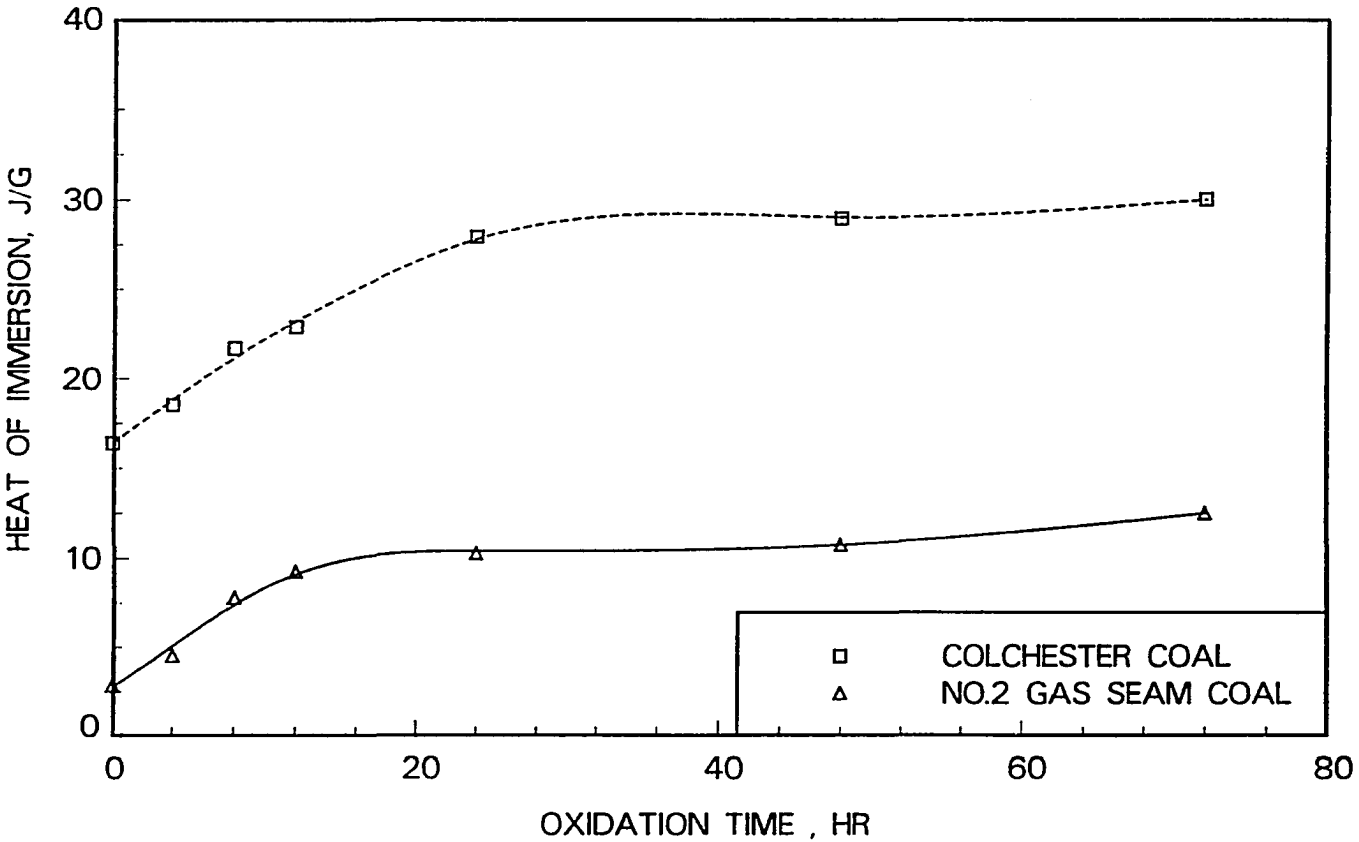

Figure 4.2: Comparison of heat of immersion in water between Colchester coal and No. 2 Gas Seam coal oxidized at 150 °C

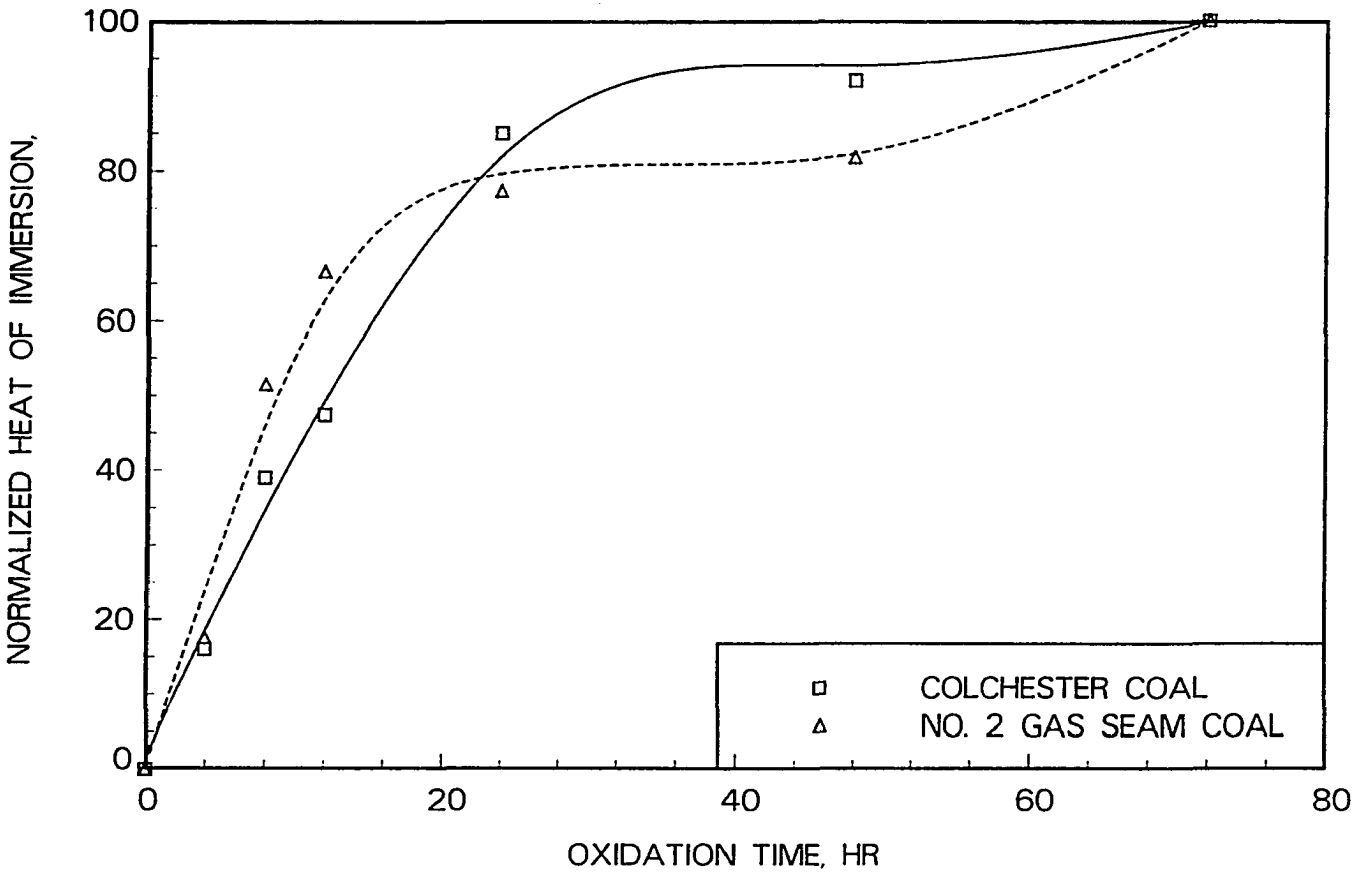

Figure 4.3: Comparison of normalized heat of immersion between Colchester coal and No. 2 Gas Seam coal

because the No. 2 Gas Seam coal originally had fewer oxygen functional groups on its surface than Colchester coal had; thus more surface sites were available to interact with oxygen in the air. The difference in the results for the two coals following 24 hr of oxidation are hard to explain. In both cases, the surface of the coal appeared to become saturated.

The FTIR spectrum was measured and the hydrophilicity index was calculated by using the formula introduced by Ye et al. [40]. Figure 4.4 shows the FTIR absorption spectra determined for the raw and oxidized Colchester coal of -200 mesh size. The difference spectra was obtained by subtracting the spectrum for the raw coal from the spectrum for oxidized coal. Spectrum A in Figure 4.5 represents the difference between coal oxidized for 4 hr and the raw coal, and F represents the difference between coal oxidized for 72 hr and the raw coal. It can be seen that with increasing oxidation extent, the absorption intensity of $-$C=O at 1710 cm^{-1} and that of -OH at 3400 cm^{-1} increase, while the absorption intensity of Ar-H at 3030 cm^{-1} and that of C-H at 2965 cm^{-1} decrease. Namely with increasing oxidation, the concentration of the hydrophobic functional groups on the coal surface decreases, while the concentration of the hydrophilic oxygen functional groups increases. The hydrophilicity index was then calculated by taking the ratio the relative absorption intensity of the hydrophilic functional groups to that of the hydrophobic functional groups as proposed by Ye et al. [40] (see Equation 4.1):

$$Hydrophilicity \quad Index = \frac{(C=O)+2(-OH)}{(R-H)+(Ar-H)} \tag{4.2}$$

However, the expression was modified by taking the absorption intensity of the $-$C=O group determined at 1710 cm^{-1} instead of the absorption intensity of the

$-COOM$ group at 1620 cm^{-1} as proposed by Ye et al. [40]. The absorption intensity at 1710 cm^{-1} was chosen because it exhibited greater change with increasing oxidation than that at 1620 cm^{-1}.

Figures 4.6 and 4.7 show how the hydrophilicity index correlated with the heat of immersion for the two coals, respectively.

Both coals showed the same general trend of increasing heat of immersion as the hydrophilicity index increased, so it may be concluded that the heat of immersion indeed depends on the oxygen functional groups content of the coal surface. The correlation between the heat of immersion and the hydrophilicity index for No. 2 Gas Seam coal appeared to be linear. A linear regression analysis produced the following results:

$$\Delta H = -0.439 + 5.627 HI$$

with a large correlation coeficient ($r^2 = 0.9856$). HI is the hydrophilicity index. However, the relationship between the heat of immersion and the hydrophilicity index for Colchester coal did not appear to be linear as observed for No. 2 Gas Seam coal. In the range of the initial oxidation period, the correlation seemed to be linear, but for oxidation longer than 24 hr, the effect of oxidation on the heat of immersion slowed down while the effect of oxidation on the hydrophilicity index continued to increase at the same pace. From consulting the peak height changes of carboxyl functional groups, The FTIR analysis showed that the carboxyl group content of Colchester coal started to decrease after the initial 24 hr period of oxidation while the carboxyl group content of No. 2 Gas Seam coal increased during the whole range of oxidation. Therefore, for Colchester coal the rate of increase in the heat of immersion slowed down because of the decrease in carboxyl functional group content. The

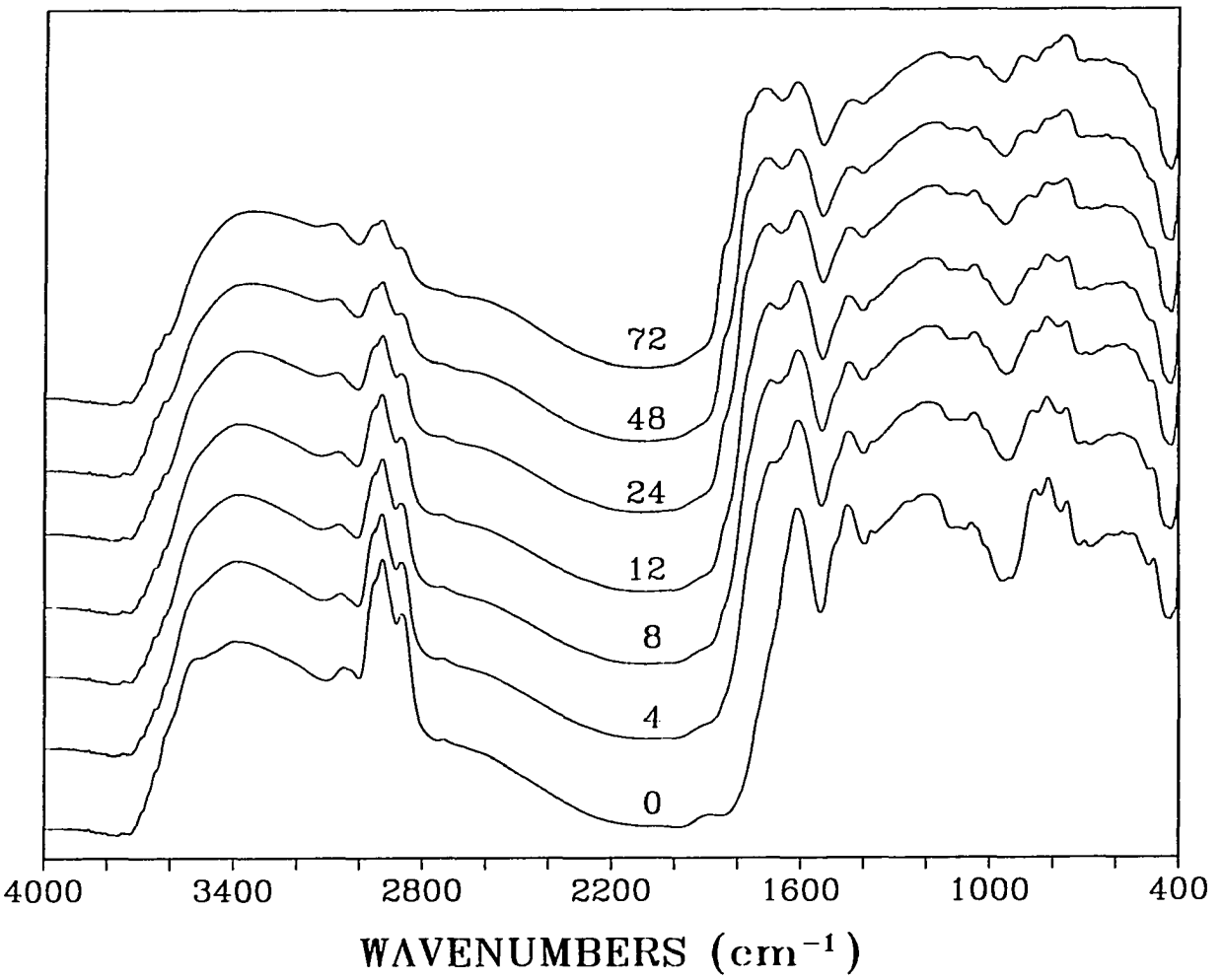

Figure 4.4: The FTIR absorption spectra for raw and oxidized Colchester coal, -200 mesh, the arabic number represents the oxidation time in hours

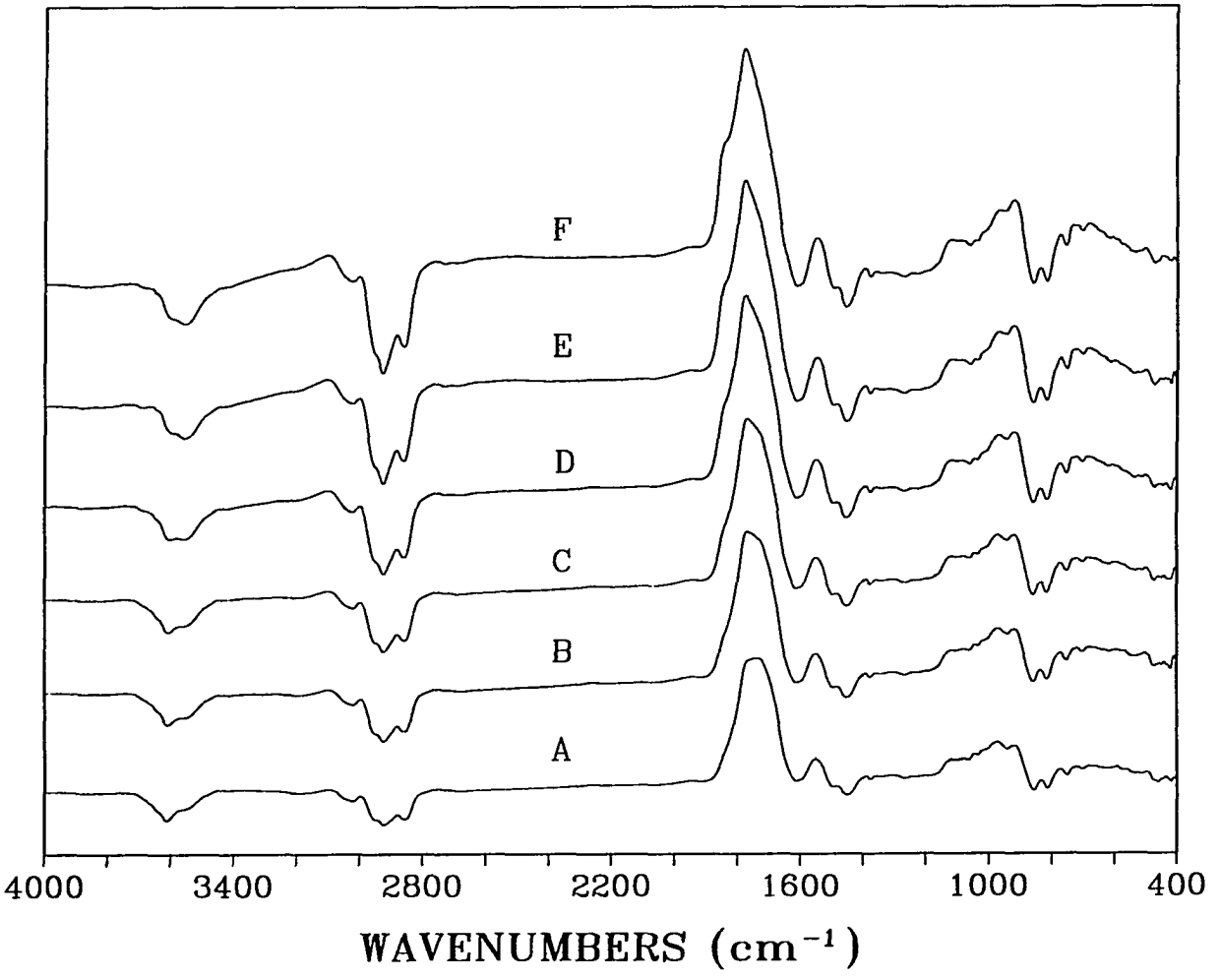

Figure 4.5: The FTIR difference spectra between oxidized and raw Colchester coal, -200 mesh

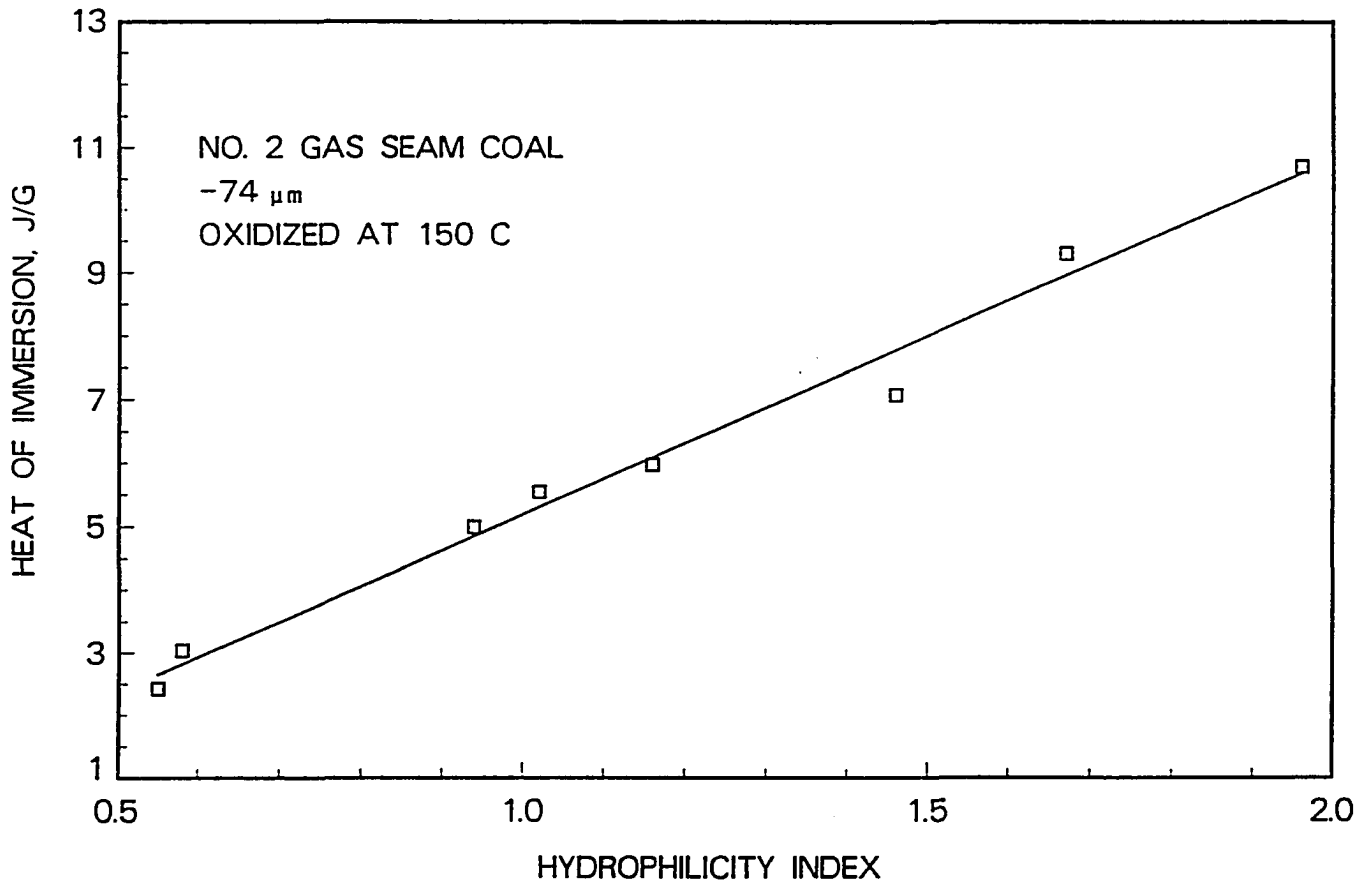

Figure 4.6: Correlation of the hydrophilicity index with the heat of immersion for No. 2 Gas Seam coal

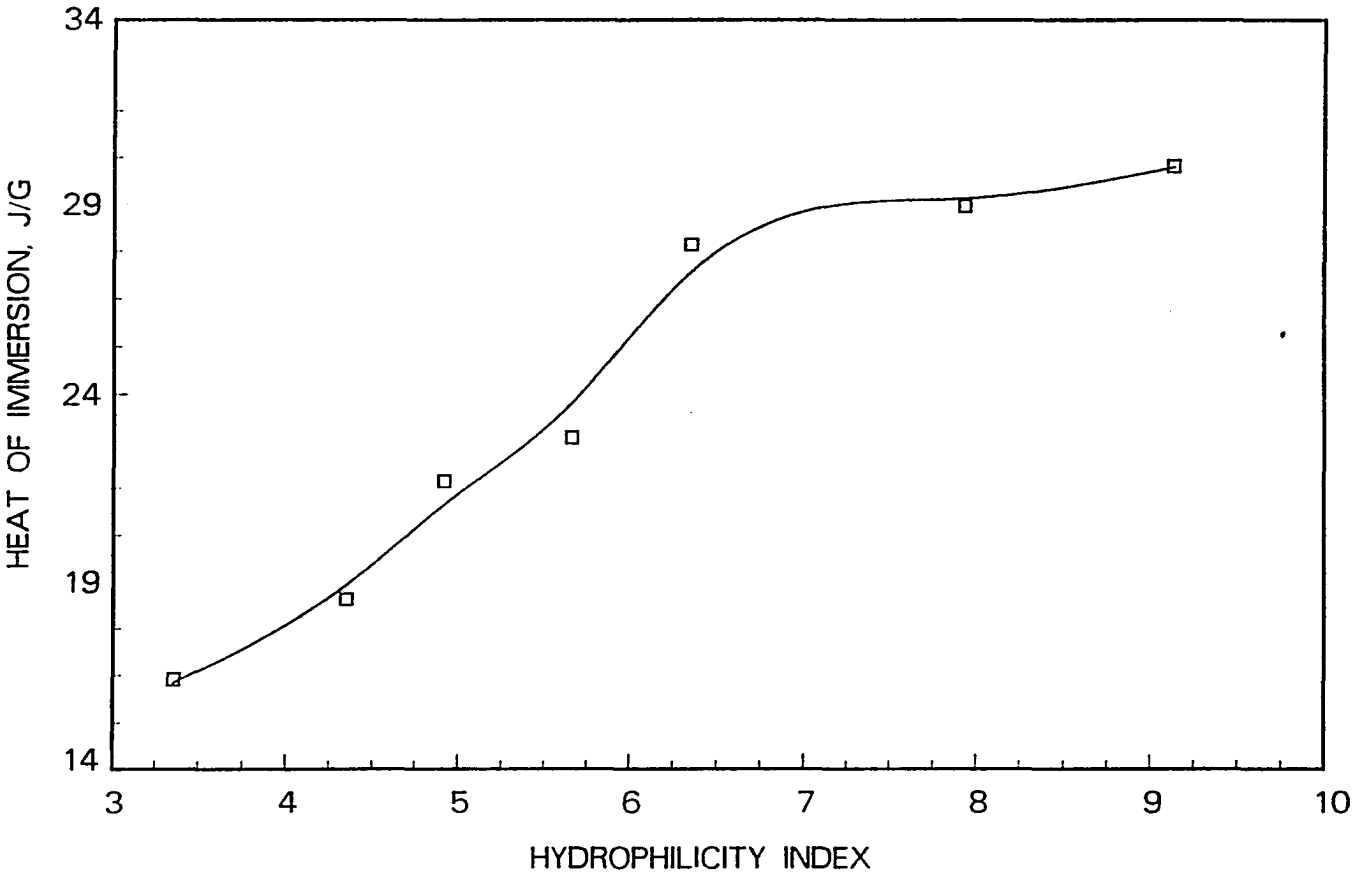

Figure 4.7: Correlation of hydrophilicity index with the heat of immersion for Colchester coal

hydrophilicity index continued to increase for Colchester coal because of the weighting factor given to the hydroxyl group content. The weighting factor for the hydroxyl group content offset the small decrease in carboxyl group content in calculating the hydrophilicity index. This implies that the heat of immersion is more responsive to the carboxyl group content on the surface. The reason that only Colchester coal showed a decrease in carboxyl group content is probably because Colchester coal originally had a higher content of oxygen functional groups than No. 2 Gas Seam coal. When the carboxyl group content reaches a certain level, some other chemical reaction may be turned on which consumes carboxyl groups. The No. 2 Gas Seam coal originally had fewer oxygen functional groups, so the carboxyl group content may not have reached the critical value during the whole period of oxidation. Also a lower rank coal such as Colchester coal is less stable than a higher rank coal such as No. 2 Gas Seam coal, therefore, it can undergo thermal decompostion at a lower temperature.

Figure 4.8 shows the turbidity of particle suspensions of oxidized Colchester coal following agglomeration with different amounts of heptane. Before the addition of heptane, the concentration of coal particles in the suspension was high, so the turbidity of the suspension was high. By adding heptane to the suspension, some coal particles were agglomerated by the heptane which decreased the concentration of fine coal particles and caused the turbidity to decrease. As the unoxidized coal had the greatest hydrophobicity, after adding 16 v/w% heptane, the turbidity of this material decreased the most. For the coal which underwent 24 hr of oxidation, the turbidity decreased less than that of the unoxidized coal for the the same heptane dosage. It is because the oxidized coal surface had become less oleophilic or hydrophobic than the

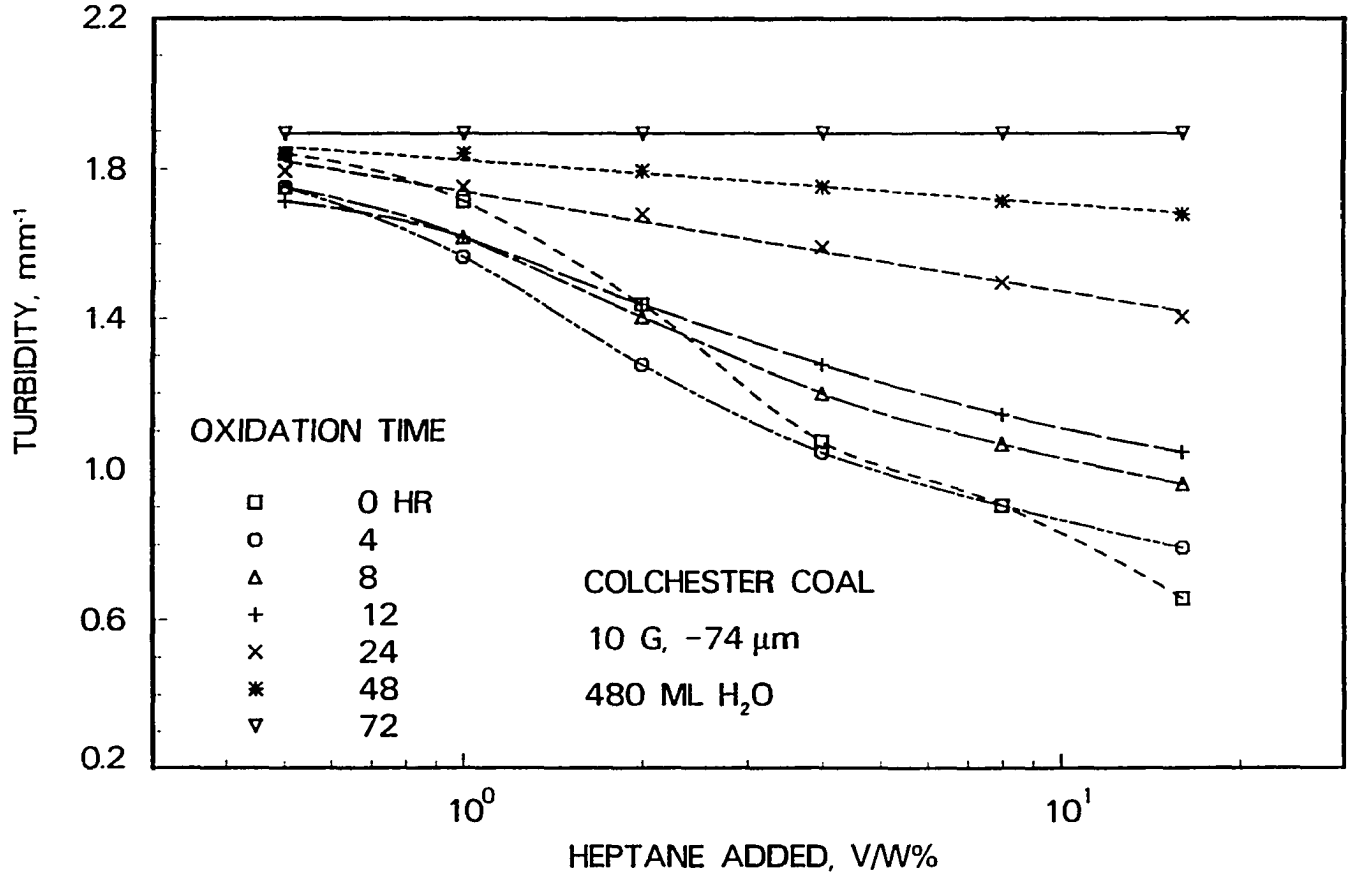

Figure 4.8: The turbidity vs. oil dosage for Colchester coal

unoxidized coal that the agglomeration tendency of the coal decreased. Hence, for the same heptane dosage fewer coal particles were agglomerated, the concentration of fine particles was higher, and the turbidity was greater. For the coal which underwent 72 hr of oxidation, the surface became so hydrophilic that the heptane could not spread on the coal surface at all so no coal particles were agglomerated, and the turbidity did not change.

Since a change in turbidity can indicate how much coal has been agglomerated, it proved instructive to use the relative turbidity change (RT) which is defined below to determine the extent of oil agglomeration:

$$RT(\%) = \frac{\tau_0 - \tau_f}{\tau_0} \times 100 \tag{4.3}$$

In this expression τ_0 is the initial turbidity of the coal/water suspension and τ_f the final turbidity of the coal water suspension. The relative turbidity change for the agglomeration of Colchester coal was calculated from the data on which Figure 4.8 was based and the results are presented in Figure 4.9.

The results in Figure 4.9 indicate that the oil agglomeration recovery determined by the traditional method, RC, is proportional to the relative turbidity change. Application of linear regression analysis produced the following equation for the straight line:

$$RC = 4.29 + 1.234RT$$

The correlation coeficient was large ($r^2 = 0.9893$). This shows that the relative turbidity change can be used to represent the agglomerability of coal. An advantage of using this parameter is that it can be determined more easily and and more rapidly than oil agglomeration recovery. In addition, it can be determined by an on line

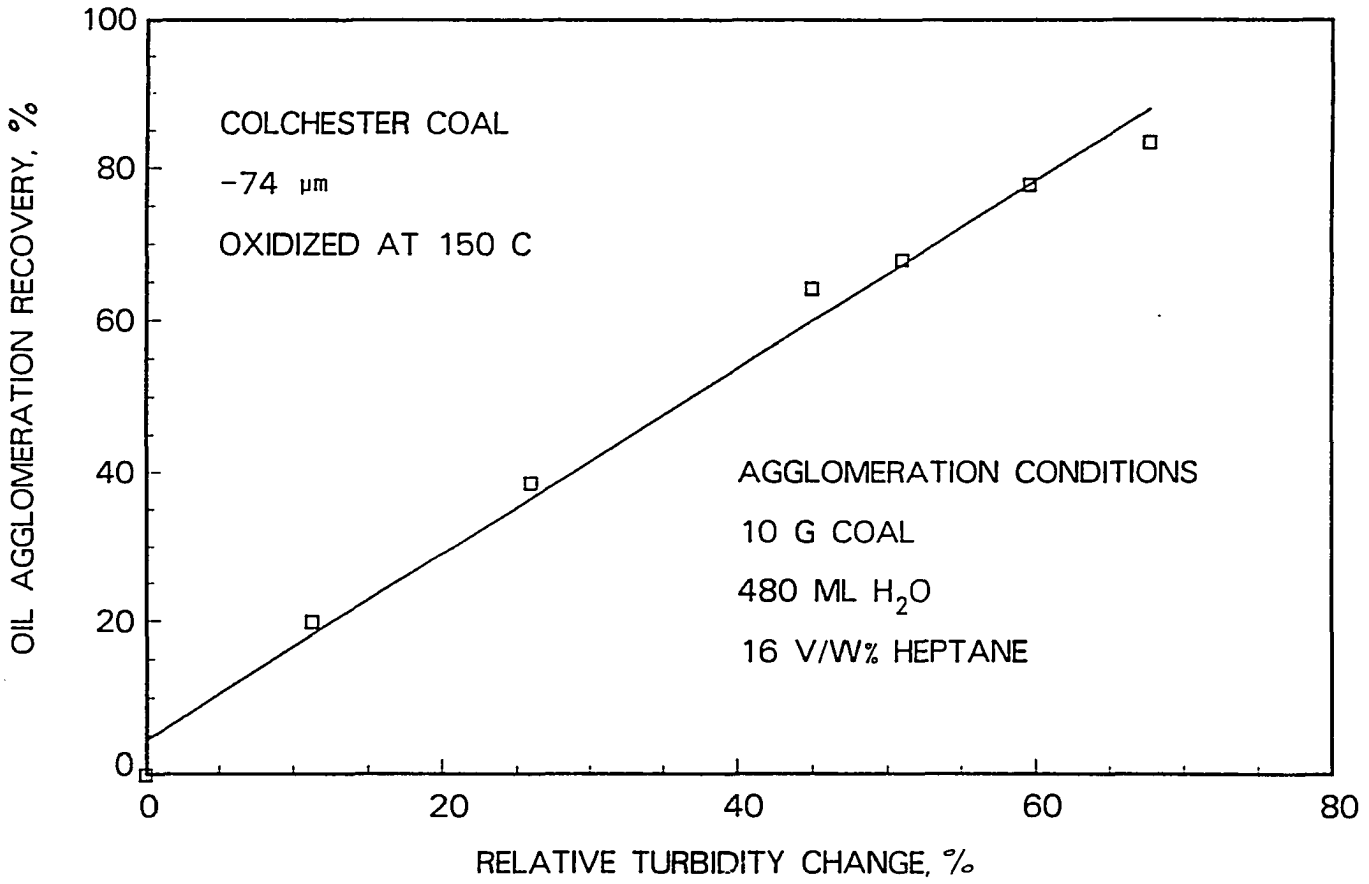

Figure 4.9: Correlation of the oil agglomeration recovery with the relative turbidity change for oxidized Colchester coal

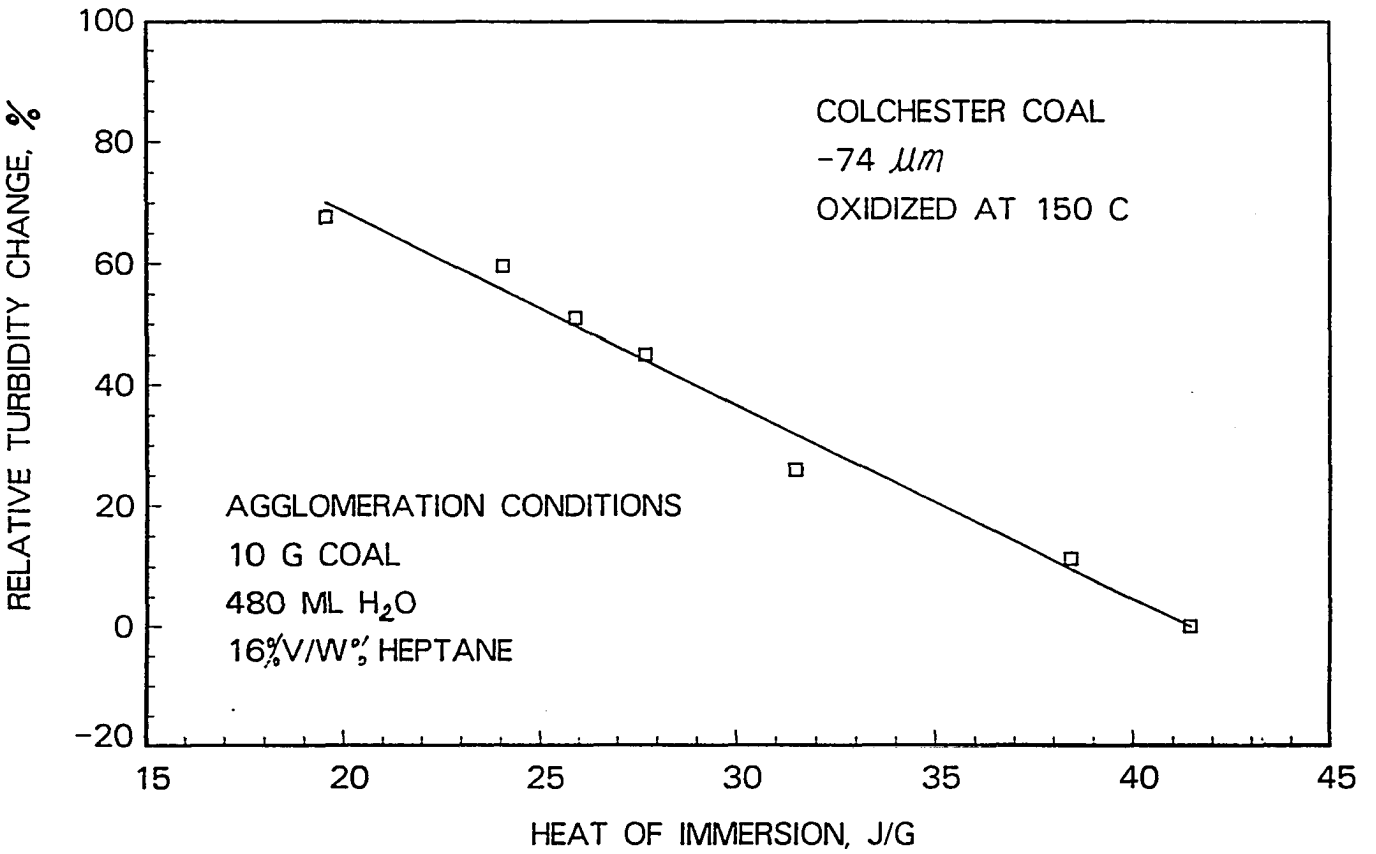

Figure 4.10: Correlation of the relative turbidity change with the heat of immersion for Colchester coal

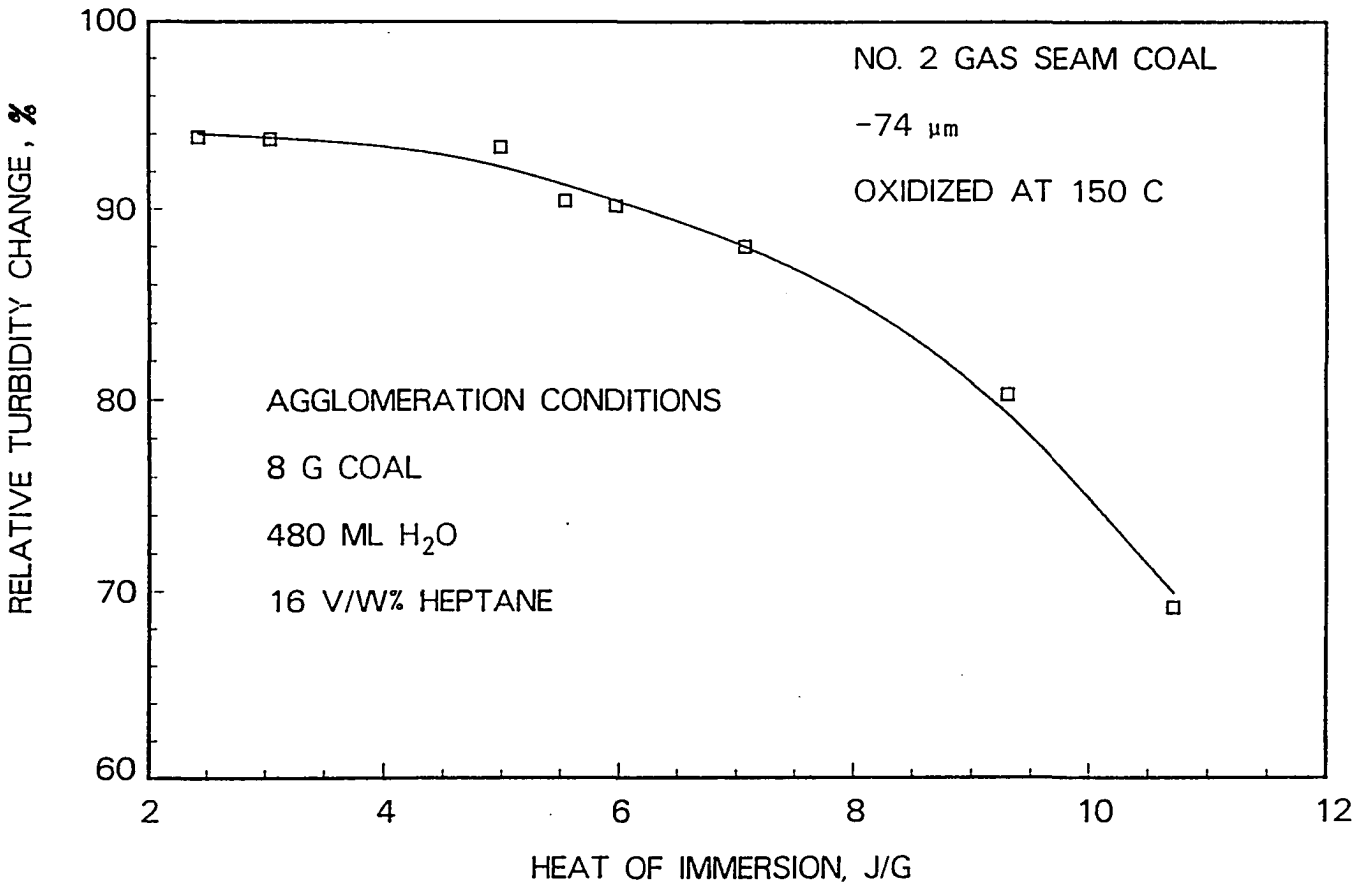

Figure 4.11: Correlation of the relative turbidity change with the heat of immersion for No. 2 Gas Seam coal

instrument and, therefore, it may also provide a way to control an industrial process.

The relationship between the relative turbidity change and the heat of immersion is shown in Figures 4.10 and 4.11, respectively, for the two coals. The relative turbidity change appeared to be inversely proportional to the heat of immersion for Colchester coal. However, for No. 2 Gas Seam coal the relationship between the relative turbidity change and heat of immersion was different. It is seen in Figure 4.11 that when the heat of immersion was small, the relative turbidity change decreased very gradually with increasing heat of immersion, but when the heat of immersion was high the heat of immersion decreased sharply. Since No. 2 Gas Seam coal was very hydrophobic originally, its response to oil agglomeration in the initial oxidation period suggests that there is a range of coal hydrophobicity in which the oil agglomeration recovery is not affected greatly by changes in surface hydrophobicity. Only when hydrophobic of coal was reduced beyond this range, did the surface properties have a significant effect on oil agglomeration recovery. On the other hand, Figure 4.10 shows that the oxidized Colchester coal which had a heat of immersion of 41.5 J/g did not respond to oil agglomeration. Therefore, there seems to be a a lower limit of hydrophobicity beyond which oil agglomeration is not possible. This range can be expressed quantitatively by heat of immersion. And this range will vary with oil agglomeration conditions such as oil type, dosage, coal particle size, and so on.

CHAPTER 5. MODIFICATION OF THE SUCTION POTENTIAL METHOD FOR THREE-PHASE CONTACT ANGLE MEASUREMENT

Review of Previous Work

In principle, almost all the methods for measuring the contact angle on a flat solid surface in a liquid-air-solid system can be applied to an oil-water-solid system to determine the three-phase contact angle. However, it has been questioned whether the contact angle measured on a polished flat coal surface will represent an actual coal surface[52]. Previous studies have shown that contact angle measurements are strongly influenced by variables such as mineral inclusions, petrographic constituents and sample preparation. Additionally, the porosity and surface roughness of the coal are important. Such studies have led at least one group to conclude that contact angles measured on polished coal surfaces may have very little relevance to the natural coal surface [52].

Many attempts have been made to measure contact angles of coal particles and even to conduct measurements on particles which may be representative of the coal separation processes [52]. Wei [53] et al. tried to measure the contact angle for individual particles using the interfacial partitioning method for a water-air-solid system. The merit of this method is that it can give the distribution of contact angles

of individual particles, therefore may give a good prediction of what the maximum separation efficiency would be. On the other hand, as the measured contact angle varies with the orientation of a single particle, and also varies from particle to particle, in order to get a statistically representative contact angle distribution for a portion of a sample, measurements must be conducted for different orientations of many particles. It may be very time consuming and expensive considering the machine time for the image analyzer.

One method which overcomes many of these problems directly measures the contact angle on ground coal particles; it is the so-called suction potential method or capillary suction method. It was first developed by Bartell and Osterhof [46] in 1927 and later modified by others [47] [48]. The method Bartell established for measuring contact angles on rough particles consisted of compacting the particles in a bed contained in a sample holder, measuring the pressure required to force a given liquid into or out of the bed, and comparing the pressure with that required to force a liquid of known contact angle into or out of the bed.

The bed of powder is assumed to resemble a bundle of equal cylindrical capillary tubes of radius, r. The pressure required to force a liquid having a surface tension, γ_1, and a contact angle, θ_1, into the bundle is:

$$P_1 = \frac{2\gamma_1 cos\ \theta_1}{r} \tag{5.1}$$

Usually the liquid of known contact angle is chosen as one that wets the solid so that the contact angle is zero. For this liquid the preceding equation reduces to the following:

$$P_2 = \frac{2\gamma_2 cos\ \theta_2}{r} = \frac{2\gamma_2}{r} \tag{5.2}$$

Bartell made the assumption that the porous medium consists of uniform cylindrical capillary tubes, all with the same radius. Hence, dividing Equation 5.1 by Equation 5.2 gives the contact angle of liquid 1 on the solid particles:

$$\frac{P_1}{P_2} = \frac{\gamma_1 cos\ \theta_1}{\gamma_2} \tag{5.3}$$

$$cos\ \theta_1 = \frac{P_1}{P_2}\frac{\gamma_2}{\gamma_1} \tag{5.4}$$

A modified version of the suction potential method was developed by Bailey and Gray [48] and their apparatus is shown in Figure 5.1. This version has been used to study dewatering and drying of coal, soil, and other minerals. Although it was considered to be a useful method, it did not gain wide use for many years, probably due to its time consuming nature. It was a common complaint of former workers that it took a very long time for a single measurement because of the slow approach to equilibrium [49]. Many days might be necessary [49] to finish a single measurement. Besides being time consuming, it was also a difficult method to use [52]. Yet it attracted the attention of research workers at the University of Nottingham [51][50] during the last decade. Brookes and Bethel [51] measured the three-phase contact angle for the oil-water-coal system. N-hexane was used as the immiscible oil. Diamine was added to the coal-water slurry before the measurement to study the effect of diamine dosage on the receding contact angle of water on coal. Handfield-Jones [50] used this method to measure the three-phase contact angle for coal and shale. Both Brookes and Bethel, and Handfield-Jones used the same version. Recently, Hanning and Rutter [52] measured the three-phase contact angle for four types of coal by this method. The data obtained was compared with that obtained by a bubble-particle attachment method. In the last few years, Ayat [54] also used this method to measure

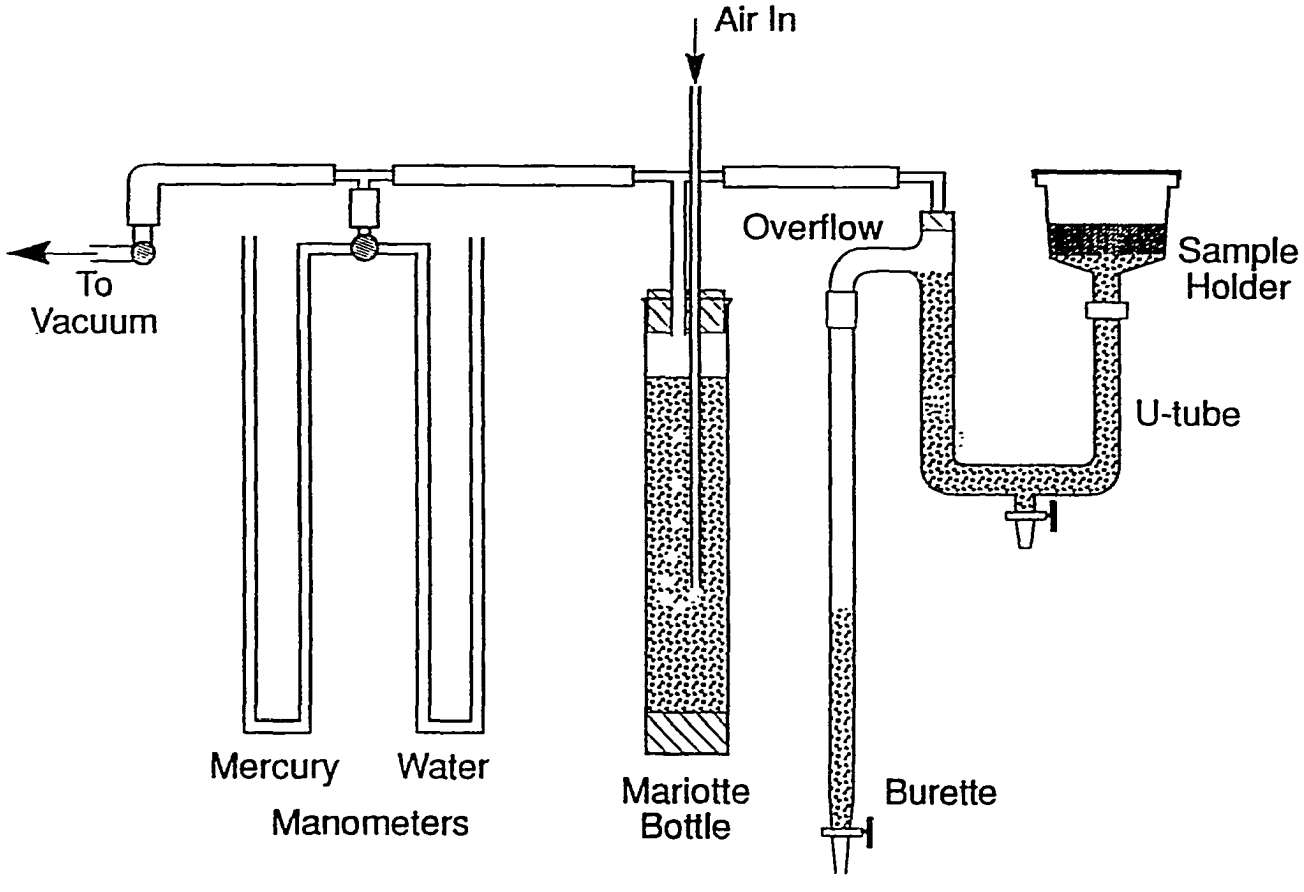

Figure 5.1: The suction potential apparatus, after Bailey and Gray[48]

the three-phase contact angle with a coal-water-n-hexane system and found that the three-phase contact angle measured through the water phase increases with carbon content for various rank of coal.

Modification of the Apparatus

Figure 5.2 illustrates the three-phase contact angles for oil and water in an ideal capillary. It should be noted that the contact angles are expressed as receding contact angles. $\theta_{o/a}$ is the receding contact angle of oil on coal, while $\theta_{w/o}$ is the receding contact angle of water on coal in the presence of oil. For water-oil and oil-air interfaces, the capillary equation may be stated respectively as:

$$P_{w/o} = \frac{2\gamma_{w/o} cos\ (\theta_{w/o})_R}{r} \tag{5.5}$$

$$P_{o/a} = \frac{2\gamma_{o/a} cos\ (\theta_{o/a})_R}{r} \tag{5.6}$$

Eliminating r leads to the following expression assuming that the receding contact angle $(\theta_{o/a})_R$ is zero, which is almost certainly the case provided a suitable paraffin oil is selected:

$$cos\ (\theta_{w/o})_R = \frac{P_{w/o}}{P_{o/a}} \frac{\gamma_{o/a}}{\gamma_{w/o}} \tag{5.7}$$

Note that the advancing contact angle for the oil phase measured through the oil phase in the presence of water, $(\theta_{o/w})_A$, is related to the receding contact angle for the water by the following equation:

$$(\theta_{o/w})_A = 180 - (\theta_{w/o})_R \tag{5.8}$$

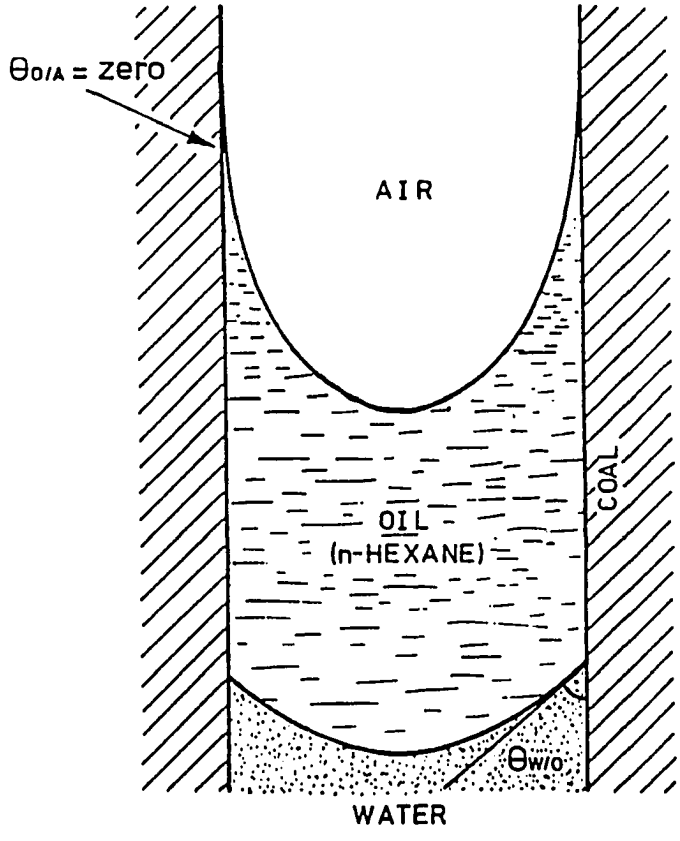

Figure 5.2: The simplified model for three-phase contact angles in an ideal capillary, after Handfield-Jones[50]

The oil advancing contact angle $(\theta_{o/w})_A$ can then be calculated from:

$$cos\ (\theta_{o/w})_A = -\frac{P_{w/o}}{P_{o/a}}\frac{\gamma_{o/a}}{\gamma_{w/o}} \tag{5.9}$$

As the oil advancing contact angle, $(\theta_{o/w})_A$, is directly related to oil displacement of water(or oil spreading against water) on a coal surface in the oil agglomeration process, the suction potential method may be a useful method for predicting oil agglomeration performance. Initially the same version of the suction potential apparatus used by Bailey and Gray [48] (see Figure 5.1) was used in this study. To determine the contact angle, a volume-suction potential curve as shown in Figure 5.3 must be obtained to give values of $P_{w/o}$ and $P_{o/a}$. The traditional method is to set a suction pressure at a value P_i, then read the volume of water drained into the burette after the flow of water has almost stopped. A preliminary experimental test indicated that this method has two major disadvantages as the former workers claimed. One is that it is time consuming. It usually takes 40-60 min. to achieve nearly a stable volume reading. To obtain a complete curve as in Figure 5.3, it usually takes 16-20 hr. The other disadvantage is that it is not easily controlled. The pressure increments must be very carefully selected in order to obtain a complete volume-suction potential curve. If the pressure increment is too big, some important points may be missed and then it is not possible to determine $P_{w/o}$ or $P_{o/a}$. On the other hand, if the pressure increment is very small, the number of readings will be too large and consequently the total time for one run will be excessive .

After careful examination (see Appendix A), the apparatus and method of operation were modified to overcome the above disadvantages. The modified apparatus is shown in Figure 5.4. A pressure adjustment tube and a stop cock were added to

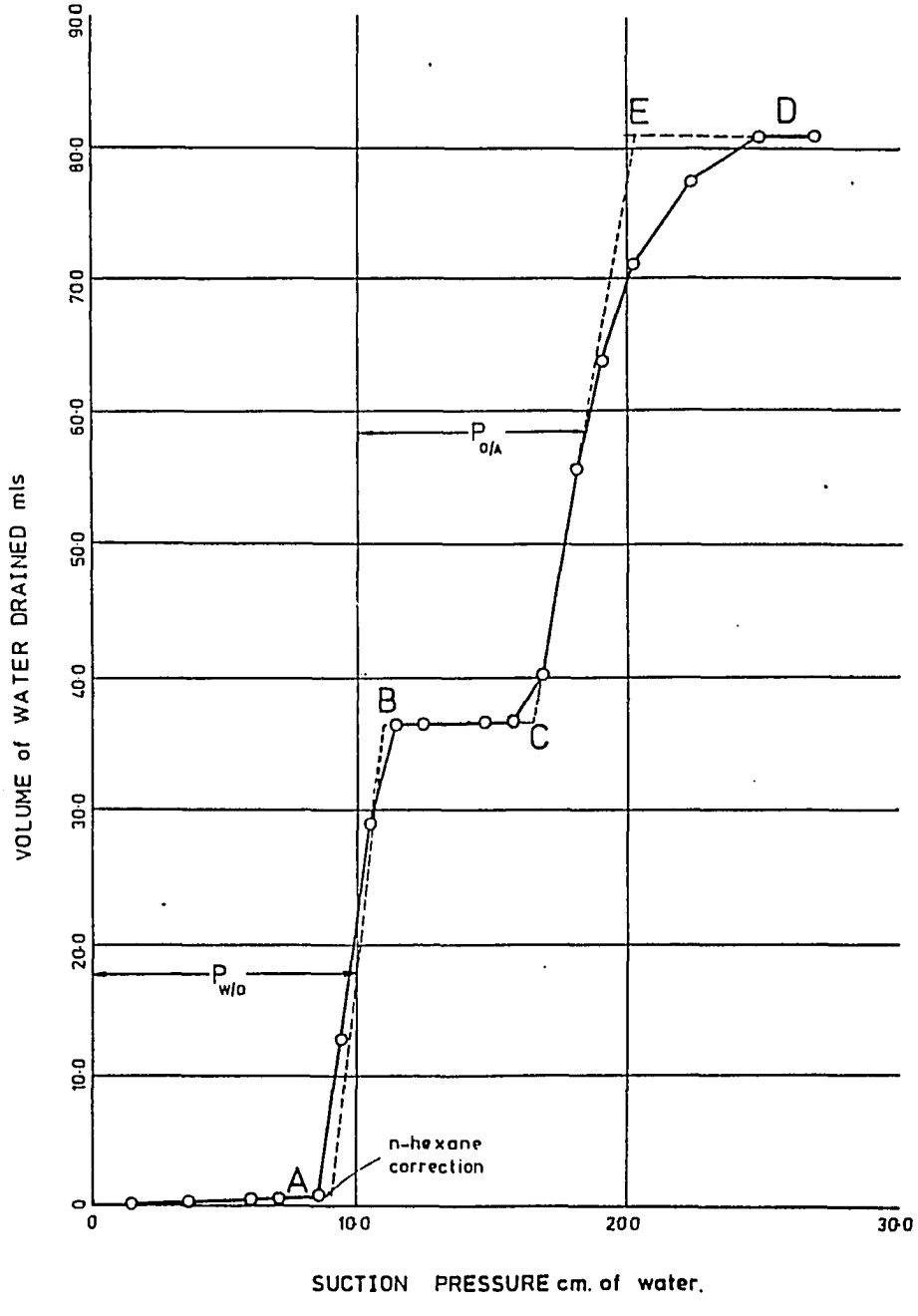

Figure 5.3: Typical volume-suction potential curve, after Handfield-Jones[50]

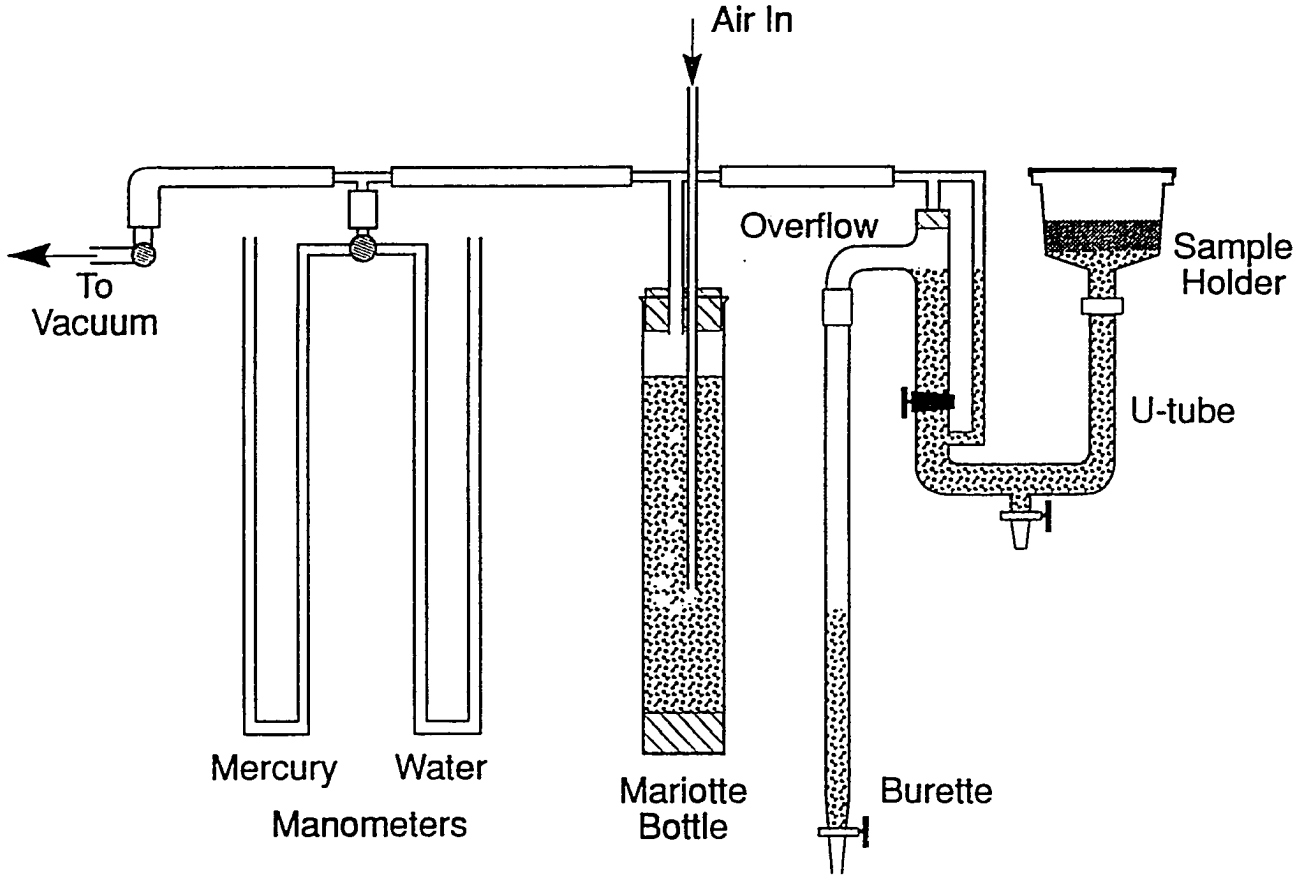

Figure 5.4: The mo lified suction potential apparatus

one side of the U-tube. The operation was modified by setting the volume instead of the pressure to obtain a point for the volume-suction potential curve. As it is easy to estimate the whereabouts of an equilibrium point on the curve from the volume, this makes the measurement controllable. Consequently, the number of points can also be reduced. Once the volume is set, the flow of water into the burette is stopped by turning the stop cock, and the pressure adjustment tube will balance the pressure and the pressure will quickly approach a stable point. Then a pressure reading can be taken. Normally, the time needed to reach a stable point is only 5-15 min. The time required for a complete run is only 2.5 to 3 hr. THe theoretical comparison of time required to reach a equilibrium point by the original and modified technique was shown in Appendix B.

Operating Procedure of Three-phase Contact Angle Measurement

The following standard operating procedure was established for the modified suction potential method:

1. Wash the sample holder, U-tube, and leveling tube with Nochromix and sulfuric acid, and rinse these pieces many times with tap water and deionized water. When washing the sample holder, fill the sample holder with wash liquid half-way above the sintered plate and then place it in a beaker and allow the wash liquid to flow through the sintered plate slowly. After 8 - 10 hrs of soaking, rinse the sintered plate with tap water and deionized water.

2. Fill the U-tube with deionized water, connect the sample holder to the U-tube, and fill the lower part of the sample holder with deionized water. Be sure that

there is no air trapped below or inside the sintered plate of the sample holder. Maintaining the water level in the sample holder slightly above the sintered plate can prevent air from collecting in the sintered plate.

3. Wet 40 - 50 g coal of a certain size fraction(M×N mesh) with deionized water in a beaker. Pour the slurry on an N mesh screen and wash off the fines with deionized water. Collect the particles above the screen and transfer them to a three-neck flask together with 200 ml water. Then degas the slurry for 20 min. by applying a vacuum of 28 in. Hg while stirring. This should get rid of the air on the coal surface. When the degassing is completed, transfer the slurry back to the beaker. The coal is allowed to settle, and the supernatant is removed by decantation to get rid of the fines produced by stirring. The coal is resuspended in deionized water.

4. Transfer the coal slurry to the sample holder and fill the sample holder with deionized water. Carefully stir the slurry and allow the coal particles to settle while tapping the rim of the sample holder gently to level and smooth the top surface of the coal bed. Skim off the floating particles with a piece of filter paper.

5. Apply suction to the sample holder to drain some water from it, and allow the water to overflow the U-tube and pass into the burette. Stop draining when the surface of the water in the sample holder is about 2 cm above the coal bed. Pipette 5 - 7 ml oil onto the water surface and cover the sample holder with a piece of filter paper and a glass plate. The coal bed should not be disturbed when pipetting oil onto the water.

6. Close the stop cock on the left side of the U-tube and allow the water in the leveling tube to balance the pressure. When the water level in the leveling tube reaches a stable value, the pressure in the system is considered equilibrated. Read the volume of water in the burette and the water manometer, and the water height in the leveling tube. The so-called suction pressure can then be calculated by means of the following equation:

$$\Delta P = h_l - h_r - (h - h_a)$$

where h_l and h_r are the heights of water in the left and right side of the manometer respectively, h_a the height of water in the leveling tube when the stop cock is open, and h the height of water in the leveling tube when equilibrium is reached.

7. After taking all the readings at one equilibrium point, open the stop cock and drain more water from the sample holder and allow another equilibrium point to be reached. Repeat the procedure described in step 6. Keep repeating this procedure until a complete ΔV versus ΔP curve is obtained as shown in Figure 5.3. Obtain at least three points for each stage.

Comparison of the Old Technique and the Modified Technique

After modifying the method for measuring the three-phase contact angle, the three-phase contact angle for oil-water-coal system was measured using both the old technique and the modified one in order to compare the reliability and reproducibility of the two methods.

The three-phase contact angle of Upper Freeport coal of 40/70 mesh size was measured using the old technique and the modified technique and using n-heptane as the oil phase. The contact angle was calculated from Equation 5.4. The contact angle determined by the old technique was 47.1 $\pm$ 0.7 degree, while the contact angle determined by the new technique was 48.2 $\pm$ 0.3 degree. The contact angle for the same coal of a narrower size fraction , 45/70 mesh, was determined by the modified technique to be 54.9 $\pm$ 0.3. These results indicate that the contact angles determined by these two techniques are very similar and that either technique is reproducible. However, the old method required 18 - 20 hr and much experience in setting the pressure increments. If by chance the pressure increment was set too large, the whole measurement would become useless. On the other hand, the modified technique only required about 3 hr.

CHAPTER 6. THE THREE-PHASE CONTACT ANGLE OF COAL AND ITS COMPARISON WITH OTHER SURFACE PROPERTIES

Introduction

It has been shown in Chapter 5 that the modified suction potential technique can be used to measure the three-phase contact angle of coal particles in an oil-water-coal system. This angle is a direct indication of the ability of oil to displace water from the coal surface. However, to make use of the three-phase contact angle for oil agglomeration process development, several related questions must be answered. These questions include: How will the coal compositions affect the contact angle value? Will the contact angle change with coal particle size? How will the three-phase contact angle correlate with the heat of immersion and hydrophilicity index? Above all, how it is correlated with oil agglomeration recovery?

In this chapter, measurements of the three-phase contact angles were made for graphite and for coals of different rank and for various particle sizes of coal. The three-phase contact angle is also reported for oxidized coal, and compared with the heat of immersion of coal in water, the hydrophilicity index calculated from the FTIR absorption spectrum and the oil agglomeration recovery.

Experimental

The coals used in this study were from several different sources as listed in Table 6.1. Their ash and total sulfur contents are listed in both Tables 6.1 and 6.2. The coals were crushed by a jaw crusher and a roll mill and screened to obtain the desired size fractions. The size fractions were collected and rescreened for 45 min to get rid of the fines.

The three-phase contact angle was measured following the operating procedure described in Chapter 5. Heptane or hexadecane was used as the oil phase since these materials were used in the oil agglomeration process.

The heat of immersion of coal in water and the hydrophilicity index were determined by the methods described in Chapter 4.

The oil agglomeration recovery of Upper Freeport coal from Pensylvania was determined by the following steps: prewet 10 g coal with 480 ml deionized water, stir for 5 min at 5500 rpm in a special closed mixing unit from which air is excluded (an air tight kitchen blender), and stir another 8 min after adding 4 ml heptane. Then pour the slurry onto a preselected screen, and collect both agglomerates and tailings. The agglomerates and tailings are dried in an oven at 120° for 4 hr and are weighed to determine the oil agglomeration recovery.

Colchester seam coal from Schuyler County, Illinois, was crushed and screened to obtain the -70/+100 mesh fraction. About 450 g of prepared coal was spread in a thin layer in four aluminum pans which were placed in an air convection oven set at 150°C. Periodically the material was mixed and riffled to obtain a set of samples. Each sample was characterized by measuring the three-phase contact angle, the heat of immersion in water at 25°C, the infrared absorption spectrum, and the recovery

of agglomerates with a given amount of hexadecane. The water receding contact angle was measured through the water phase for each sample by the modified suction potential method described above. The heat of immersion and hydrophilicity index were determined by the methods previously reported. A portion of each sample was suspended in water and agglomerated with hexadecane. The agglomerates were recovered on a 50 mesh screen while the tailings passed through the screen. Both agglomerates and tailings were dried overnight at $100 - 110^{\circ}C$ and weighed to calculate the recovery.

Results and Discussion

1. Three-phase Contact Angle vs. Rank and Ash Content of Coal

The three-phase contact angle was determined for graphite and several coals from different sources; the size fraction was chosen to be -45/+75 mesh. Heptane was used. The three-phase contact angle was measured through the water phase and calculated by means of Equation 5.7. Table 6.1 lists the experimental values of the contact angle. Graphite had the highest contact angle, while for other coals, the contact angle seemed to decrease with decreasing rank. The measured contact angle seemed to decrease with increasing ash content except for Illinois No. 6 coal. Illinois No. 6 coal had the smallest contact angle although its ash content was significantly lower than that for Upper Freeport coal and Pittsburgh No. 8 coal. Illinois No. 6 coal rank was the lowest and it would have had a higher oxygen functional group content than Upper Freeport coal. This would have accounted for the lower contact angle for Illinois No. 6 coal. This suggests that ash content is not the only factor which would affect the three phase contact angle of coal. Interestingly, Ayat [54]

Table 6.1: Source, rank, ash content and total sulfur content of coals and graphite, -45/+70 mesh size, and three-phase contact angle measured through water phase. Oil phase was heptane

Materials	Source	Rank	Ash, wt. %	Total sulfur, wt. %	Contact angle, degrees
Graphite	Sri Lanka		0.4	0	85.5± 0.8
No. 2 Gas Seam coal	West Virginia	High volatile A bituminous	2.9	0.76	61.6± 0.6
Upper Freeport coal	Pennsylvania	Medium volatile bituminous	17.9	2.02	41.6 ± 1.0
Pittsburgh No. 8 coal	Ohio	High volatile C bituminous	29.5	4.69	36.6± 1.0
Illinois No. 6 coal	Illinois	High volatile C bituminous	5.0	3.39	31.6 ± 0.5

did not find a good correlation between the ash content of coal and the three-phase contact angle in the hexane-water-coal system.

2. Three-phase Contact Angle vs. Coal Particle Size

There have been many studies reported in the literature about the dependency of contact angle on coal particle size [55]– [57]. Yet the fundamental reason for this dependency remains unclear.

Vargha-Butler et al. [55] used the advancing solidification front technique, an indirect method, to determine the critical solidification velocity of coal particles. The particle surface tension was subsequently calculated by using the measured critical solidification velocity of coal particles. Their results showed that the surface tension of coal particles increases with increasing particle size. This would have resulted in the decrease of contact angle with increasing particle size. They suggested that the decrease in contact angle with increasing particle size was due to an increase of inorganic matter in the coal. However, their results showed a very small variation of particle surface tension among coals of various ranks. Since the percentage change in inorganic mineral content among different sizes of coal particles was much smaller than that among coal particles representing different ranks, their explanation for the dependency of contact angle on coal particle size was not convincing. So far, no other study has addressed the dependency of the oil-water-coal, three-phase contact angle on coal particle size. In the present study, the three-phase contact angle was determined for Upper Freeport coal of various size fractions in the coal-heptane-water system and the results were listed in Table 6.2 along with the corresponding ash and total sulfur contents.

Table 6.2: Three-phase contact angle and oil agglomeration recovery of Upper Freeport coal with heptane. The oil dosage for agglomeration was 40 v/w %

Particle Size, mesh (U.S. Std.)	Average Size, micron	Ash, %	Total Sulfur, %	Contact Angle, degree	Oil Agglomeration Recovery, %
-20/+45	530	18.22	2.06	31.2 ± 1.7	69.7
-45/+70	280	18.09	2.02	41.6 ± 2.3	75.0
-70/+100	179.5	17.31	2.02	46.6 ± 2.2	82.6
-100/+200	111.5	17.64	2.05	59 ± 3	98.0

Figure 6.1 shows that the heptane-water-coal, three-phase contact angle measured through the water phase decreases with increasing particle size. This trend is similar to that calculated by Vargha-Butler et al. [55] for the liquid-air-coal system. However, Table 6.2 shows no significant difference in the ash and total sulfur contents among the different size fractions of coal. Therefore, the results were affected by some factor other than the mineral content. No convincing explanation has been found to explain the relationship shown in Figure 6.1. Perhaps the dependency of contact angle on particle size is due to an apparent difference in surface roughness for coal particles of different size. It has been shown that surface roughness [58] [59] has a dramatic effect on the contact angle. On the other hand, it has also been observed that smaller coal particles tend to have a more regular shape and are more spherical than are large particles. Also spikes are usually higher on larger particles than on smaller particles. Therefore, large particles probably have a rougher surface compared to smaller particles, resulting in a smaller contact angle. This coincides with the results of Brown et al. [63] as well who found that oil spread more easily on a highly polished surface than on a rough surface.

As shown in Figure 6.2, the oil agglomeration recovery of Upper Freeport coal with 40 v/w % heptane (10 g coal, 4 ml heptane) decreased with increasing average particle size in a manner similar to the decrease in contact angle shown in Figure 6.1. When the oil agglomeration recovery was correlated with the contact angle for Upper Freeport coal, a linear correlation was found (see Figure 6.3) which was represented by the following equation:

$$R = 34.77 + 1.04\theta$$

The correlation coeficient was large ($r^2 = 0.958$). This indicates that for the given

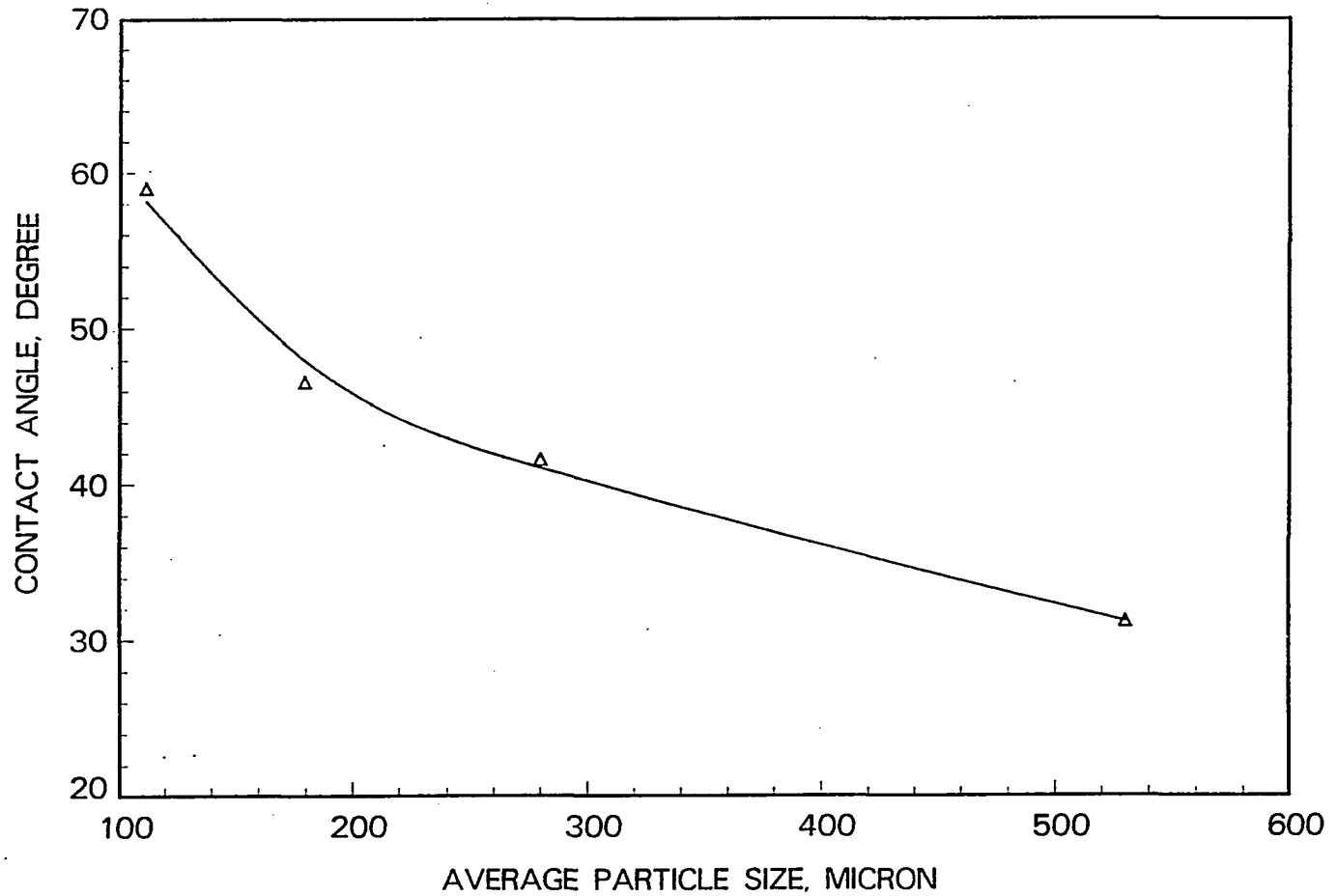

Figure 6.1: Correlation between three-phase (heptane-deionized water-coal) contact angle and average particle size of Upper Freeport coal from Pennsylvania

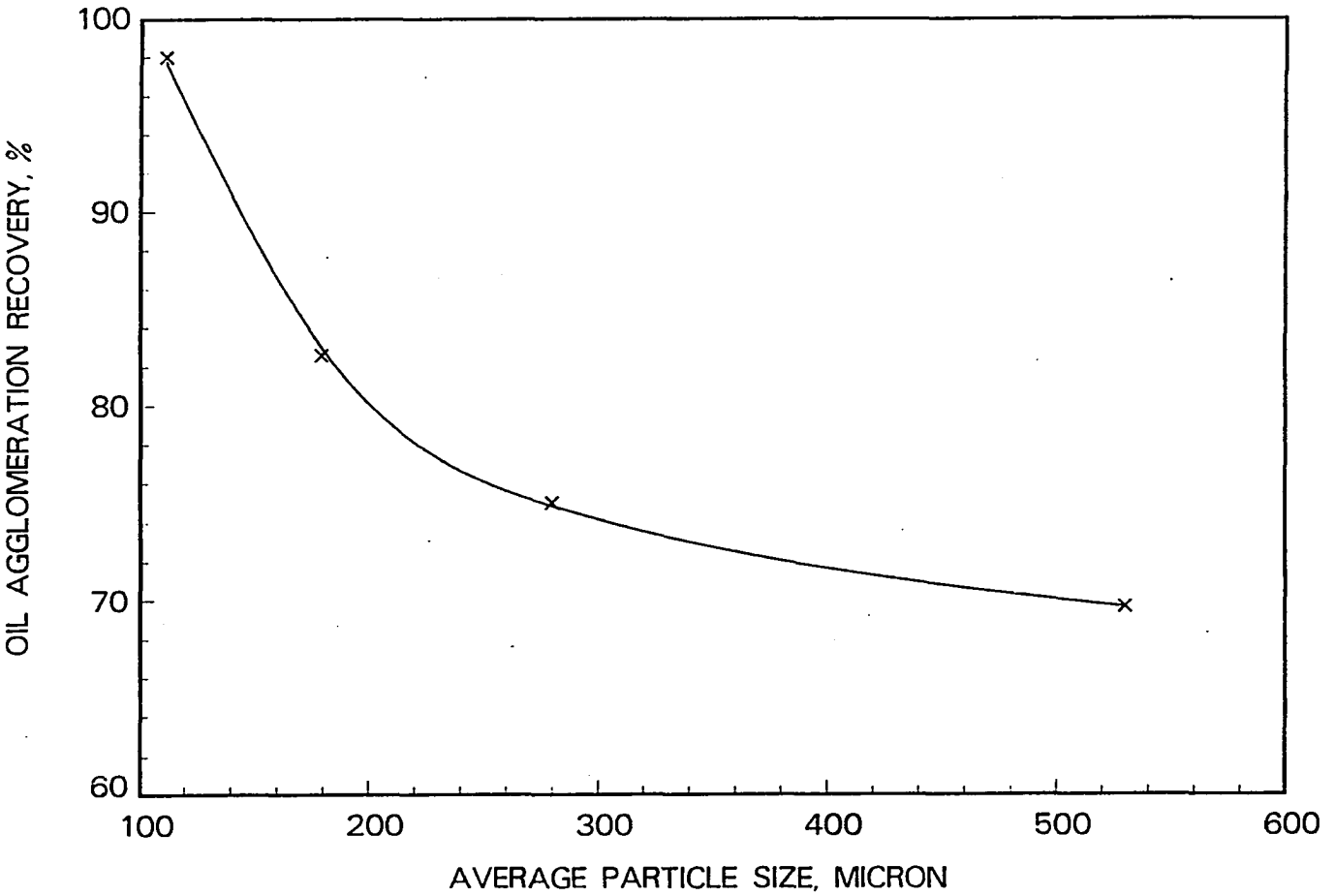

Figure 6.2: Correlation between oil agglomeration recovery with heptane and the average particle size of Upper Freeport coal from Pennsylvania

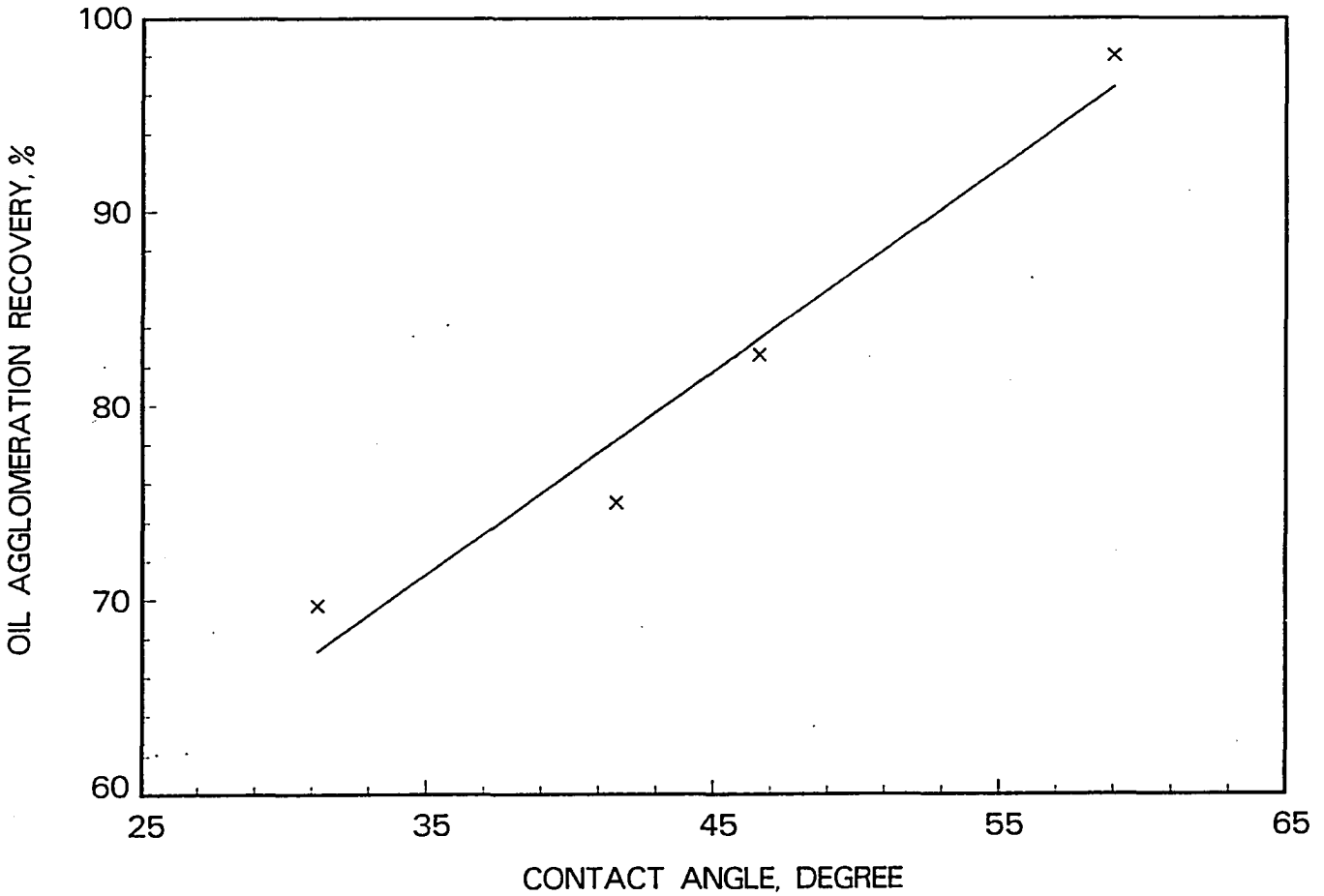

Figure 6.3: Correlation between oil agglomeration recovery with heptane and the three-phase (heptane-water-coal) contact angle for Upper Freeport coal from Pennsylvania

agglomeration conditions (stirring speed, oil dosage, etc.), the oil-water-coal, three-phase contact angle was a most important factor in determining the oil agglomeration recovery.

3. The Results of a Coal Oxidation Experiment

In order to compare and correlate the results of several different surface characterizatin methods, a sample of coal from the Colchester Seam in Schuyler County, Illinois, was oxidized in air at 150 °C. Small portions of the coal were collected at intervals and characterized by measuring the three-phase contact angle, the heat of immersion in water, and the FTIR absorption spectrum. In addition, the response of the coal to agglomeration was determined. Hexadecane was used for oil agglomeration and contact angle measurements.

a. Comparison of Different Surface Properties of Oxidized Coal

Figure 6.4 shows the change in the three-phase contact angle measured through the water phase, θ, with increasing oxidation time. The contact angle decreased from 78° for the raw coal to 25° for coal which had been oxidized for 72 hr; most of the change appeared to take place during the first 24 hr of oxidation. This indicates that the ability of oil to displace water from the coal surface decreased with increasing oxidation. In other words, the coal surface became less oleophilic with increasing oxidation time.

Figure 6.4 also shows that $\cos\theta$ increased as oxidation time increased. This pattern is very similar to the effect of oxidation on the heat of immersion in water and the hydrophilicity index calculated from the FTIR absorption spectrum (see Figures 6.5 and 6.6). Relative values of the hydrophilicity index and the other two

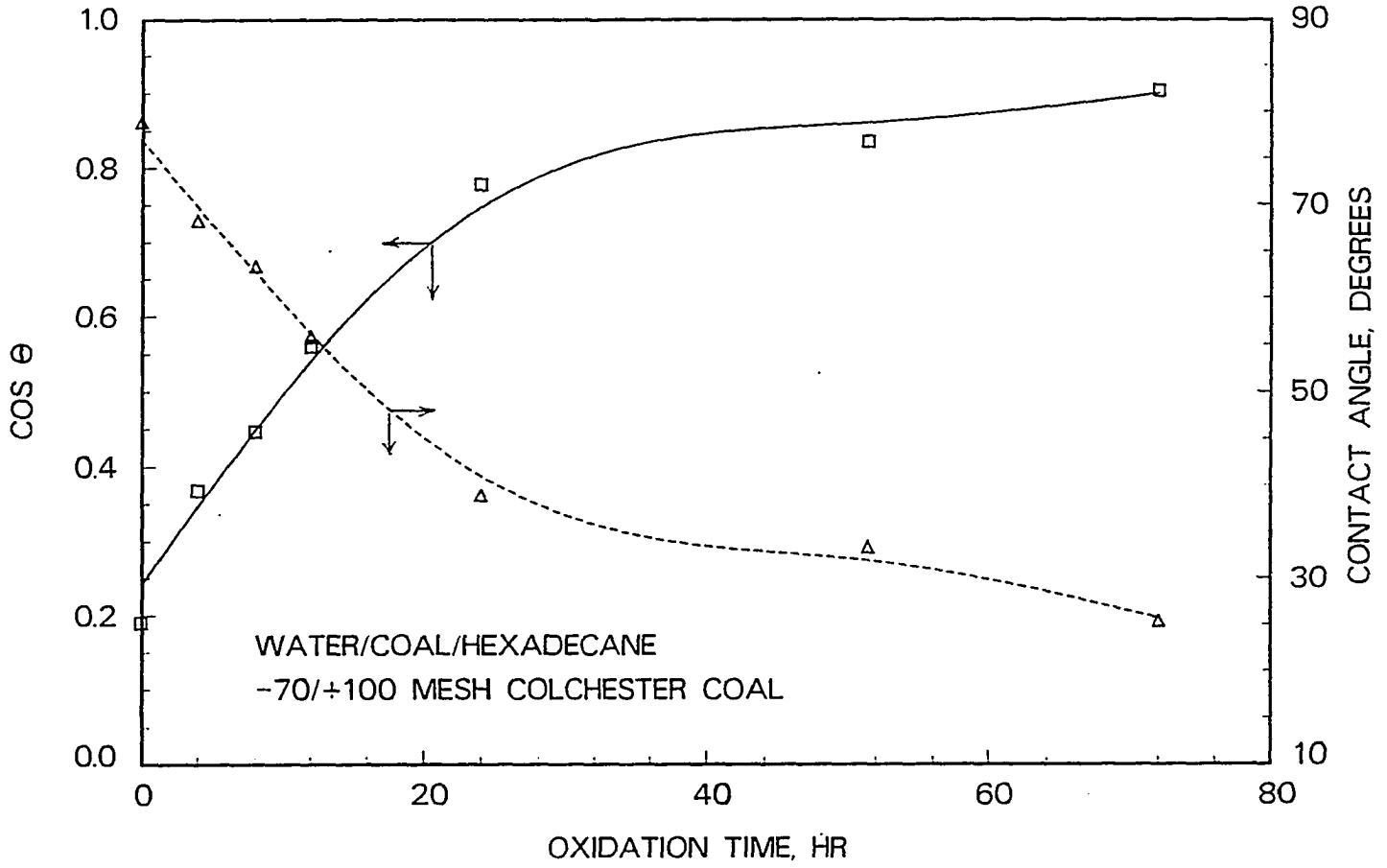

Figure 6.4: Effect of oxidation time on the three-phase contact angle for -70/+100 mesh Colchester coal

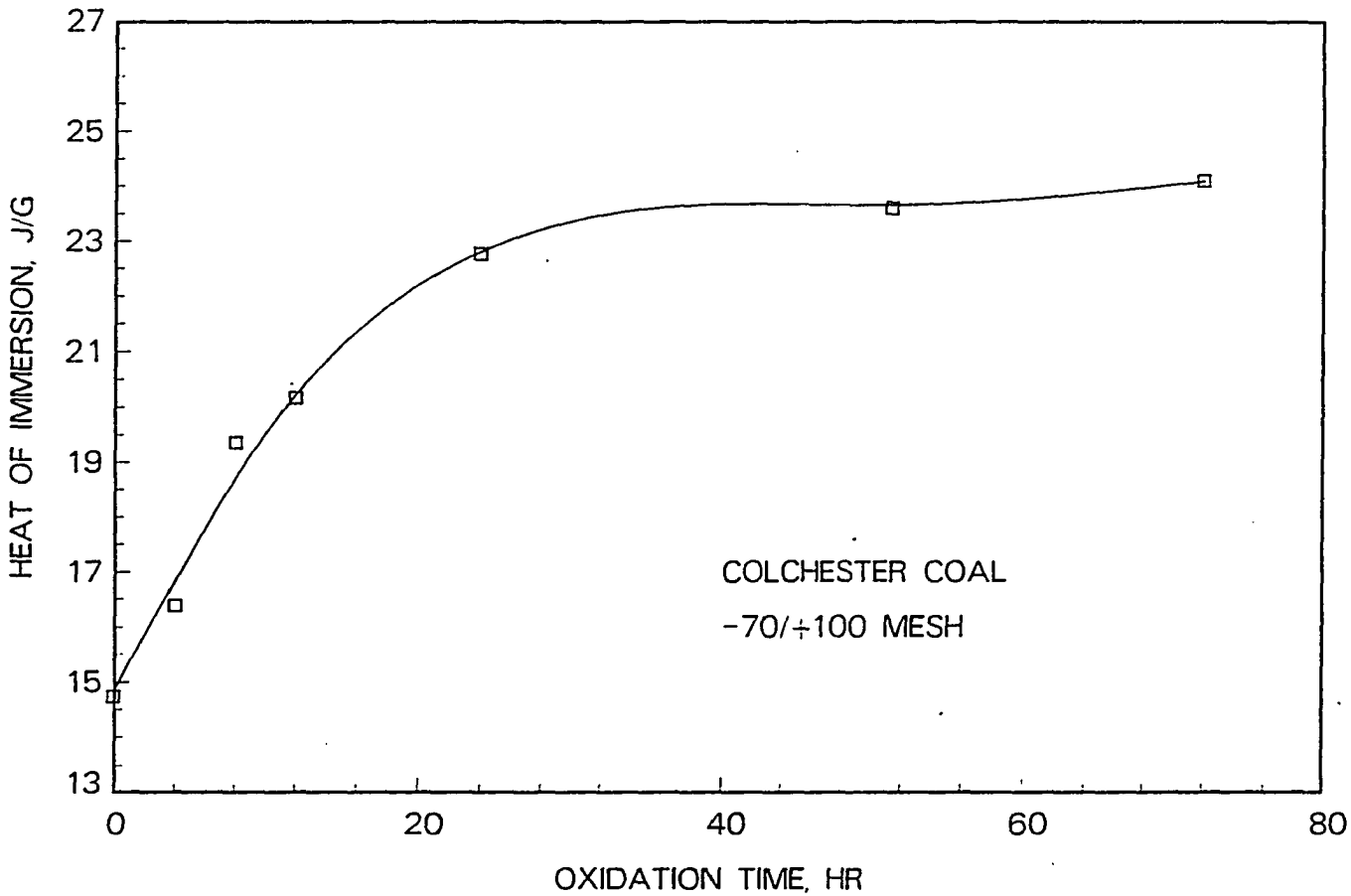

Figure 6.5: Effect of oxidation time on the heat of immersion of -70/+100 mesh Colchester coal

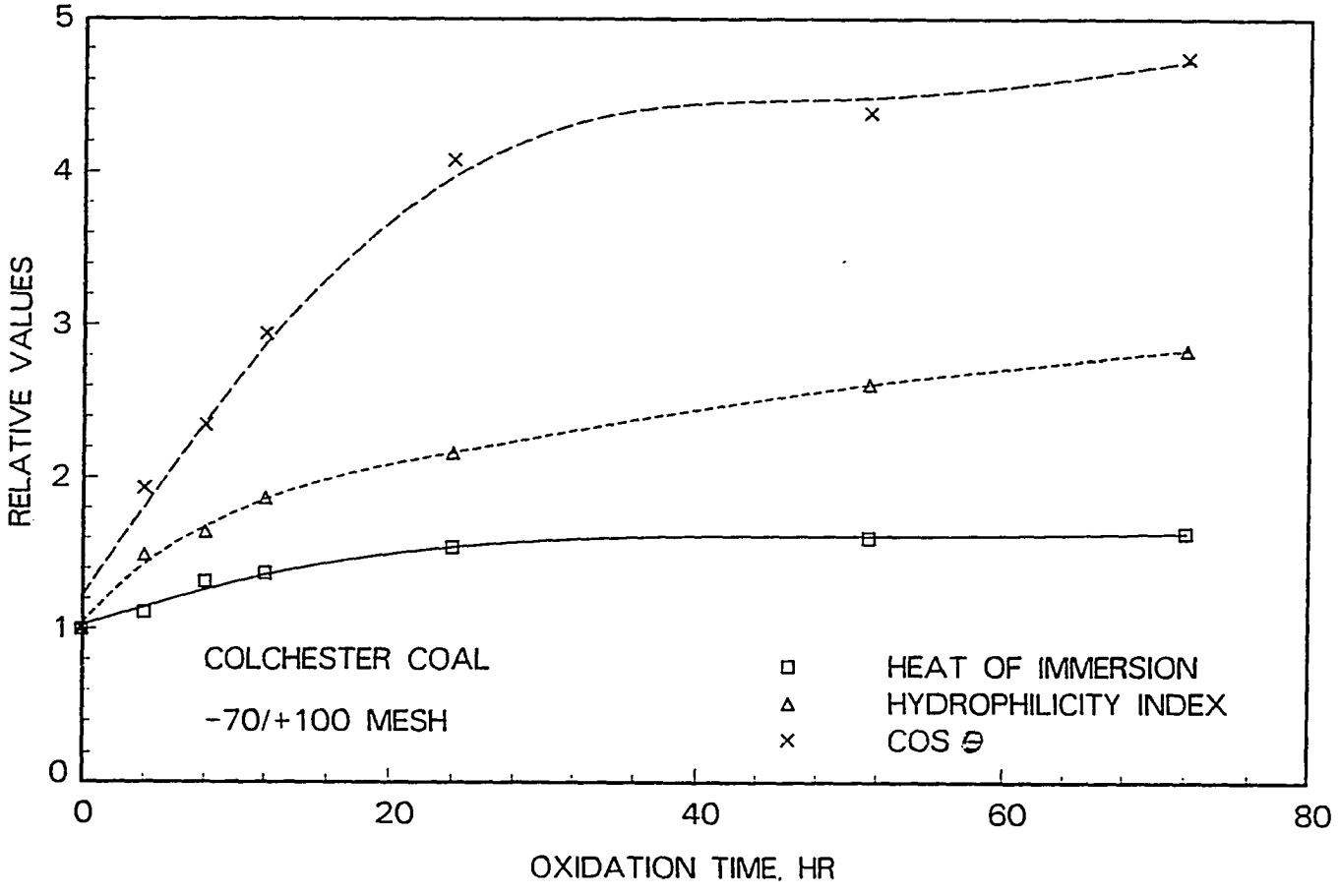

Figure 6.6: Relative values of the three different surface characteristics for -70/+100 mesh Colchester coal; oil phase was hexadecane.

surface properties described above are shown in Figure 6.6 as a function of oxidation time. The relative value of a given surface property is the ratio of the surface property for a particular oxidation time to its initial value. Figure 6.6 showed that the relative value of $\cos\theta$ increased the most and the relative value of the heat of immersion increased the least for any given time of treatment. This suggests that the three-phase contact angle may be more sensitive than the other surface properties to changes in the coal surface produced by oxidation. Therefore, $\cos\theta$ was compared with the heat of immersion in water and the hydrophilicity index. As shown in Figures 6.7 and 6.8, both the heat of immersion in water (ΔH) and the hydrophilicity index (H.I.) varied directly with $\cos\theta$. Linear regression analysis produced the following expressions:

$$\Delta H = 12.04 + 14.15\cos\theta \tag{6.1}$$

for which $r^2 = 0.977$ and

$$H.I. = 0.765 + 3.29\cos\theta \tag{6.2}$$

for which $r^2 = 0.966$. The heat of immersion in water also varied directly with the hydrophililicity index as shown in Figure 6.9. The correlation produced by the linear regression is shown below:

$$\Delta H = 9.11 + 4.17 H.I. \tag{6.3}$$

For this expression the correlation coeficient was again large (r^2 was 0.949).

Equation 6.1 relates the heat of immersion to the three-phase contact angle; that is, it relates the surface property of coal measured in a water-air-coal system to the surface property of coal measured in an oil-water-coal system. Equations 6.2 and 6.3 relate the contact angle and the heat of immersion in water to the relative concentrations of various organic functional groups on the coal surface. These results show that

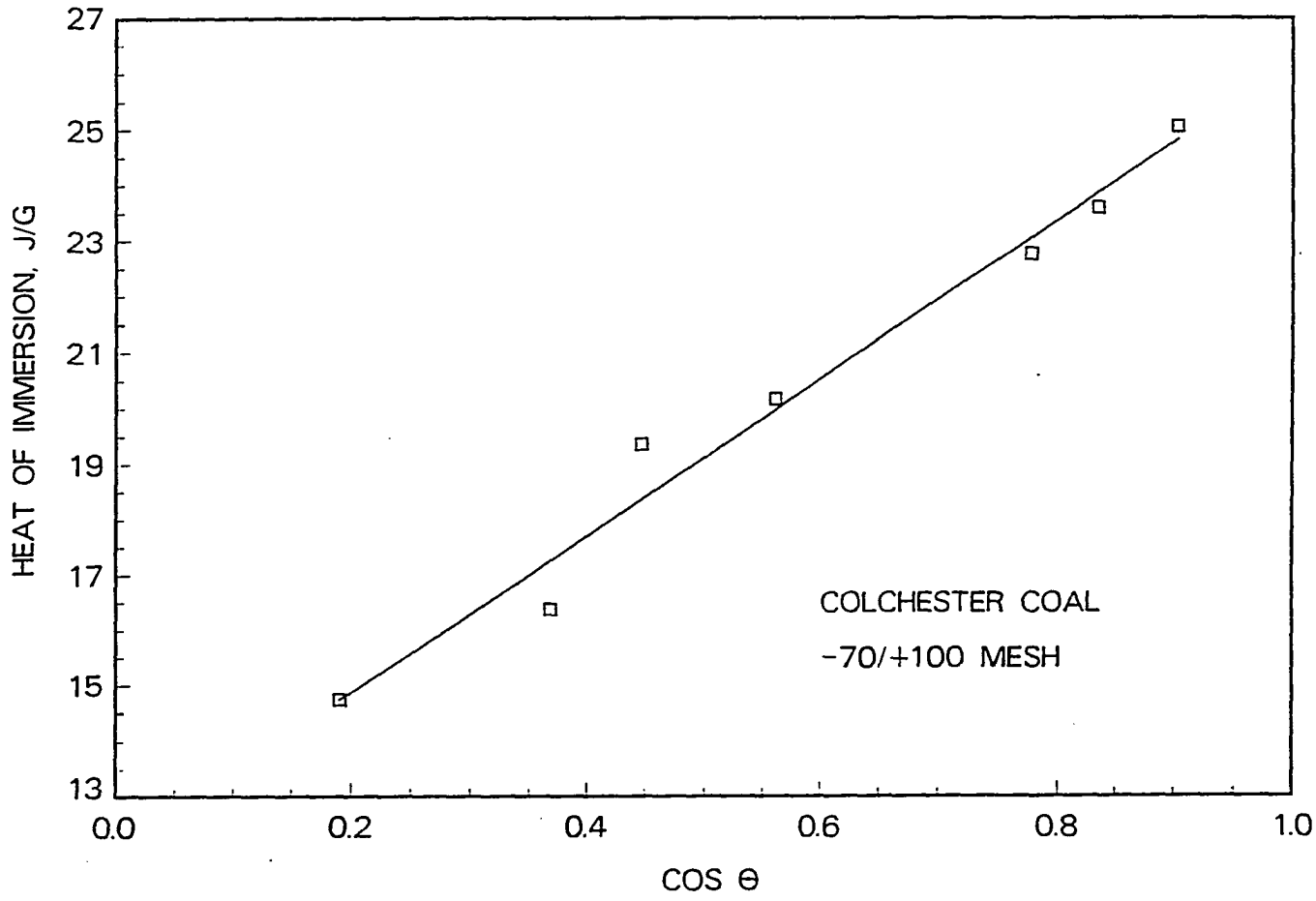

Figure 6.7: Correlation between the heat of immersion and $\cos\theta$ for -70/+100 mesh Colchester coal: oil phase was hexadecane.

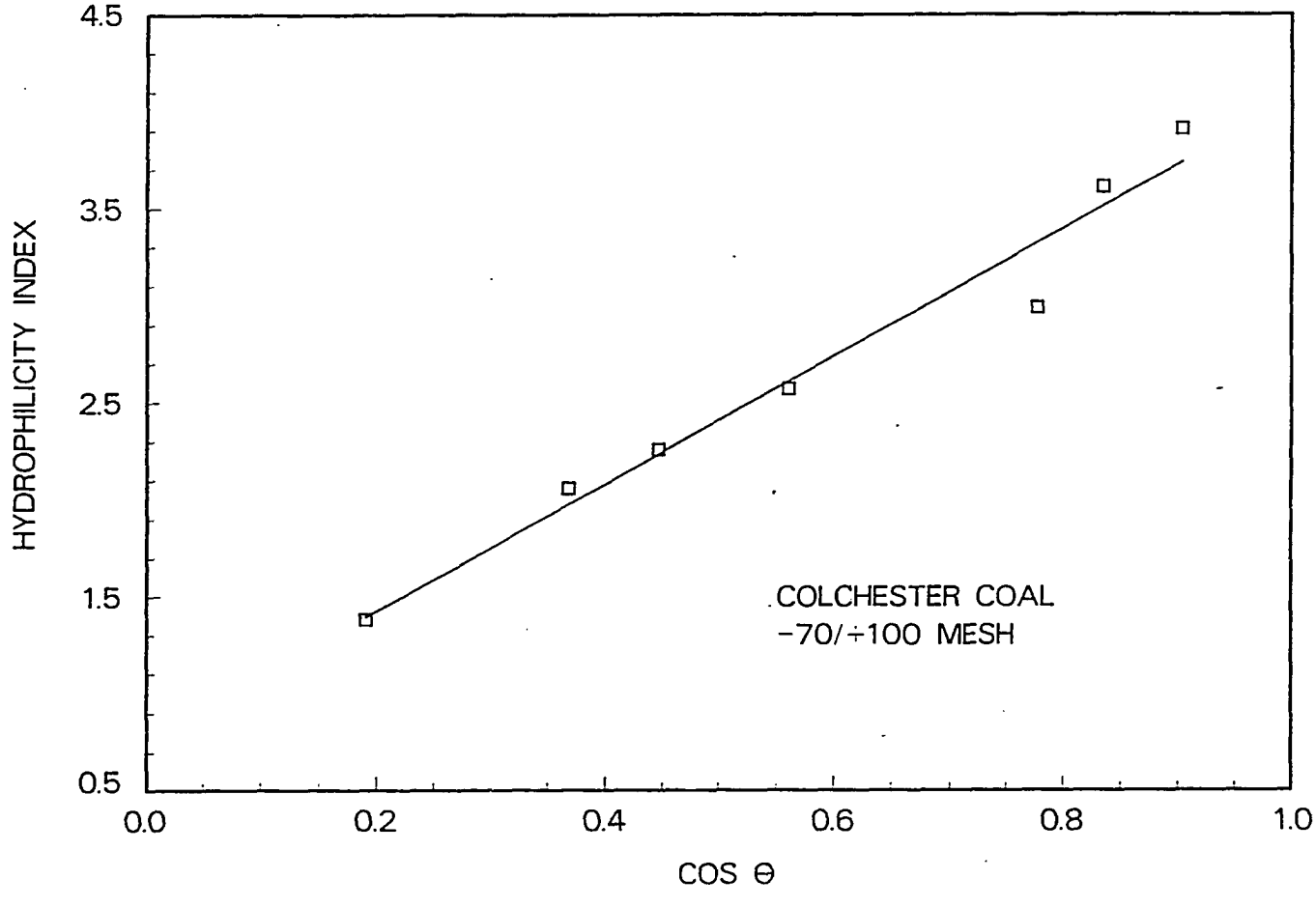

Figure 6.8: Correlation between the hydrophilicity index and $\cos\theta$ for -70/+100 mesh Colchester coal; oil phase was hexadecane.

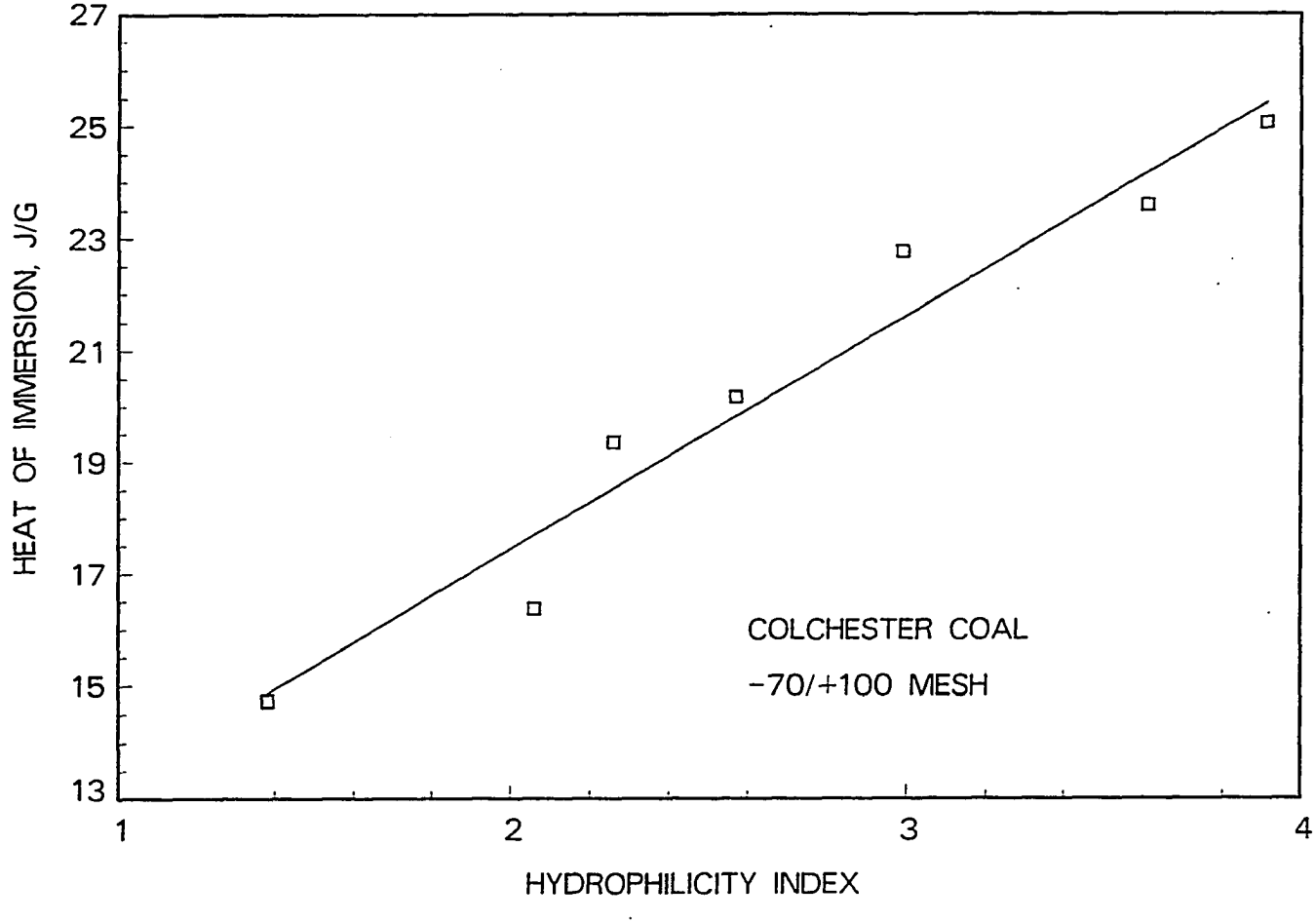

Figure 6.9: Correlation between the heat of immersion in water and the hydrophilicity index for -70/+100 mesh Colchester coal

the different surface characteristics are more or less equivalent or interchangeable for oxidized coal at a given particle size and moisture content.

b. Correlation between Oil Agglomeration Recovery and Surface Properties

The oil agglomeration recovery of oxidized Colchester coal was determined and correlated with each of the following surface properties: the three-phase contact angle (θ), $\cos\theta$, the heat of immersion in water, and the hydrophilicity index.

The results shown in Figure 6.10 indicate that oil agglomeration recovery increased with increasing contact angle. They also indicate that with increasing oxidation, the coal surface became less oleophilic, and it was more difficult for hexadecane to displace water from the coal surface. Therefore, during the oil agglomeration process, there would have been less tendency for oil droplets to attach to the oxidized coal particles which resulted in lower oil agglomeration recovery. The recovery of agglomerated coal was directly proportional to the three-phase contact angle for oxidized coal samples. When a straight line was fitted to the data by linear regression, the point corresponding to the raw coal was omitted since it did not appear to be in line with the others. These results suggest that the oil agglomeration recovery does not decrease significantly as a consequence of oxidation in the upper range of contact angle values. Although the contact angle decreased considerably during the first few hours of oxidation, it remained relatively large (above 70°). The tendency for oil to displace water from the coal surface was still strong enough for oil to readily attach to the coal particles, so the oil agglomeration recovery remained high. This phenomenon is very similar to what was observed previously with No. 2 Gas Seam

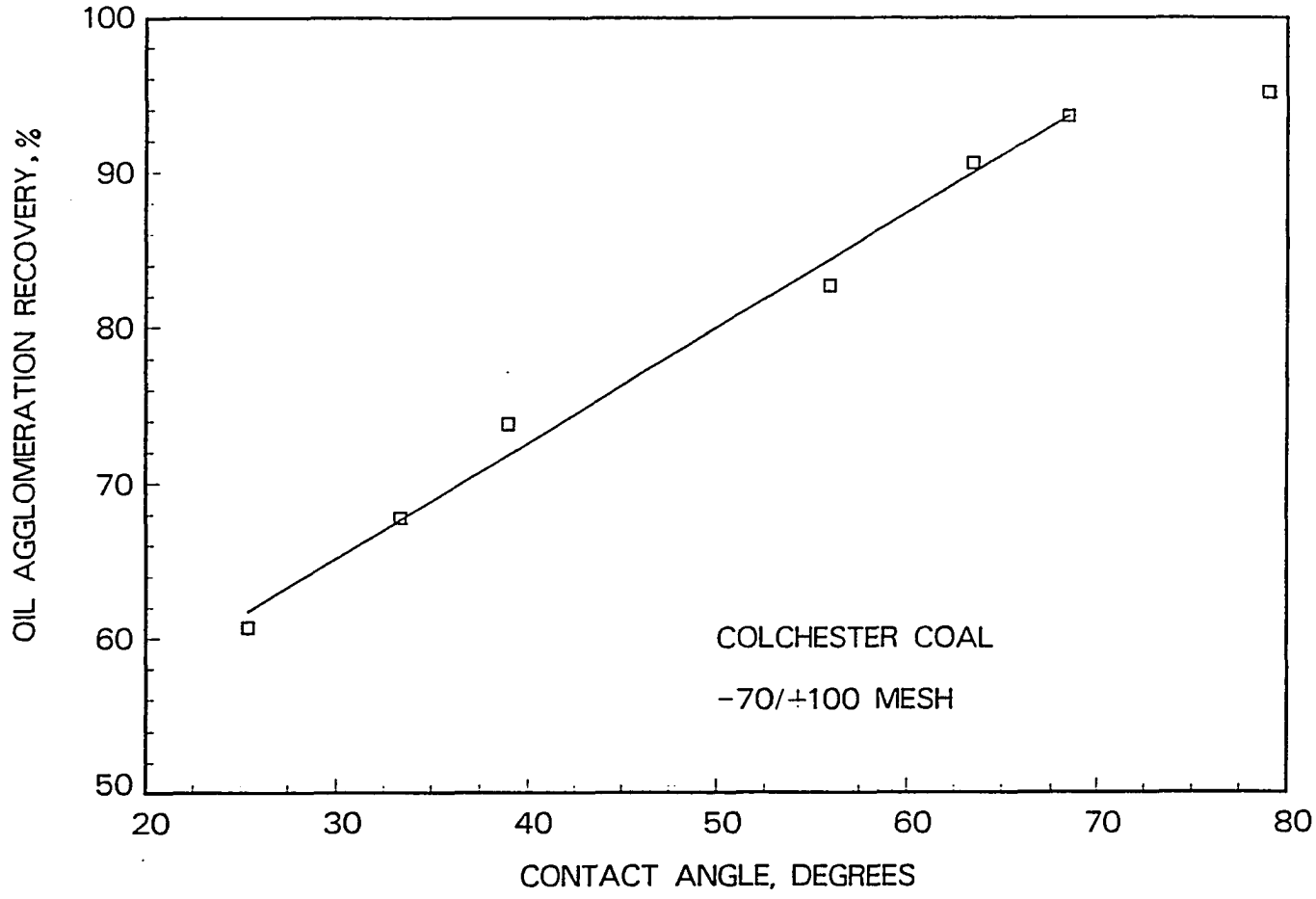

Figure 6.10: Correlation between oil agglomeration recovery and the three-phase contact angle for -70/+100 mesh Colchester coal, 20 v/w % hexadecane added for agglomeration

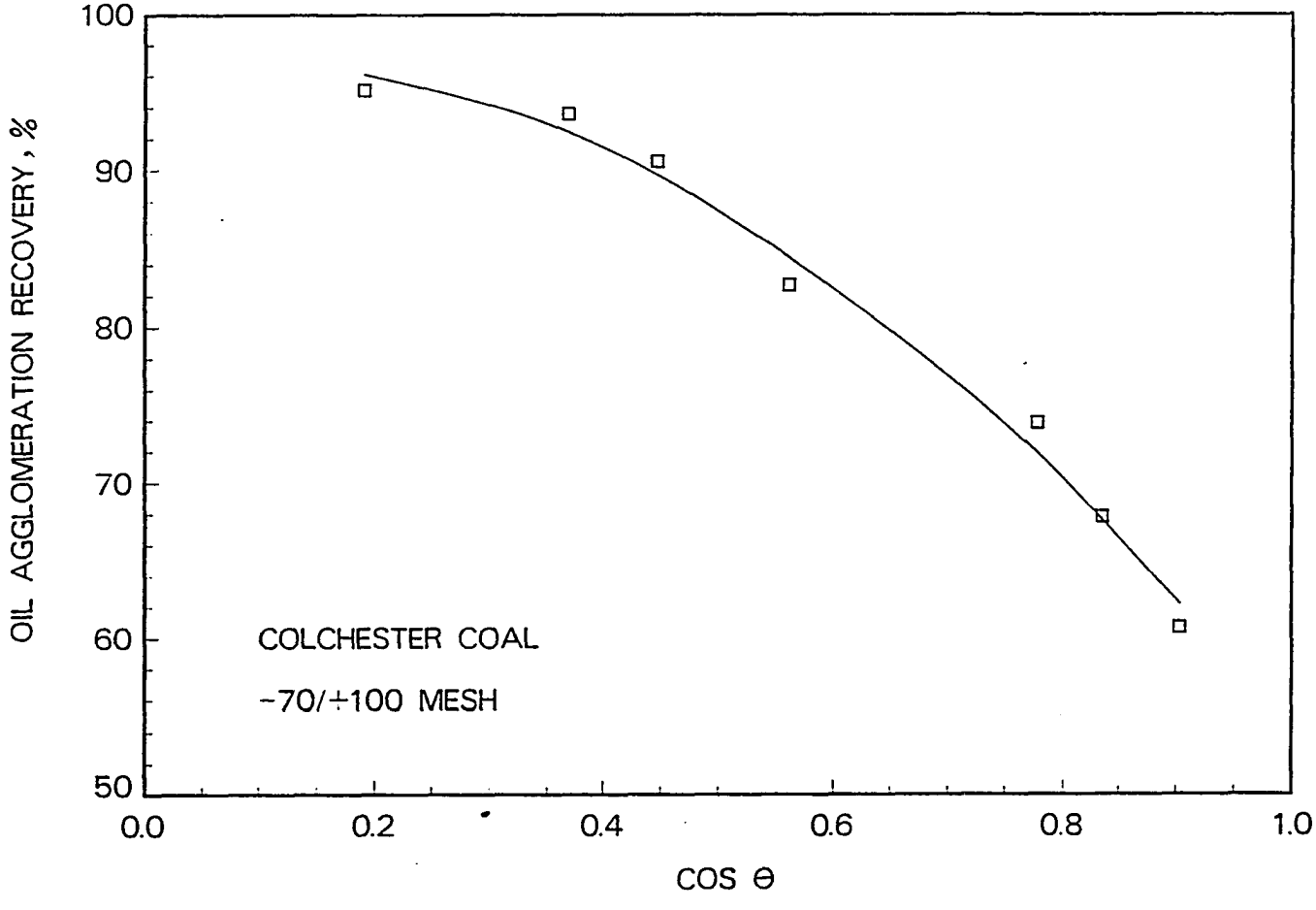

Figure 6.11: Correlation between oil agglomeration recovery and cos θ for -70/+100 mesh Colchester coal, 20 v/w % hexadecane added for agglomeration

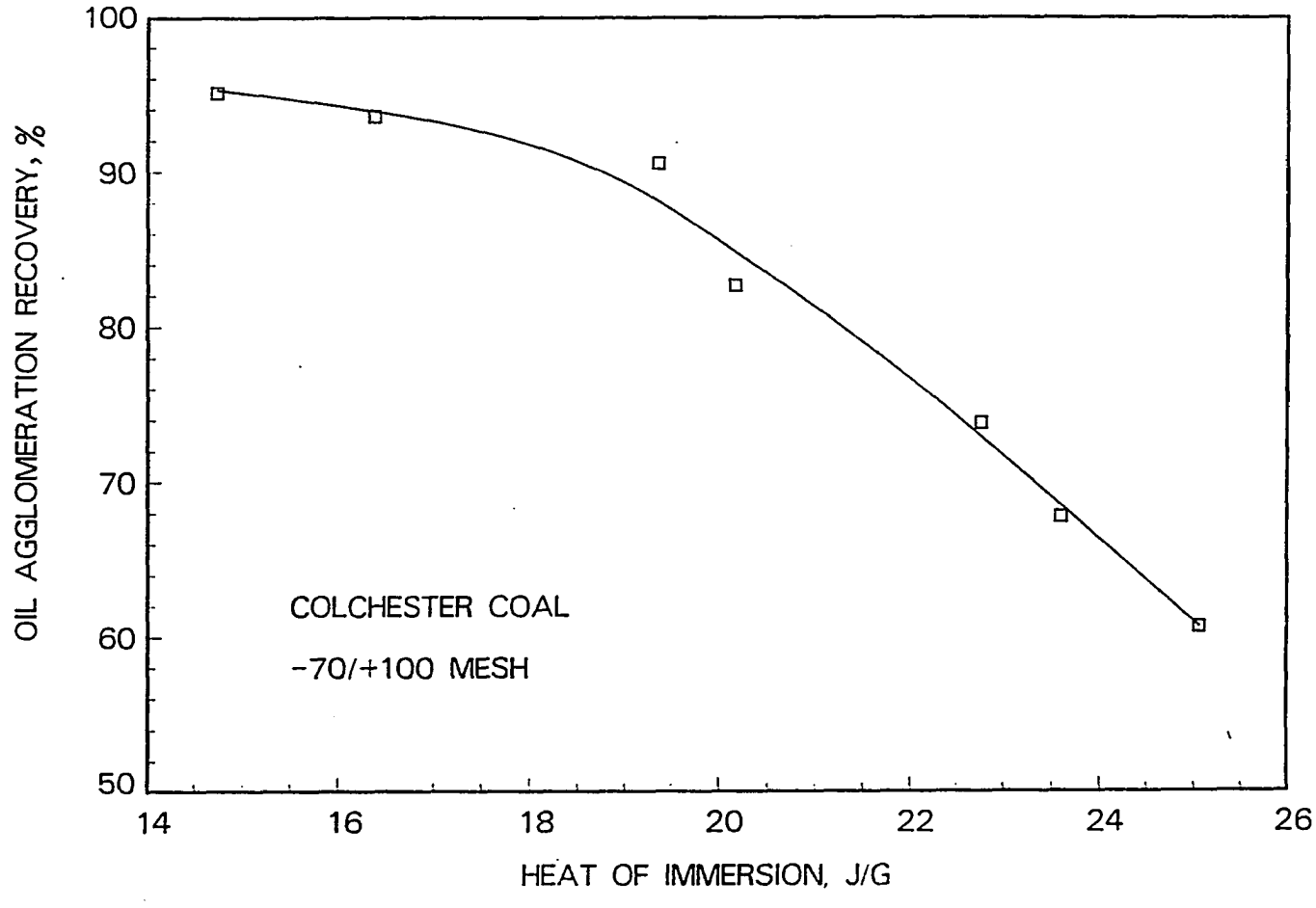

Figure 6.12: Correlation between oil agglomeration recovery and the heat of immersion in water for -70/+100 mesh Colchester coal, 20 v/w % hexadecane added for agglomeration

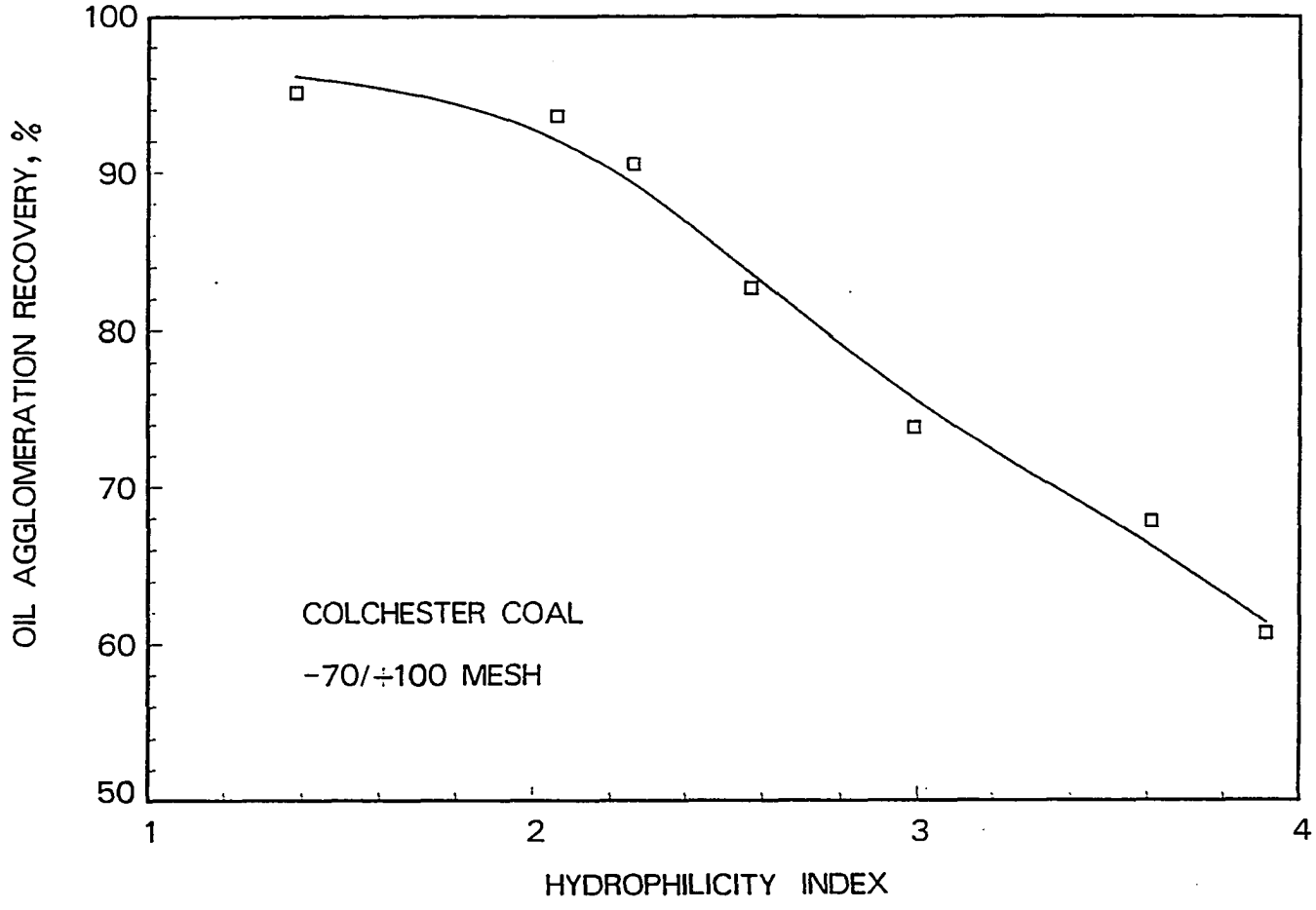

Figure 6.13: Correlation between oil agglomeration recovery and the hydrophilicity index for -70/+100 mesh Colchester coal, 20 v/w % hexadecane added for agglomeration

coal. The regression line in Figure 6.10 is represented by the following expression:

$$Recovery(\%) = 4.58 + 0.668\theta \tag{6.4}$$

for which $r^2 = 0.972$.

The oil agglomeration recovery of Colchester coal appeared to correlate equally well with either $\cos\theta$, the heat of immersion in water, or the hydrophilicity index for the series of oxidized samples. This can be seen by comparing the results presented in Figures 6.10 to 6.13, respectively. However, in most cases the correlations are nonlinear. The possible exception is the correlation of the agglomeration recovery with the hydrophilicity index. If the first point, which represents the raw coal, is disregarded, the remaining points can be fitted to a straight line. Choosing between these methods for characterizing the surface of coal will probably depend on other considerations. The three-phase contact angle is the only one of the properties which directly accounts for the interactions among the oil,water, and coal phases which are involved in the agglomeration process. Therefore, it should provide a more direct measure of the oleophilicity of coal in a water environment and be the best predictor of oil agglomeration performance. It can be used to determine the interaction between different coal and oil types. The FTIR absorption spectrum cannot serve this purpose, and it would be, though not impossible, much more difficult and indirect to obtain such information from the heat of immersion measurement. Measurement of the contact angle requires a closely sized sample, but the measurement is unaffected by the moisture content of the sample. On the other hand, the heat of immersion is sensitive to both particle size and moisture content. The hydrophilicity index is also affected by particle size and moisture content, but it does not seem as sensitive to these factors as the heat of immersion appears to be. Furthermore, the hydrophilicity

index can be determined easily and quickly when an FTIR spectrophotometer is available. However, the greatest disadvantage of the hydrophilicity index is that it is a relative value. The absolute value does not indicate the surface hydrophilicity unless the value is compared with a known standard. It is actually a good index for characterizing the surface of one type of coal. The three-phase contact angle and the heat of immersion are better indicators for comparing coals from different sources. Also the three-phase contact angle represents an absolute measure of surface and interfacial properties.

CHAPTER 7. THE EFFECTS OF COAL SURFACE PROPERTIES, OIL PROPERTIES, AND AIR ON THE OIL AGGLOMERATION PROCESS

Introduction

The oil agglomeration of coal in an aqueous suspension is a process for separating coal particles from mineral particles based on the difference in surface properties of coal and minerals. The factors which are usually considered to affect the agglomeration kinetics and recovery are the surface properties of the solids, oil type and dosage, intensity of agitation, and the presence of air. Drzymala et al. [60] studied the influence of air on oil agglomeration of carbonaceous solids in aqueous suspension. Their results for the graphite-heptane-water system showed that generally the oil agglomeration recovery was higher in the presence of air than in the absence of air. Microscopic examination of the agglomerates produced when air was present revealed the incorporation of air bubbles in the agglomerates. The effect of n-alkanes of different molecular weights on the recovery of Illinois No. 6 coal was also studied, and it was found that in the absence of air, the recovery was nearly independent of oil type. However, when air was present, lower molecular weight alkanes such as pentane and heptane gave a higher recovery than when air was absent. In the presence of air, the recovery seemed to correlate with the vapor pressure of the lower molecular weight

alkanes. For octane and higher molecular weight alkanes, the presence or absence of air had little effect on coal recovery.

Recently, Allen and Wheelock [62] studied the effect of air on the kinetics of oil agglomeration of No. 2 Gas Seam coal and Colchester coal and found with air present the initial agglomeration rate was faster than when it was absent.

The effect of air on agglomeration is an interesting and important phenomenon which is due to the mechanism of oil-agglomeration. The separation process could be improved if the mechanism of attachment and spreading of oil droplets on coal under water were better understood. Such understanding would also facilitate the design of the oil-agglomeration process. More specifically, this understanding could be used to predict minimum residence time for best separation.

Brown [63] studied the spreading of oil on a wet coal surface, hoping to find conditions under which the spreading coefficient or the work of spreading was zero, that is the conditions under which oil would spread spontaneously on a wet coal surface. He was interested in finding reagents which would improve the hydrophobicity of coal for use in the froth flotation method of coal cleaning. This method like the oil agglomeration process depends on surface properties. Conventional wisdom suggested that the easier the oil spread on the wet coal surface, the higher the recovery would be by froth flotation. However, Brown found that the best flotation reagents were those which spread least readily if the flotation reagents were pure hydrocarbon oils. But no satisfactory explanation was given. Also, he found that surface-active agents, which increased the contact angle of oil on a coal surface in water and decreased the interfacial tension, decreased the work of spreading and made the spreading of oil on coal easier. He pointed out that when the coal pores are filled with water, it is not

possible for oil to penetrate the pores. For oil to penetrate the coal pores, the coal pores need to be at least partially filled with air.

Moxon et al. [64] studied the effects of surface spreading and pore penetration by oil on the froth flotation process for cleaning coal. The maximum flotation yield was obtained with a hydrocarbon chain length corresponding to dodecane. The flotation yield obtained with shorter chain hydrocarbons was thought to be retarded by the penetration of the hydrocarbons into the coal pores, thereby reducing the surface concentration of oil. The yield with longer chain hydrocarbons was retarded seemingly by the greater viscosity of these materials which reduced their rate of spreading on the coal surface. The viscosity effect was overcome by providing a longer conditioning time prior to flotation. Although the effect of viscosity was discussed, the theory seemed not to fit all the experimental data.

The present study was aimed at determining how the presence of air on a coal surface affects the interaction between oil and coal and how the mechanism of oil agglomeration is consequently affected. The three-phase contact angle for the oil-water- coal system was determined for degassed and non-degassed coal with several oil types and the corresponding oil agglomeration response was determined.

Theory

1. Definition of Spreading Coefficient

In the literature, the spreading coefficient for a liquid on a solid or for a liquid on another liquid is mainly defined in two ways [9]: (a) the difference between the work of adhesion and the work of cohesion, or (b) the partial derivative of the Gibbs free energy with respect to the interfacial area when the temperature and chemical

potential of the system are constant. However, both definitions lead to the same overall results.

a. The first way of defining the spreading coefficient can also be expressed as [61]:

$$S = W_A - W_C \tag{7.1}$$

where W_A is the maximum reversible work of adhesion by the system, and W_C is the reversible work of cohesion of the liquid that spreads. The work of adhesion can also be expressed as follows:

$$W_A = \gamma_{sv} + \gamma_{lv} - \gamma_{sl} \tag{7.2}$$

where γ_{sv} and γ_{lv} are the surface tension of the solid and liquid, respectively, and γ_{sl} is the interfacial tension between the solid and the liquid. The work of cohesion of the liquid can be expressed as follows:

$$W_C = 2\gamma_{lv} \tag{7.3}$$

If the liquid spontaneously spreads on the solid, the maximum reversible work of adhesion of the liquid on the solid is greater than the work of cohesion of the liquid; then the spreading coefficient becomes

$$S = W_A - W_C = \gamma_{sv} - \gamma_{lv} - \gamma sl \tag{7.4}$$

For spreading, $S \geq 0$; nonspreading, $S < 0$.

b. The second way of defining the spreading coefficient is shown below:

$$S = -\left(\frac{\partial G}{\partial A}\right)_{T,P} \tag{7.5}$$

G is the Gibbs free energy of the system.

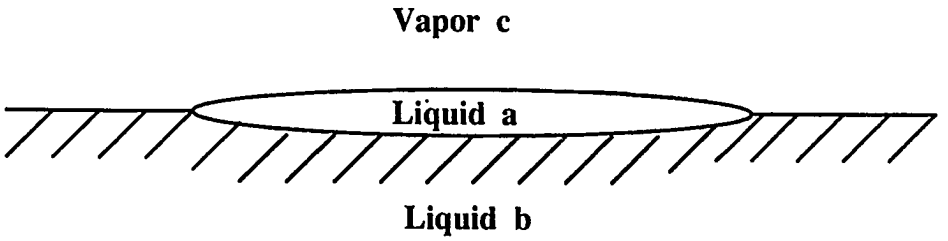

Figure 7.1: A layer of liquid "a" placed on another immiscible liquid "b" [8]

Consider a system where one liquid is placed on another immiscible liquid as in Figure 7.1 [8]. At constant temperature and pressure a small change in the surface free energy of the system can be written as

$$dG = \left(\frac{\partial G}{\partial A_{a/c}}\right)_{T,P} dA_{a/c} + \left(\frac{\partial G}{\partial A_{a/b}}\right)_{T,P} dA_{a/b} + \left(\frac{\partial G}{\partial A_{b/c}}\right)_{T,P} dA_{b/c}$$

For an ideal system it can be assumed that the changes of surface area are

$$-dA_{b/c} = dA_{a/b} = dA_{a/c}$$

Noting that by definition, the spreading coefficient of "a" on "b" is

$$S_{a/b} = -\left(\frac{\partial G}{\partial A_{a/b}}\right)_{T,P}$$

and

$$\gamma_{ij} = \left(\frac{\partial G}{\partial A_{ij}}\right)_{T,P}$$

the above equation can be then written as

$$S_{a/b} = \gamma_{b/c} - \gamma_{a/c} - \gamma_{a/b} \tag{7.6}$$

2. Spreading of Oil on a Coal Surface in a Water Environment

The preceding equation can be applied to the water-coal-oil system depicted in Figure 7.2 if the assumption about the change in surface area still holds.

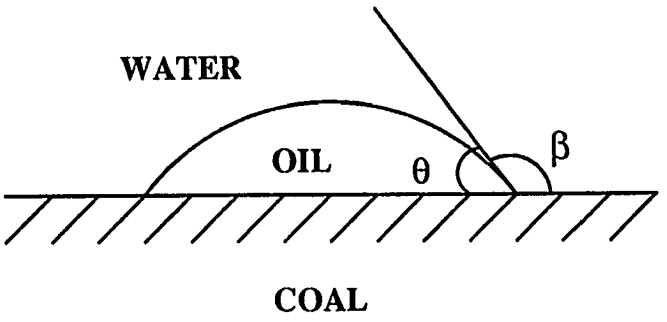

Figure 7.2: An oil-water-coal system. θ is the three-phase contact angle measured through the oil phase and β is the three-phase contact angle measured through the water phase

Then the spreading coefficient for oil on coal in the water environment can be written as

$$S_{o/c/w} = \gamma_{w/c} - \gamma_{o/w} - \gamma_{o/c} \tag{7.7}$$

Substituting the Young-Laplace equation,

$$\gamma_{w/c} - \gamma_{o/c} = \gamma_{o/w} \cos\theta$$

into Equation 7.7 gives

$$S_{o/c/w} = \gamma_{o/w}(\cos\theta - 1) \tag{7.8}$$

or since $\cos\theta = -\cos\beta$, the equation can also be written as

$$S_{o/c/w} = -\gamma_{o/w}(\cos\beta + 1) \tag{7.9}$$

As Zisman [9] pointed out, an "initial spreading coefficient" exists for the condition that can initiate spreading; a "final spreading coefficient" exists for the conditions that once spreading has occurred the liquid can remain spread. Noting that the Young-Laplace equation corresponds to the mechanical equilibrium of a drop resting on a flat solid surface, the spreading coefficient calculated by means of Equation 7.8 or Equation 7.9 then corresponds to the so-called "final spreading coefficient" which describes the equilibrium state. Therefore, the value and sign of the spreading coefficient directly relates to the readiness of spreading of a liquid on a solid surface. When $S_{o/c/w} = 0, \theta = 0$, the oil spreads or completely wets the coal; when $S_{o/c/w} > 0$, $\theta > 0$, and the oil partially wets the coal. Straight chain hydrocarbon oils such as heptane and hexadecane usually spread spontaneously on a dry coal surface. However, droplets of these oils placed on coal surfaces immersed in water did not spread spontaneously over the surface, but remained as discrete droplets displaying a finite contact angle between the oil-water interface and the coal surface [63] - [66]. Also the contact angles reported in Chapter 6 for the oil-water-coal system were finite.

3. Spreading of Oil on a Coal Surface in an Air Environment

An equation similar to Equation 7.9 can be written for the coal-oil-air system as follows:

$$S_{o/c/a} = \gamma_{o/a}(\cos\theta_{o/c/a} - 1) \tag{7.10}$$

where $\theta_{o/c/a}$ is the contact angle for an oil drop formed on a dry coal surface measured through the oil phase.

4. Liquid Bridges and Binding Force Between Coal Particles

Liquid bridges and the binding force between coal particles are important in the formation and stabilization of agglomerates in suspension [67] [68]. Jacques et al. [67] analyzed the stability of a particle attachment to immiscible liquid droplets dispersed in a bulk liquid phase in terms of the change in free energy. Factors such as the dispersed liquid droplet/particle size ratio (n), three-phase contact angle (θ) and liquid-liquid interfacial tension (γ_{ij}) were considered. The most stable state was shown to result when $\theta \rightarrow 0$, and $n \rightarrow \infty$, corresponding to a small three-phase contact angle and a large dispersed droplet.

Good and Islam [68] analyzed the stability of agglomerates in terms of the mechanical force provided by a liquid bridge between two coal particles. Good and Islam [68] and Good et al. [69] assumed that in oil agglomeration coal particles are enveloped in oil and water droplets serve as liquid bridges between coal particles, providing cohesive mechanical strength for the agglomerates. In cases where coal is very hydrophobic or very oleophilic as in the case of anthracite, the oil may coat the anthracite particles. Water may serve as the liquid bridge between anthracite particles. However, this binding mechanism may not be true for other coals.

In oil agglomeration, when oil is added to a coal-water suspension under agitation, oil becomes the dispersed phase. When oil droplets attach to coal particles in water, they tend to form a finite three-phase contact angle. As shown in Chapter 6, the three-phase contact angle measured through the water phase ranged from 61.6 degree for No. 2 Gas Seam coal (high volatile A bituminous) to 31.6 degree for Illinois No. 6 coal (high volatile C bituminous). Therefore, the oil could not completely displace water from the surface of such coal particles, and since the oil was the dis-

persed phase, it served as the liquid bridge between coal particles. The configuration of the liquid bridge between two coal particles similar to that proposed by Good and Islam [68] is indicated in Figure 7.3. This diagram differs from that by Good and Islam [68] because oil is considered as the bridge.

The net force, f, between the plates shown in Figure 7.3 is given by

$$f = 2p \cdot \gamma_{ow} \cdot \sin\theta \tag{7.11}$$

where p is the perimeter of the circle in which the drop surface intesects the solid. The oil-water-coal three-phase line is assumed to be stationary and hysteresis of the contact angle allows the contact angle to vary when the distance between the two plates, d, changes [68]. Equation 7.11 shows that as the contact angle, θ, decreases between 90 and 180 degrees, the net force, f, also increases; that is, the resistance of the two particle aggregate to an increase in the distance between the two plates, d, increases. In other words, if a coal is hydrophobic which corresponds to a large contact angle, the probability of an agglomerate sustaining a shearing force is also large, which may result in a high agglomeration recovery.

The preceding configuration will also hold for pyrite and other mineral particles (see Figure 7.4). The three-phase contact angle determined for fresh pyrite was 34.6 degrees and for oxidized pyrite 42 degrees. The particle size in both cases corresponded to -70/+100 mesh. When the distance, d, increases, θ will increase, and the net force, f, will increase. The oil bridges between pyrite particles will still be able to resist an increase in d. However, since the contact angle, θ, for pyrite is smaller than that for high rank coals, the force binding a pyrite agglomerate will be smaller than that binding a coal agglomerate.

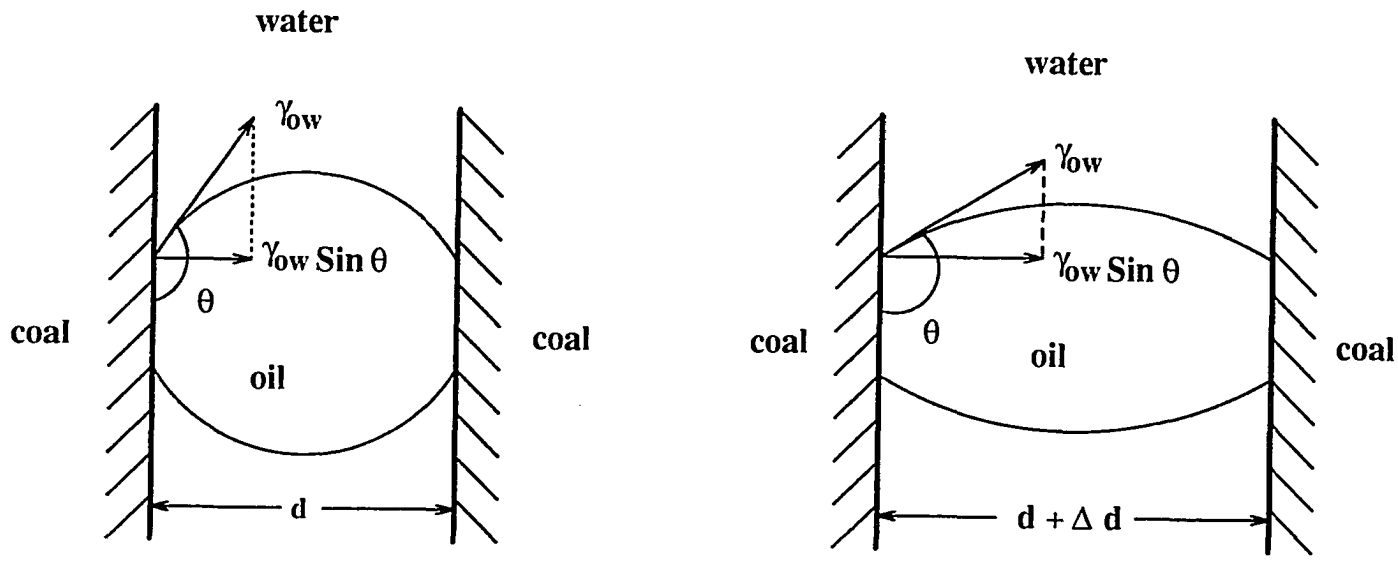

Figure 7.3: A liquid bridge, formed by a droplet of oil in water between two coal particles, responses to an increase in distance between coal particles

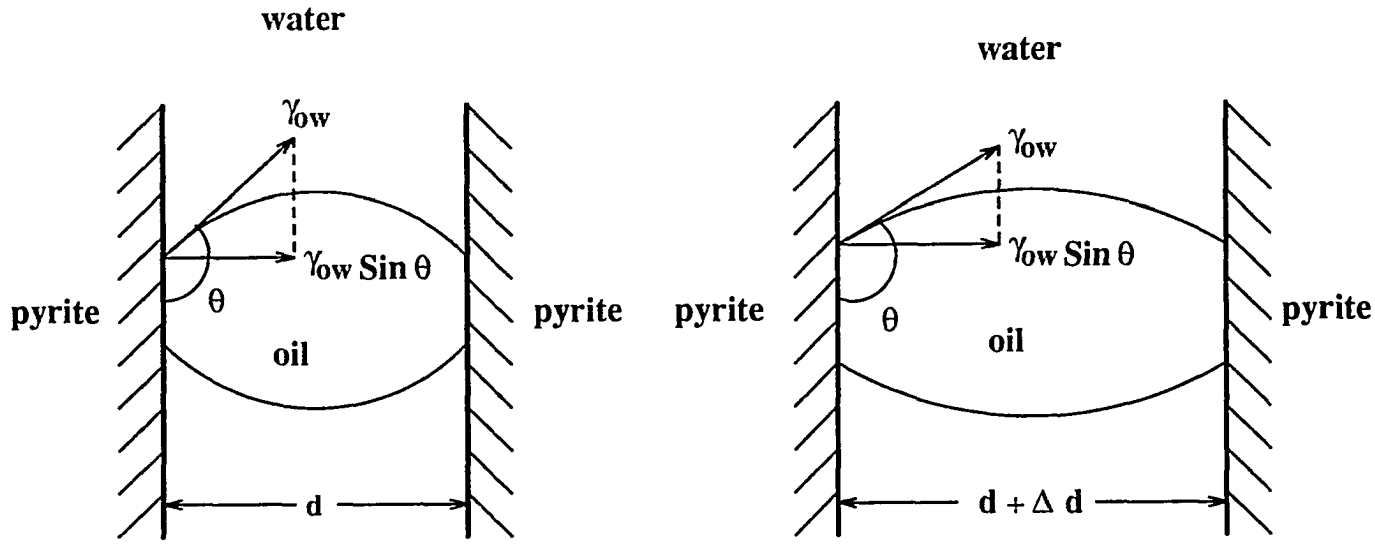

Figure 7.4: A liquid bridge, formed by a droplet of oil in water between two pyrite particles, responses to an increase in distance between pyrite particles

Experimental

1. Three-phase Contact Angle for Degassed and Nondegassed Coal Particles

No. 2 Gas Seam coal from West Virginia was used for the three-phase contact angle measurement. The coal was crushed by a jaw crusher and ground in a roll mill. The -45/+70 mesh size fraction was used. The ash and total sulfur contents of this specific size fraction were 2.9 % and 0.76 %, respectively. The coal sample was divided into a number of portions by a spinning riffle. Each portion weighing about 35 g was used for a single measurement. The coal was wetted with deionized water in a beaker and poured onto a 70 mesh screen. The coal was washed on the screen with deionized water in order to remove most of the fine particles which passed through the screen. The washed coal was mixed with water to form a slurry. In some cases the coal slurry was degassed while in other cases it was not degassed before being put into the sample holder for determining the three-phase contact angle. The nondegassed coal slurry was stirred in a open beaker for 5 min. with a Cole-Palmer laboratory stirrer. The coal slurry which was to be degassed was stirred in a closed flask connected to a vacuum pump. Stirring was continued for 15 – 20 min while applying a vacuum of −660 mmHg. The three-phase contact angle was determined by the modified suction potential technique described in Chapter 5.

Four oils were used. They included: pentane from Kodak (BP 35°C), heptane from Burdick and Jackson Lab, Inc. (distilled in glass, BP 98 – 99°C), 99.7 mol% decane form Fisher Scientific, and 99 mol% hexadecane from Aldrich.

2. Oil Agglomeration Tests

No. 2 Gas Seam coal from Raleigh County, West Virginia, and Colchester Seam coal from Schuyler County, Illinois, were used. No. 2 Gas Seam coal was much more hydrophobic than Colchester coal and, therefore, more difficult to wet. Both coals were ground in the dry state with a high-speed impact mill to pass a 200 mesh (75 μm) screen. The ground material was divided with a spinning riffle into a number of 8 g portions to use in the individual agglomeration tests.

To degas the coal, 8 g of coal was first added to 200 ml of water in a beaker which was stirred with a magnetic stirring bar until the coal appeared completely wetted. The mixture was transferred to a round bottom flask which was fitted with a mechanical agitator and connected to a vacuum pump. Over a period of 5 min. the vacuum was increased gradually to − 660 mmHg while the suspension was stirred. The vacuum was then maintained for another 10 min. The suspension was transferred to the closed system agglomeration unit where sufficient water was added to completely fill the 480 ml vessel. The suspension was conditioned for 2 to 3 min. by stirring at 5500 rpm. An agglomerant was subsequently added in a series of small measured increments while the turbidity of the suspension was monitored with a photometric dispersion analyzer. After each addition the turbidity was allowed to stabilize before recording its value. The reproducibility for the turbidity measurement was determined to be 96 % to 98 %.

For the tests which did not involve degassing, 8 g of coal was added to 300 ml water in the agglomeration vessel. The mixture was stirred briefly at 5500 rpm to wet the coal. Sufficient water was added to completely fill the 480 ml vessel, and the suspension was conditioned, and the agglomeration was carried out as described for

the degassed coal.

A series of agglomeration experiments was conducted using different paraffinic hydrocarbons which ranged from pentane with a chain length of five carbon atoms to a purified paraffin oil having an average chain length of 30 carbon atoms. The latter was a mixture of relatively long-chain hydrocarbons obtained from Fisher Scientific. The other hydrocarbons were the same as those used for the three-phase contact angle measurements described previously.

Results and Discussion

1. Effects of Air on the Coal Surface

The relative turbidity for both degassed and nondegassed No. 2 Gas Seam coal was plotted against the oil dosage, v/w%, for different types of oil in Figures 7.5 to 7.10. The relative turbidity plotted in these figures is the ratio of the turbidity achieved with a given oil dose to the initial turbidity of the coal suspension. Most of the oils were straight chain paraffinic hydrocarbons ranging from pentane with five carbon atoms to a purified paraffin oil having an average chain length of 30 carbon atoms. Except for pentane and n-octanol, the extent of agglomeration achieved with smaller oil doses was considerably greater for nondegassed suspensions than for degassed suspensions. However, when the oil dosage increased to 8 v/w% and beyond, the results were very similar for degassed and nondegassed suspensions.

In order to complete the picture, the same experimental study was conducted for Colchester coal and the results are plotted in Figures 7.11 - 7.15. The results with Colchester coal showed that the presence or absence of air had little or no effect on the agglomeration process, as the extent of agglomeration for both degassed and

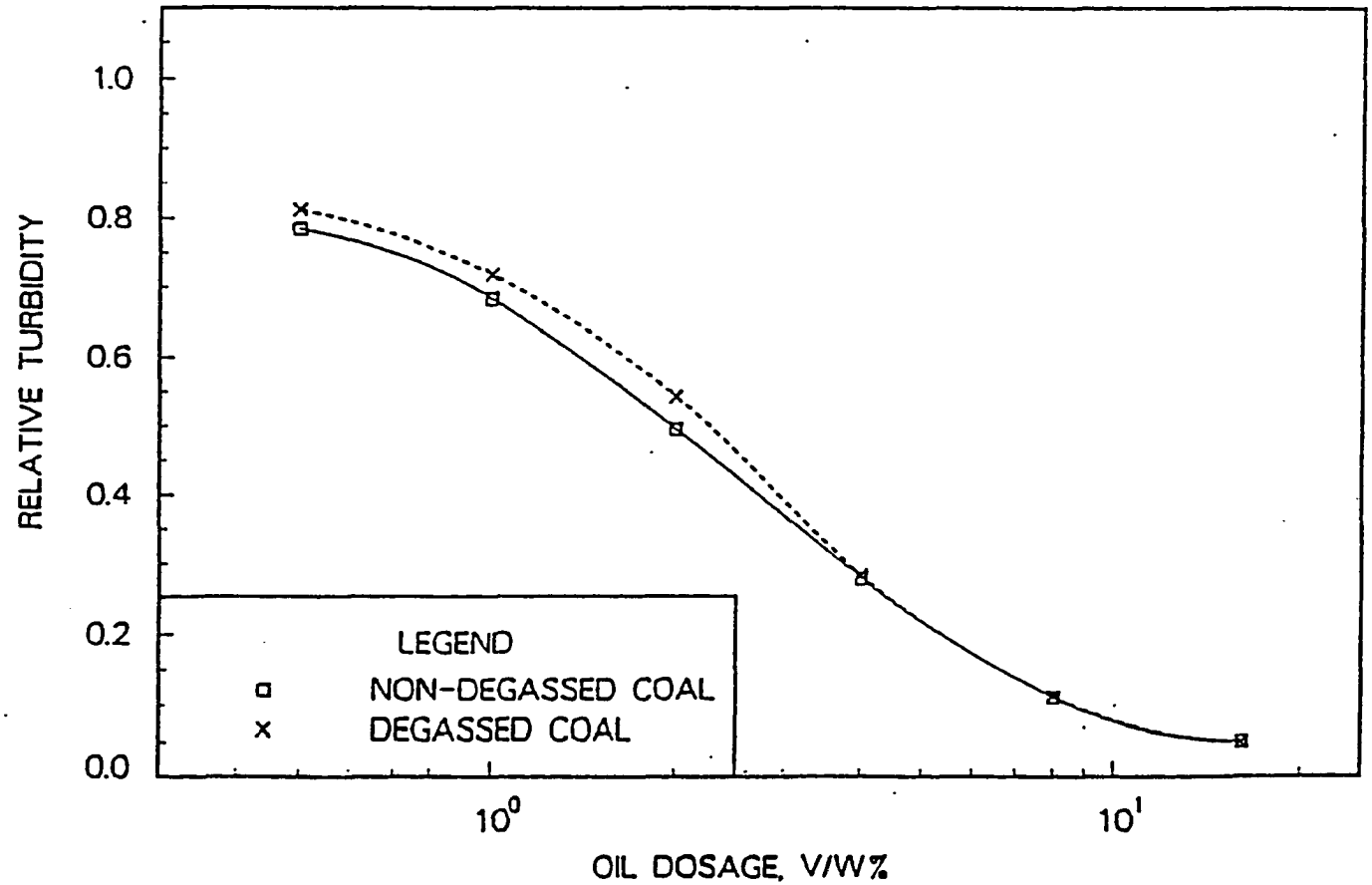

Figure 7.5: Effect of degassing on turbidity of suspensions of No. 2 Gas Seam coal after agglomeration with pentane

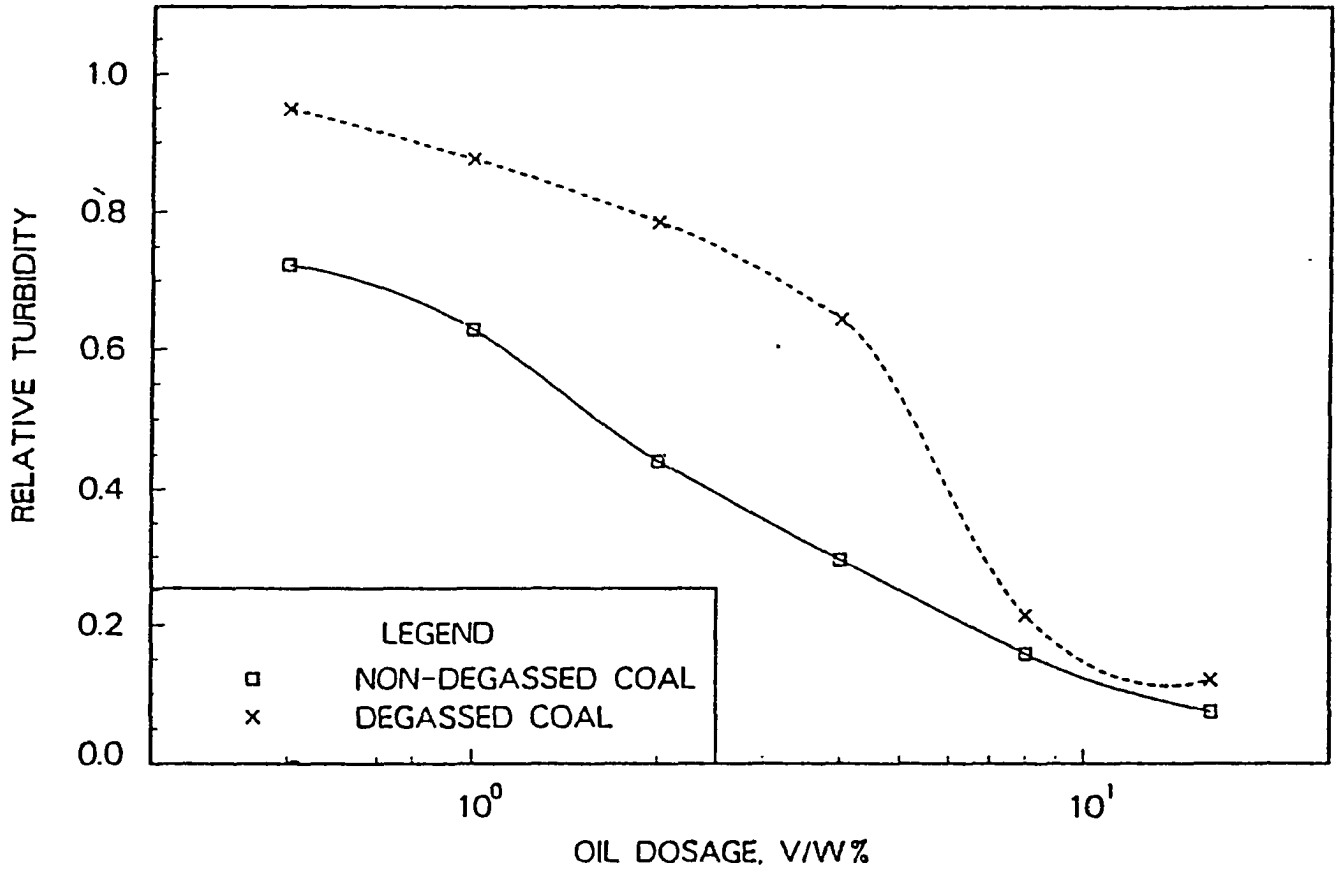

Figure 7.6: Effect of degassing on turbidity of suspensions of No. 2 Gas Seam coal after agglomeration with heptane

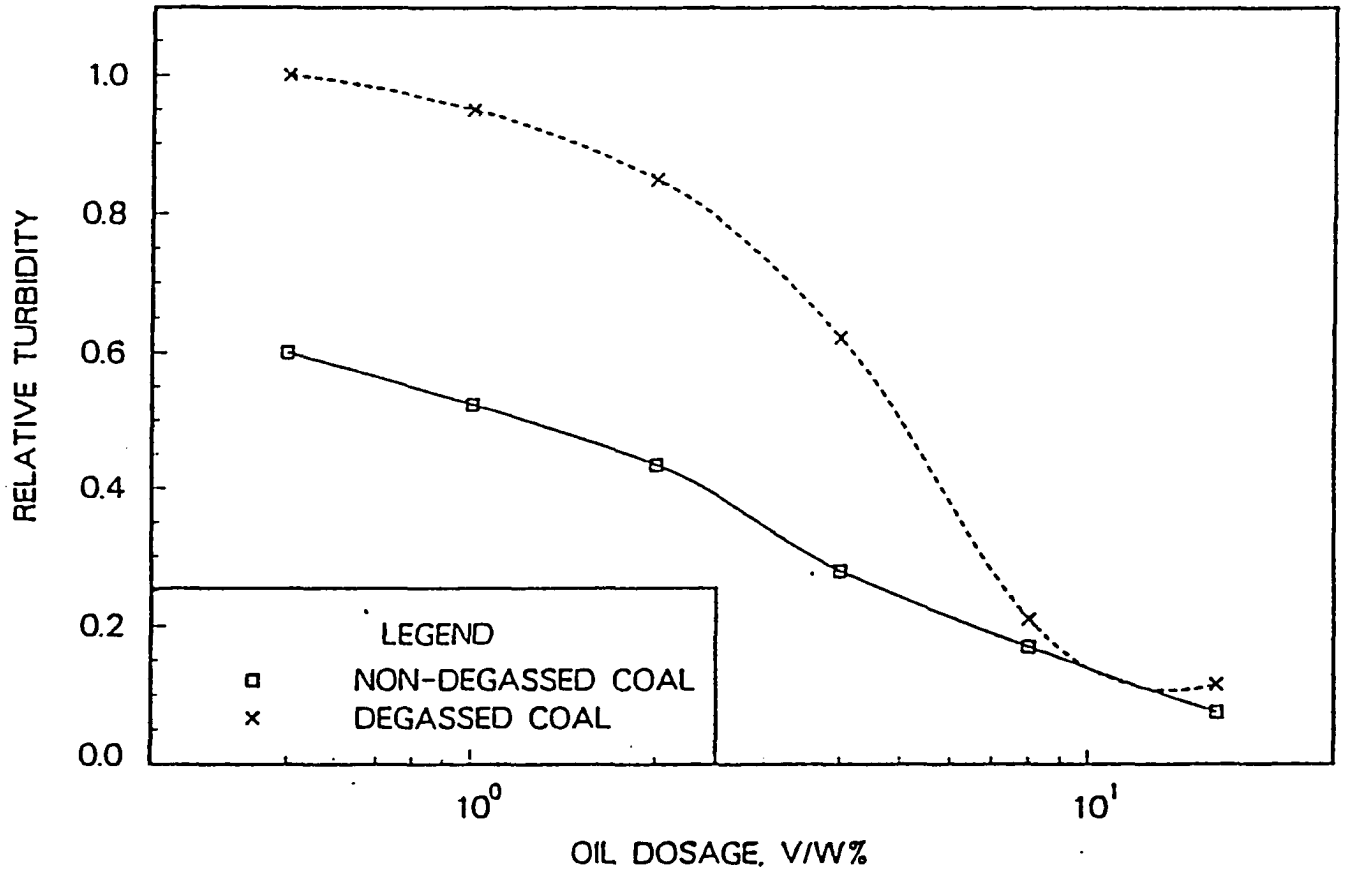

Figure 7.7: Effect of degassing on turbidity of suspensions of No. 2 Gas Seam coal after agglomeration with decane

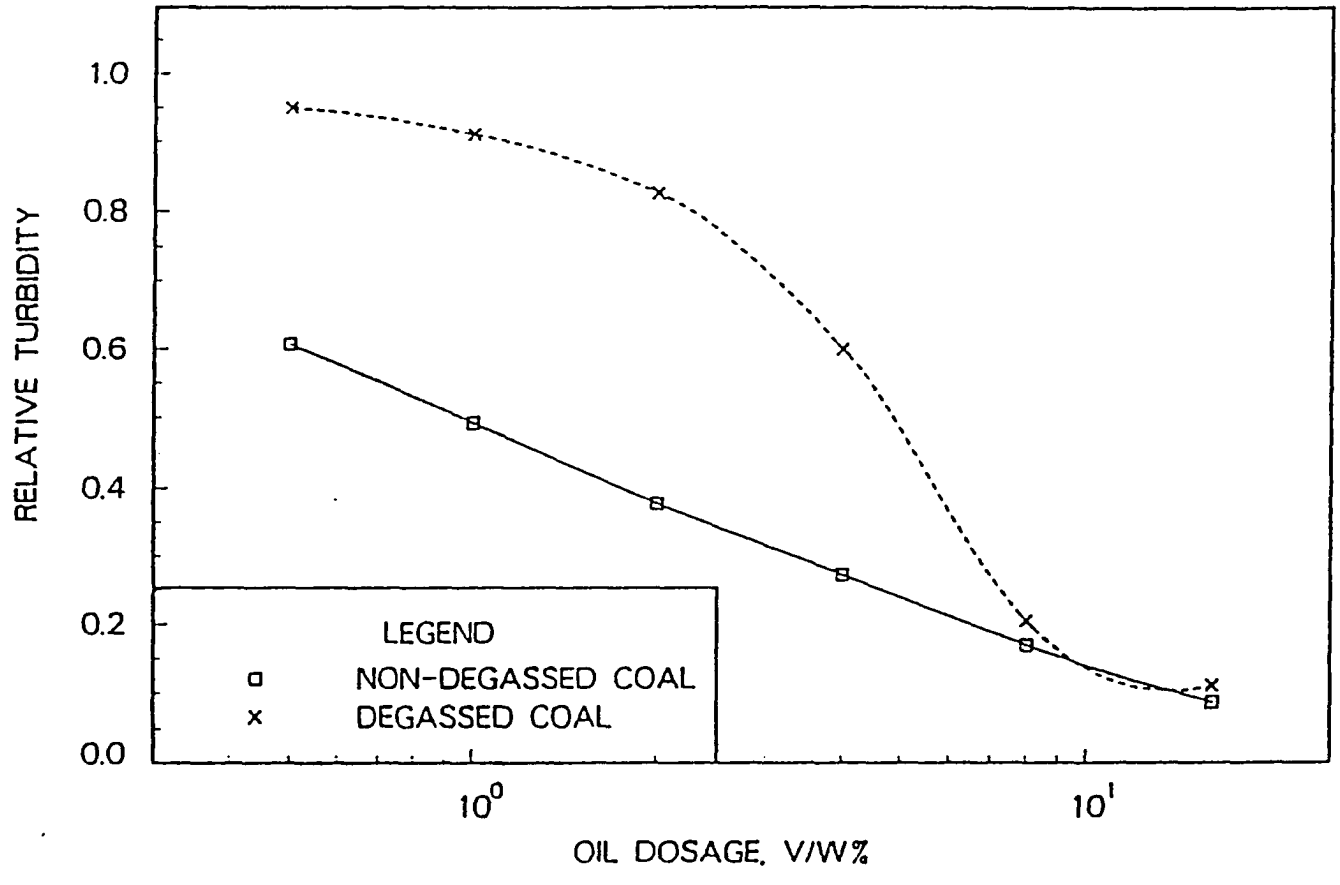

Figure 7.8: Effect of degassing on turbidity of suspensions of No. 2 Gas Seam coal after agglomeration with hexadecane

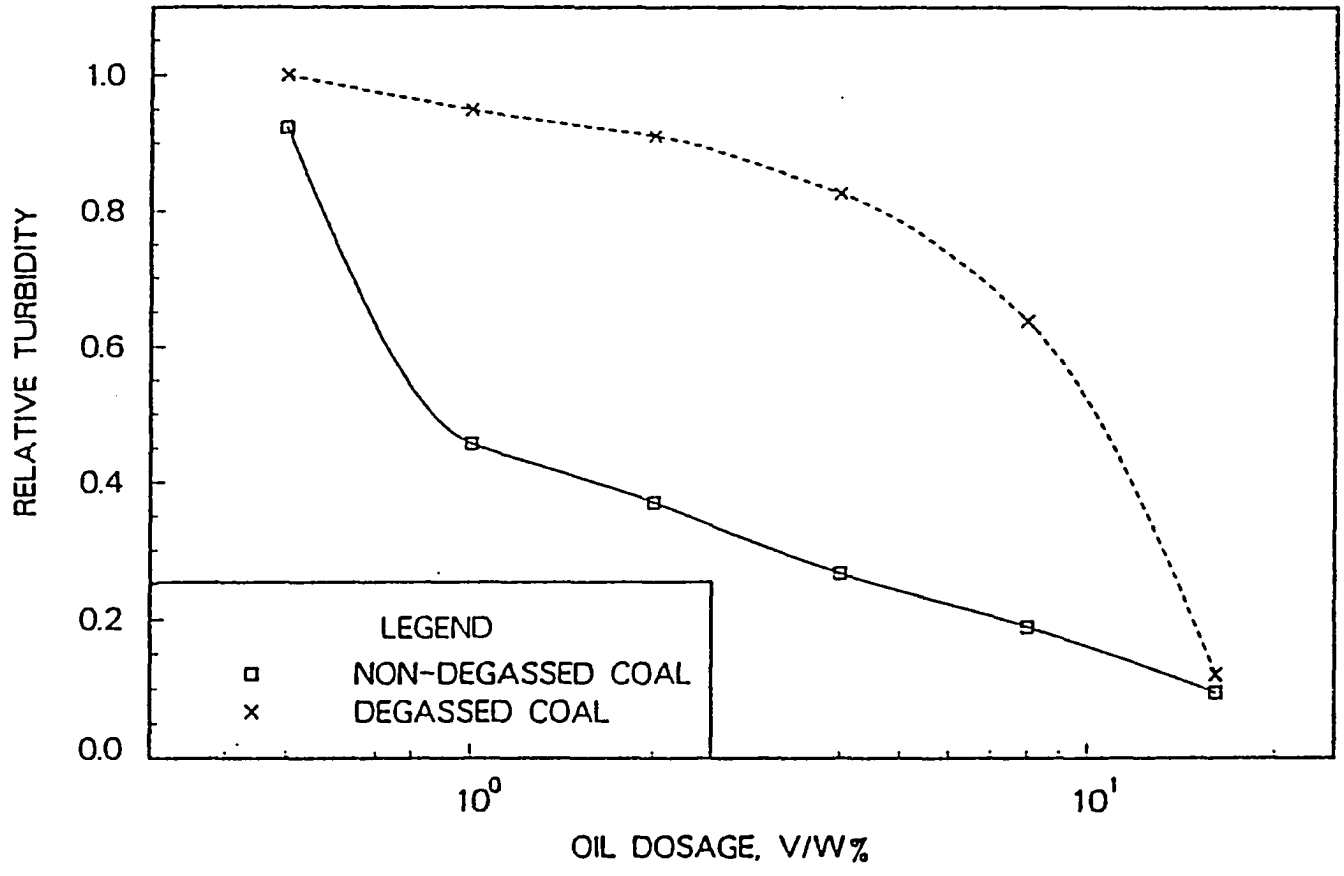

Figure 7.9: Effect of degassing on turbidity of suspensions of No. 2 Gas Seam coal after agglomeration with paraffin oil

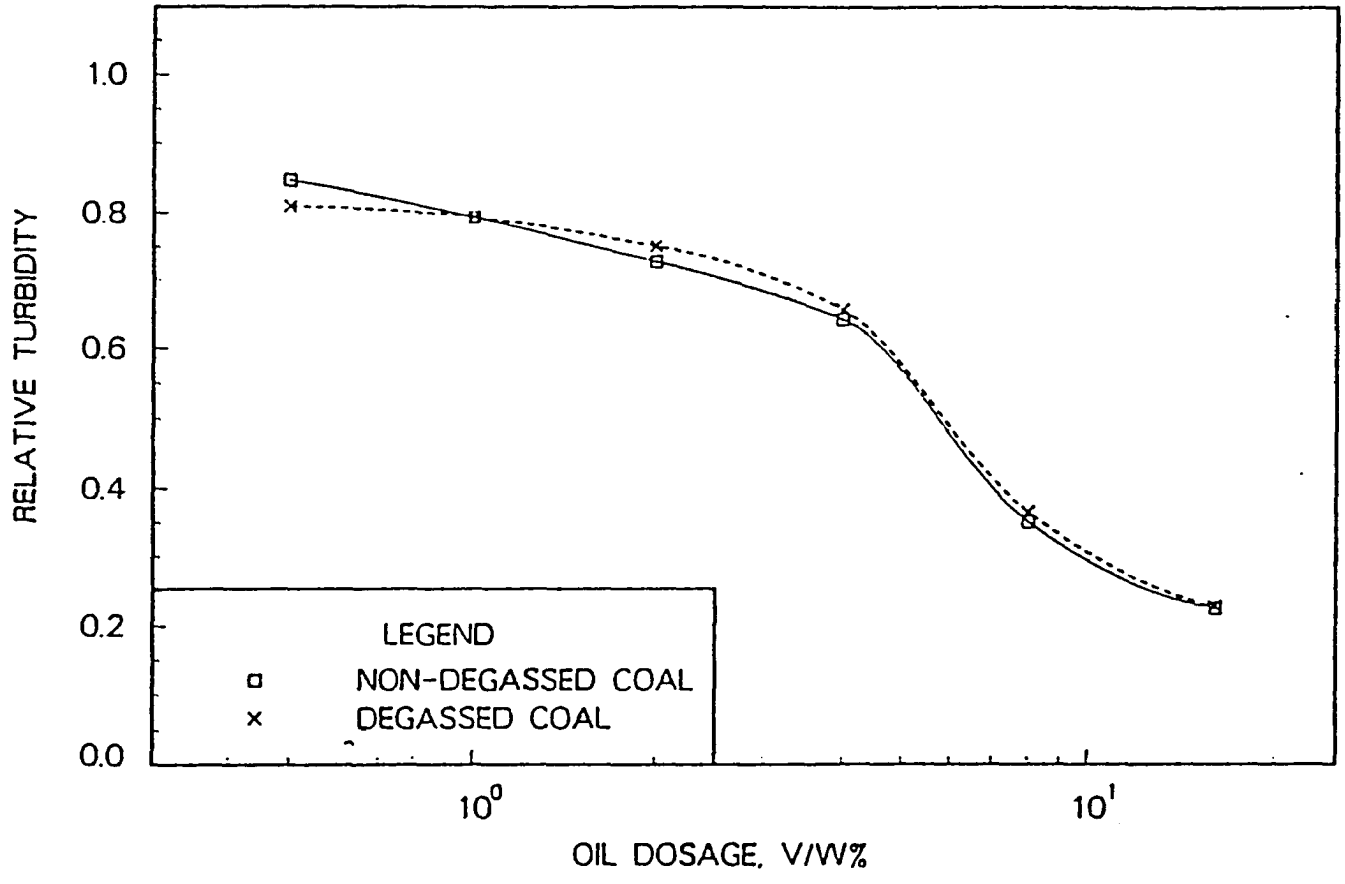

Figure 7.10: Effect of degassing on turbidity of suspensions of No. 2 Gas Seam coal after agglomeration with octanol

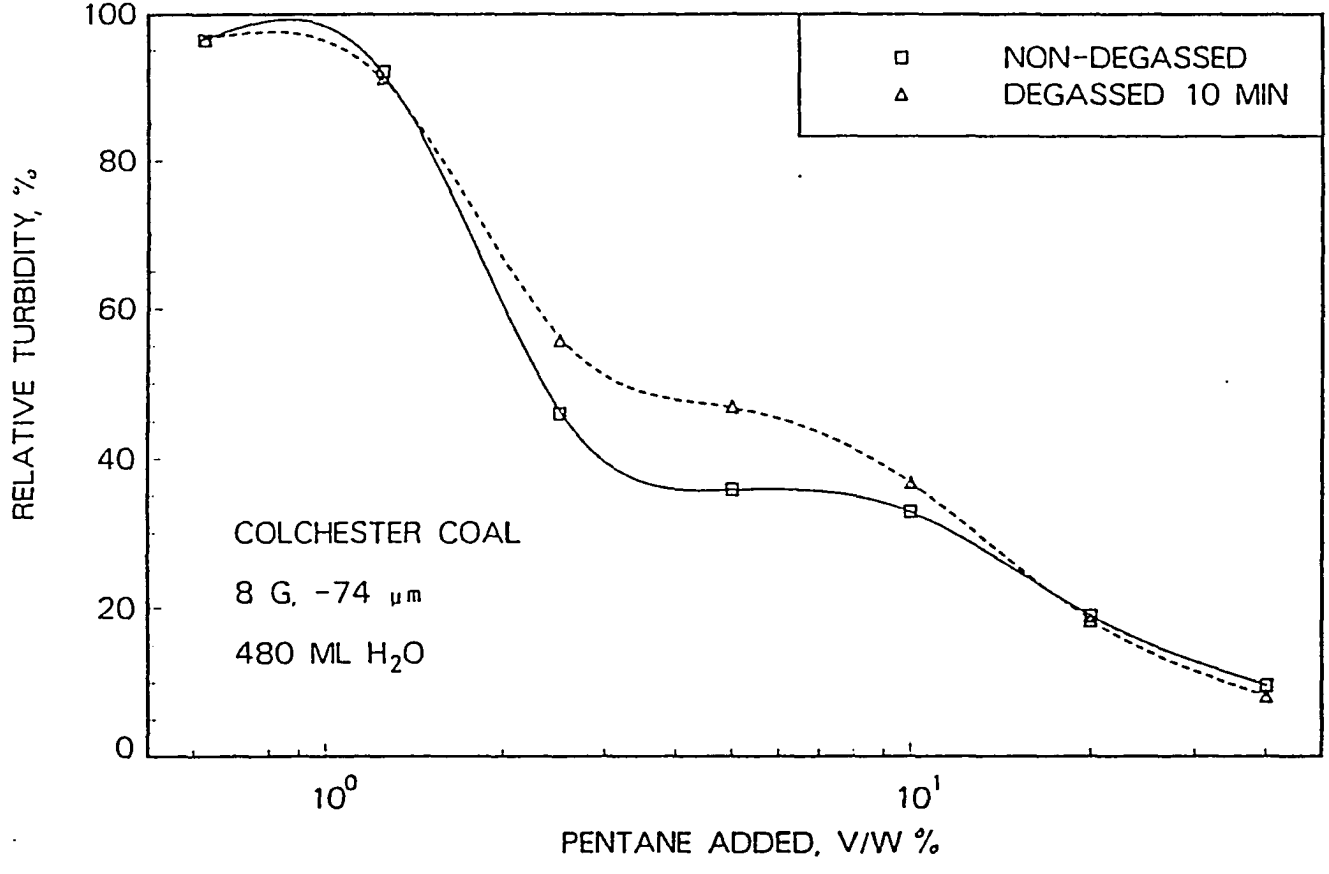

Figure 7.11: Effect of degassing on turbidity of suspensions of Colchester coal after agglomeration with pentane

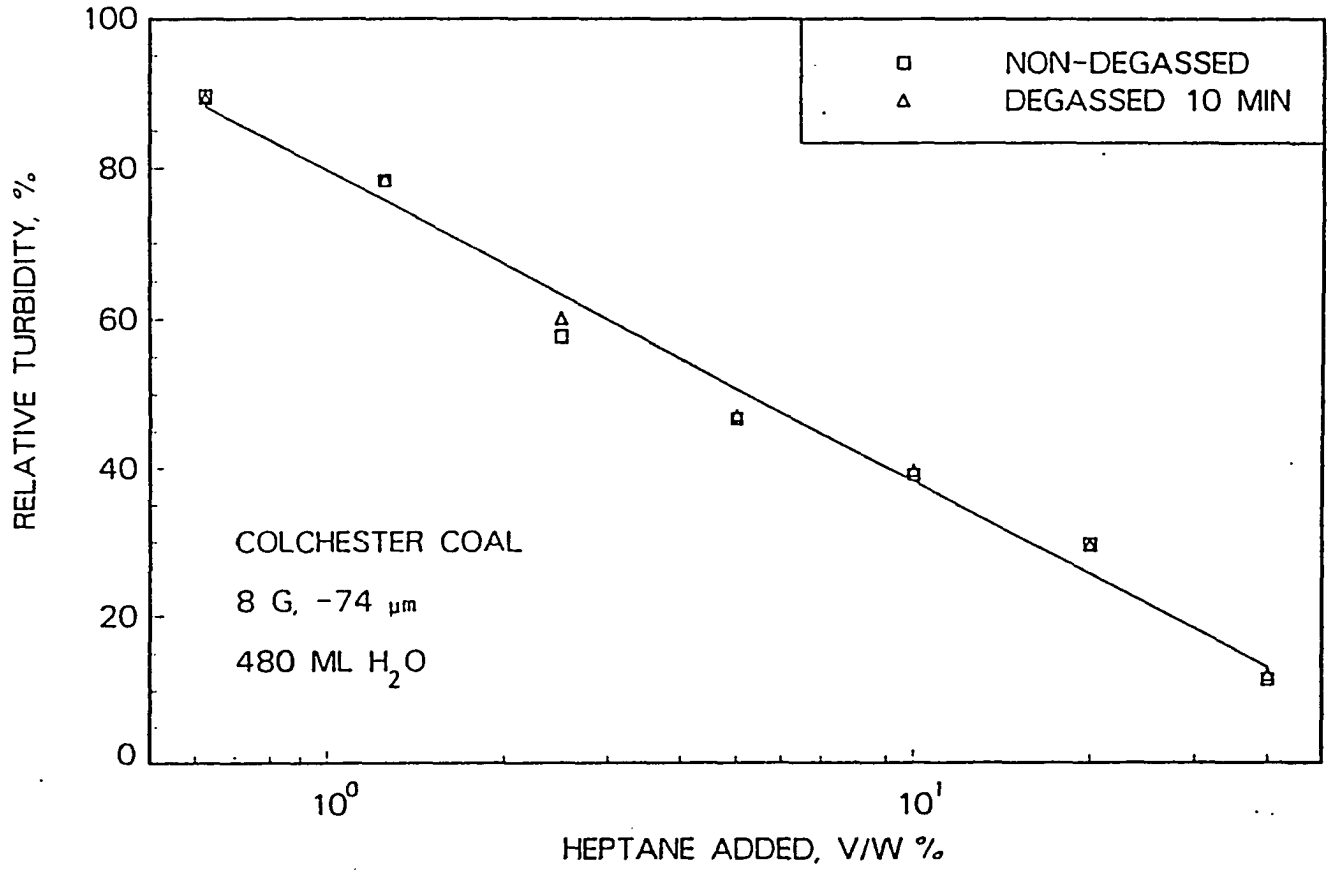

Figure 7.12: Effect of degassing on turbidity of suspensions of Colchester coal after agglomeration with heptane

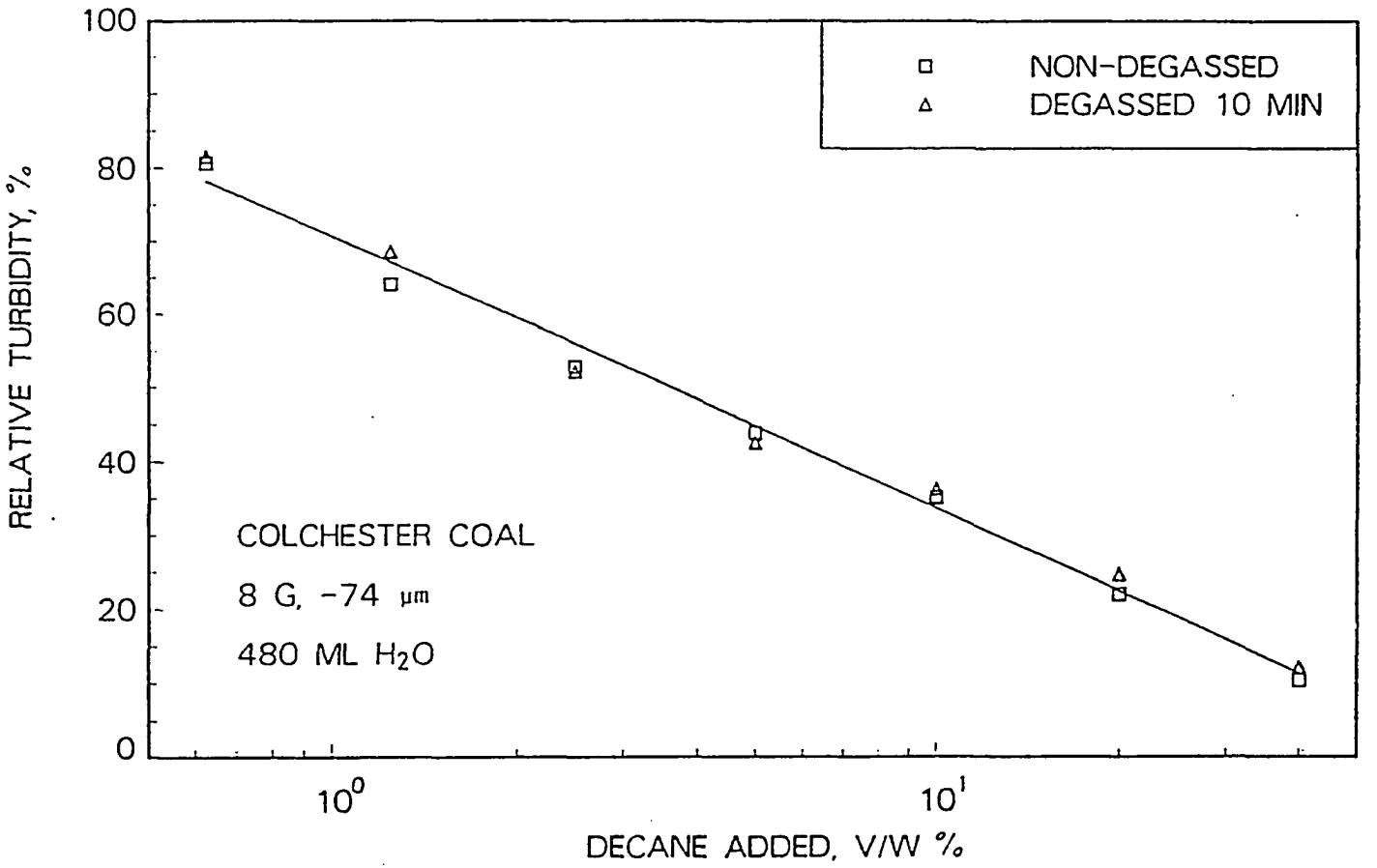

Figure 7.13: Effect of degassing on turbidity of suspensions of Colchester coal after agglomeration with decane

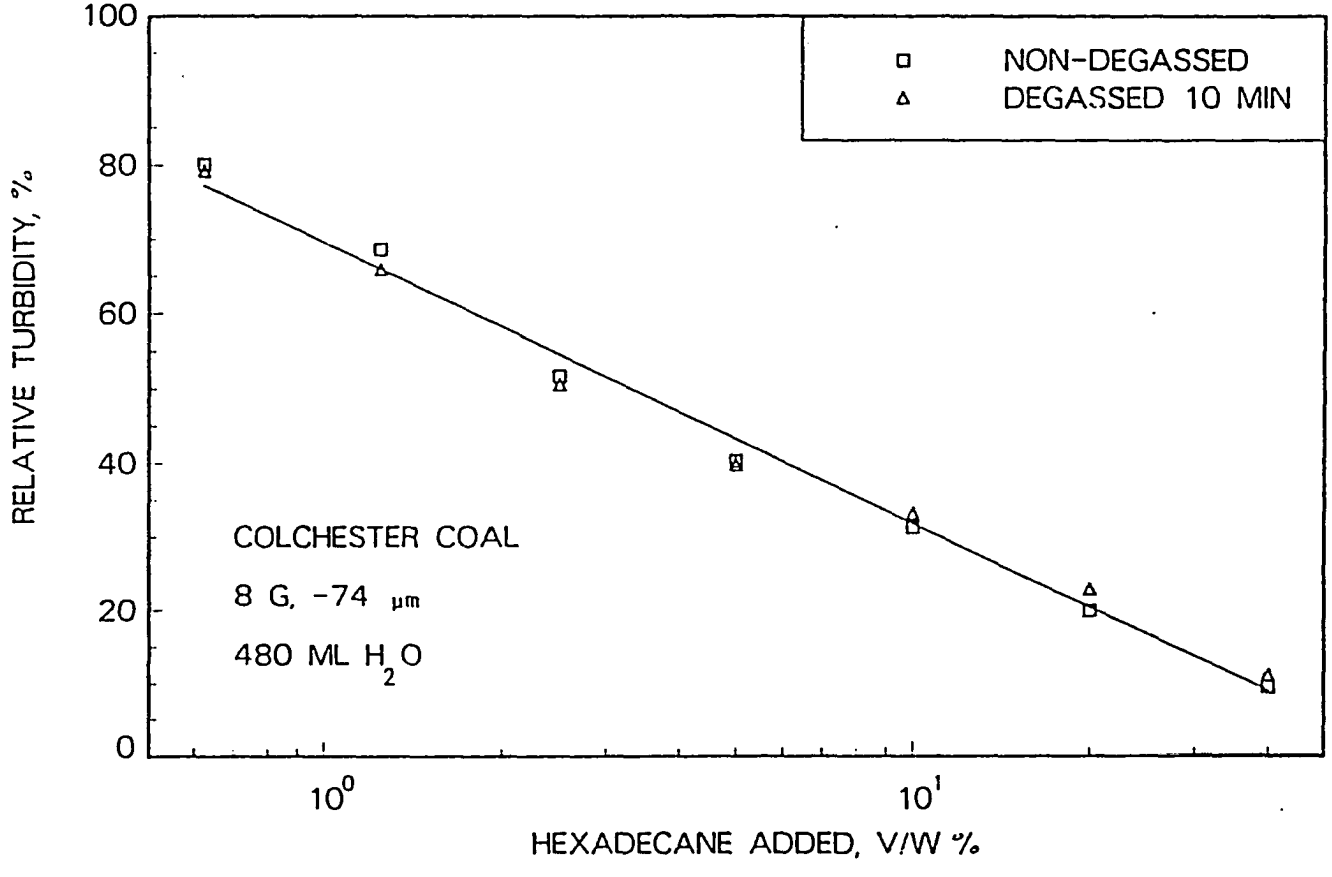

Figure 7.14: Effect of degassing on turbidity of suspensions of Colchester coal after agglomeration with hexadecane

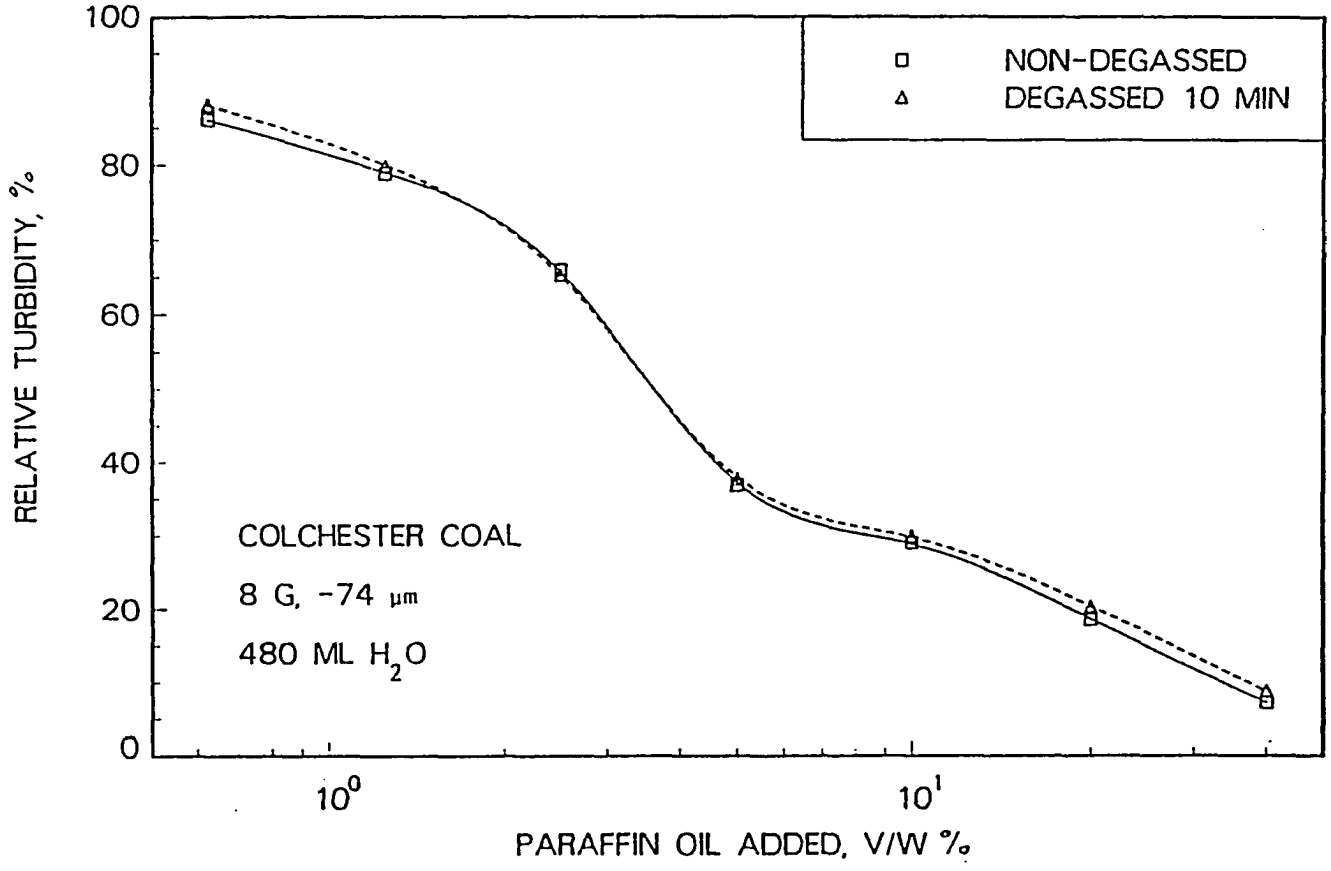

Figure 7.15: Effect of degassing on turbidity of suspensions of Colchester coal after agglomeration with paraffin oil

nondegassed coal was almost identical.

A reasonable explanation for the difference in the extent of agglomeration for degassed and nondegassed No. 2 Gas Seam coal suspensions could be that it is easier for oil to displace air than water from the surface of the coal.

To prove this theoretically, the spreading coefficient was calculated and compared for degassed and nondegassed coal. For degassed coal, no air bubbles or air film exist on the coal surface. An oil droplet must replace water from the coal surface in order to attach to the coal particle. In this case the spreading coefficient $So/c/w$ can be calculated by Equation 7.9 using the contact angle measured for the degassed coal (see Table 7.1). The calculated spreading coefficient for degassed No. 2 Gas Seam coal is listed in Table 7.2 for each of the oils. The spreading coefficient $S_{o/c/w}$ for several hydrocarbons on No. 2 Gas Seam coal is smaller than zero, therefore, work is needed for these oils to displace water from the coal surface. It was observed that water does not readily spread on the surface of No. 2 Gas Seam coal and it was very difficult to get the coal surface completely wetted unless degassing was used; that is, air bubbles or an air film existed on the surface of nondegassed No. 2 Gas Seam coal. When air bubbles or a film existed on the coal surface, oil droplets contacting the air bubbles or film tended to become attached to the air bubbles or film and then replaced the air from the coal surface.

In our study of the interactions among oil, air, and coal, a flat polished surface of No. 2 Gas Seam coal was immersed in deionized water. With no degassing, there were many air bubbles on the coal surface which could be seen under a microscope. Figure 7.16 shows the observed phenomenon when a tiny oil droplet was placed onto an air bubble. The oil first spread over the air-water interface towards the coal-

Table 7.1: Three-phase contact angle measured through the water phase for degassed and nondegassed No. 2 Gas Seam coal, -45/+70 mesh

Oil type	$\gamma_{o/a}$, dyne/cm	$\gamma_{o/w}$, dyne/cm	Contact angle, degrees	
			Degassed coal	Nondegassed coal
Pentane	16.0	49.0	45±1	74±1.5
Heptane	20.1	50.1	61±1	66±1.5
Decane	23.8	51.2	61±1	69±1.5
Hexadecane	27.47	50.1	61±1	67±1.5

Table 7.2: Spreading coefficient for different types of oil to replace water or air from the surface of No. 2 Gas Seam coal

Oil type	Spreading coefficient, for oil to replace water, $S_{o/c/w}$, dyne/cm.	Spreading coefficient for oil to replace air, $S_{o/c/a}$, dyne/cm.
Pentane	-83.65	0
Heptane	-74.39	0
Decane	-76.02	0
Hexadecane	-74.39	0

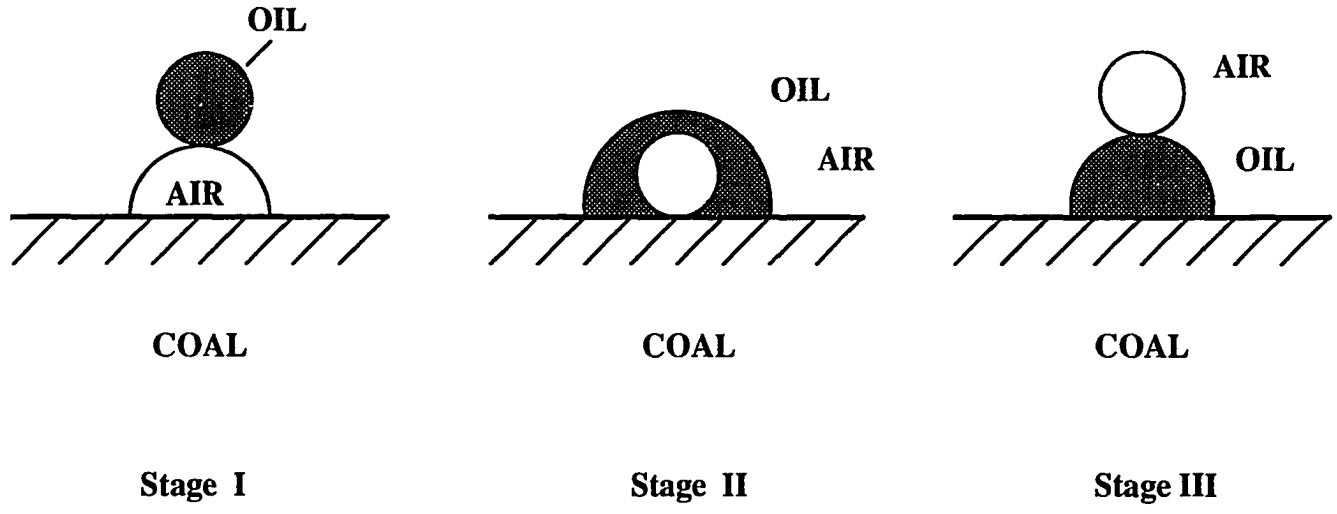

Figure 7.16: The process whereby an oil droplet replaces an air bubble from a No. 2 Gas Seam coal surface immersed in water

air interface (stage I). When the oil reached the coal surface, the air-coal interface was totally replaced by the oil-coal interface, and the air bubble became detached from the coal surface (stage II). The detached air bubble inside the oil droplet then rose to the top of the oil droplet (stage III), and became detached from the oil droplet. Equation 7.10 could then be applied to calculate the corresponding spreading coefficient. Since the oils listed in Table 7.2 readily spread on the surface of coal in an air environment, the contact angle, $\theta_{o/w/a}$, is zero for each of these oils, therefore, the spreading coefficient, $S_{o/c/a}$, calculated by Equation 7.10 is zero for each of these oils (see Table 7.2) which means that no work is required for these oils to displace air from the coal surface. Therefore, it is easier for an oil droplet to displace air than water from coal surface for No. 2 Gas Seam coal.

Consider the attachment of oil droplets to coal particles as taking place in two stages: (a) collision of oil droplets and coal particles and (b) displacement of water or air from the coal surface. The probability of oil becoming attached to coal, P, can be related to the probability of collision between coal particles and oil droplets, P_1, and the probability of displacement of water or air from the coal surface by oil, P_2, by the following expression:

$$P = P_1 \times P_2$$

where

$$P_2 \propto \frac{1}{S_{o/c/w}} \quad or \quad \frac{1}{S_{o/c/a}}$$

Since $S_{o/c/a}$ is greater than $S_{o/c/w}$, the presence of air increases the overall probability of attachment of oil droplets to coal particles, and consequently increases the extent of agglomeration with low oil dosage. However, since there are only a limited number of air bubbles on the surface of nondegassed coal, most of the air

bubbles will be displaced by oil during the early stage of agglomeration. Therefore, as the presence of agglomeration is continued by adding more oil, the initial advantage of having air present on the surface will be lost and the response of degased coal to oil agglomeration will be similar to that of nondegassed coal. This probably explains why the coal recovery was higher for nondegassed coal than for degassed coal at low oil doses but not at high oil doses, as reported in Figures 7.6 - 7.10.

With increasing oil dosage, the number of oil droplets in the suspension increases and so does the probability of oil droplets colliding with coal particles, P_1. The overall probability of oil droplets becoming attached to degassed coal will increase too. Figures 7.6 - 7.10 show that when the oil dosage increased to 8 v/w% or more, there was a sharp drop in relative turbidity for degassed coal suspensions, which seems to support this theory.

When pentane was used, the difference in oil agglomeration response between degassed and nondegassed No. 2 Gas Seam coal was very small (see Figure 7.5), and this may have been because in the case of a nondegassed coal suspension, a portion of the pentane was carried away by air bubbles and was not available for agglomerating coal particles (details are described in next section). Although the presence of air bubbles made it easier for attachment between pentane droplets and the coal particles, the loss of pentane causd by air bubbles offset this effect.

In comparison with the other hydrocarbons, pentane is more soluble in water which may retard the decrease of turbidity of the suspension in the low oil dosage range, as less oil is available for agglomerating coal particles. This may explain why the behavior of Colchester coal with pentane (see Figure 7.11) is different from that observed with other hydrocarbons (see Figures 7.12 - 7.15).

When a long chain alcohol(n-octanol) was used as an agglomerant, the turbidity of the coal suspension declined very little until more than 4 v/w% (or 0.32 ml) n-octanol had been added (see Figure 7.10). Up to this point, most of the n-octanol would have dissolved in the water and would not have been available for agglomerating coal particles.

Degassing appeared to have little or no effect on the agglomeration response of Colchester coal suspensions(see Figures 7.11 - 7.15). It was observed that water readily spread on the surface of Colchester coal. In other words, Colchester coal was completely wetted by water without degassing. This meant that water would have displaced air almost completely from the surface of Colchester coal. Since air would not have been present coal surface, degassing would have had no effect. This explains why Figures 7.11 - 7.15 indicate no difference in the extent of agglomeration between degassed and nondegassed Colchester coal.

2. Effects of Oil Types on Agglomeration Response

Figure 7.17 compares the oil agglomeration response of degassed No. 2 Gas Seam coal with various hydrocarbons. In the absence of air, the oil viscosity and spreading coefficient may be the two most significant factors which affect the oil agglomeration response.

Figure 7.18 compares the oil agglomeration response of nondegassed No. 2 Gas Seam coal with different hydrocarbons. In the low oil dosage range (4 v/w% and below), the suspension with hexadecane underwent the largest change in relative turbidity, while the suspension with pentane underwent the smallest change. The relative turbidity (RT) of the suspensions with various oils decreased in the following

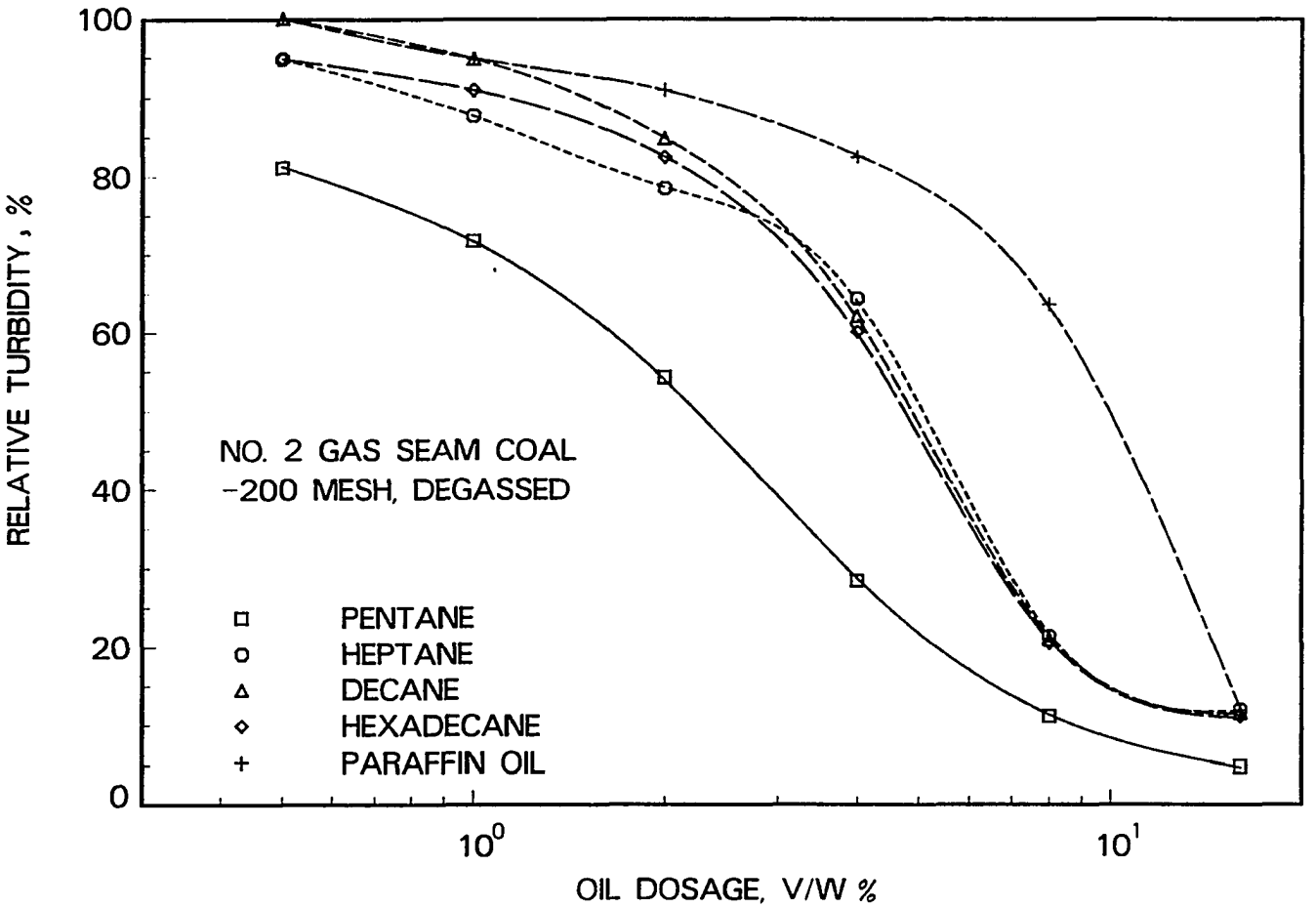

Figure 7.17: Results of agglomerating degassed No. 2 Gas Seam coal with various hydrocarbons

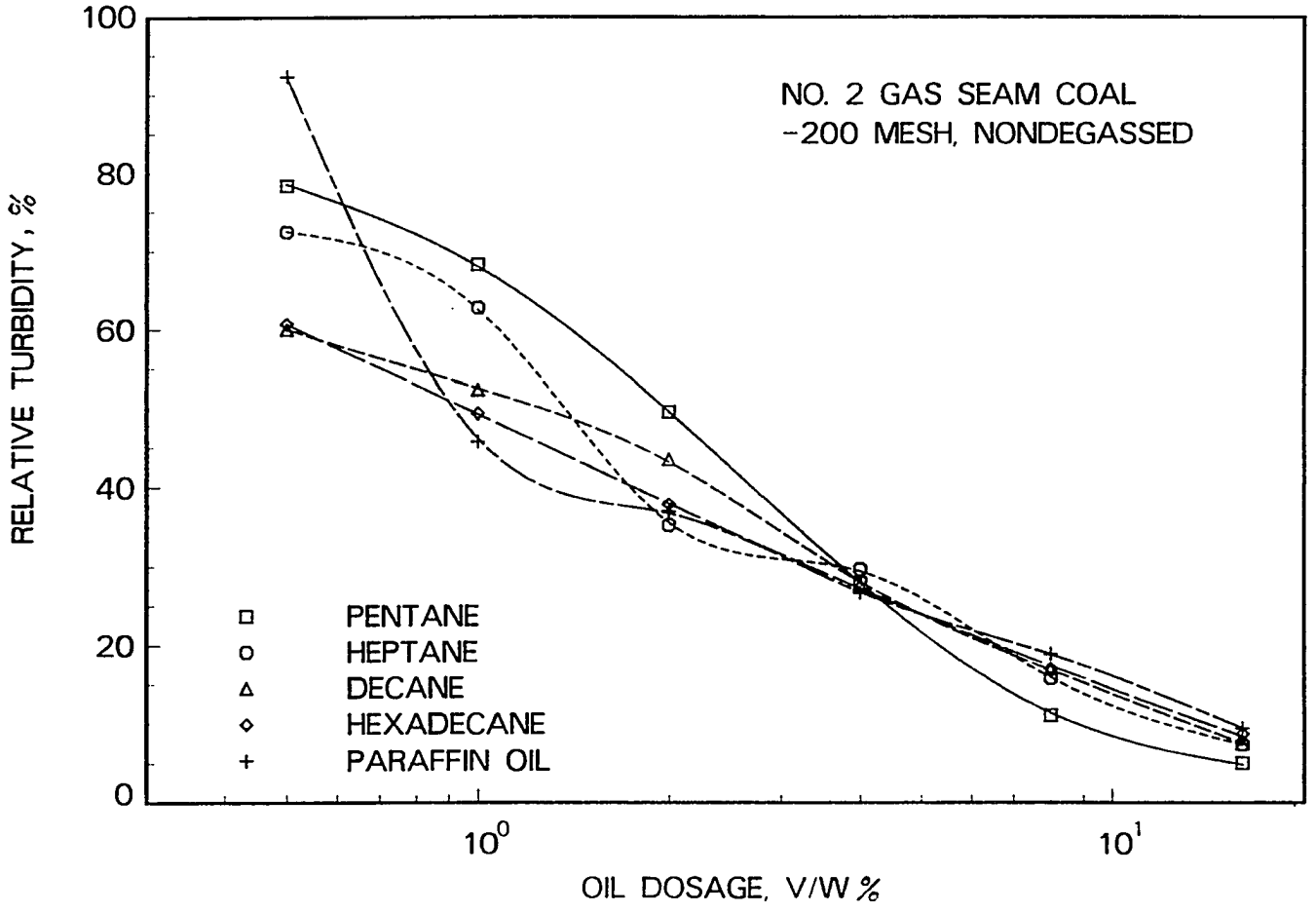

Figure 7.18: Results of agglomerating nondegassed No. 2 Gas Seam coal with various hydrocarbons

order:

$$RT_{pentane} < RT_{heptane} < RT_{decane} < RT_{hexadecane} < RT_{paraffin}$$

This order is similar to the order of the surface tension ($\gamma_{o/a}$) of these oils:

$$\gamma_{pentane} < \gamma_{heptane} < \gamma_{decane} < \gamma_{hexadecane} < \gamma_{paraffin}$$

The following theory is offered to explain the effect of different oils on agglomeration response. Since the surface tension of pentane is very small, pentane can very easily spread on air bubbles. Therefore when pentane displaces an air bubble from the coal surface in water, some of the pentane will be removed with the air bubble instead of coating the coal [63]. This results in less pentane being available to bridge between coal particles, and consequently reduces the oil agglomeration response which is reflected by a smaller change in relative turbidity. A hydrocarbon having a longer chain length and larger surface tension will spread less readily than pentane and less will be carried away by air bubbles. Therefore, more oil will be available for oil agglomeration, and the relative turbidity change will consequently be larger.

The preceding analysis does not explain the larger relative turbidity corresponding to a paraffin oil dosage of 0.5 v/w%. This anomaly may have been due to both the high viscosity and high surface tension of the oil which made it difficult to disperse in water.

Figure 7.18 also indicates an inversion point in the order of relative turbidity of coal suspensions with different oils. At an oil dosage of 4 v/w % the relative turbidity is almost identical for coal suspensions agglomerated with different oils. With an oil dosage higher than 4 v/w %, the order in the relative turbidity produced by different oils is opposite to that produced by different oils applied in smaller doses. This

Table 7.3: Three-phase contact angle and oil agglomeration response for degassed and nondegassed No. 2 Gas Seam coal with various oils, oil dosage was 16 v/w%

	Degassed coal		Nondegassed coal	
Oil	Contact angle, degrees	Relative turbidity change, %	Contact angle, degrees	Relative turbidity change, %
Pentane	45±1	95	74±1.5	95
Heptane	61±1	88	66±1.5	93
Decane	61±1	88	69±1.5	92
Hexadecane	61±1	89	67±1.5	91

suggests that with an oil dosage greater than 4 v/w %, most of the air bubbles have been displaced by oil; therefore, the effect of air no longer exists. The probability of oil droplets becoming attached to coal particles then only depends on the same oil-water-coal interactions as for degassed coal. Hence, the order in relative turbidity change becomes the same as for degassed coal.

As has been discussed previously, no air existed on Colchester coal in a stirred suspension. Hence, the difference in relative turbidity between different hydrocarbons shown in Figure 7.19 for Colchester coal is similar to that for degassed No. 2 Gas Seam coal.

Table 7.3 compares the measured three-phase contact angle and the relative turbidity change for degassed and nondegassed No. 2 Gas Seam coal with different hydrocarbons. It can be seen that degassed coal corresponds to smaller three-phase contact angles than nondegassed coal, which explains the lower relative turbidity

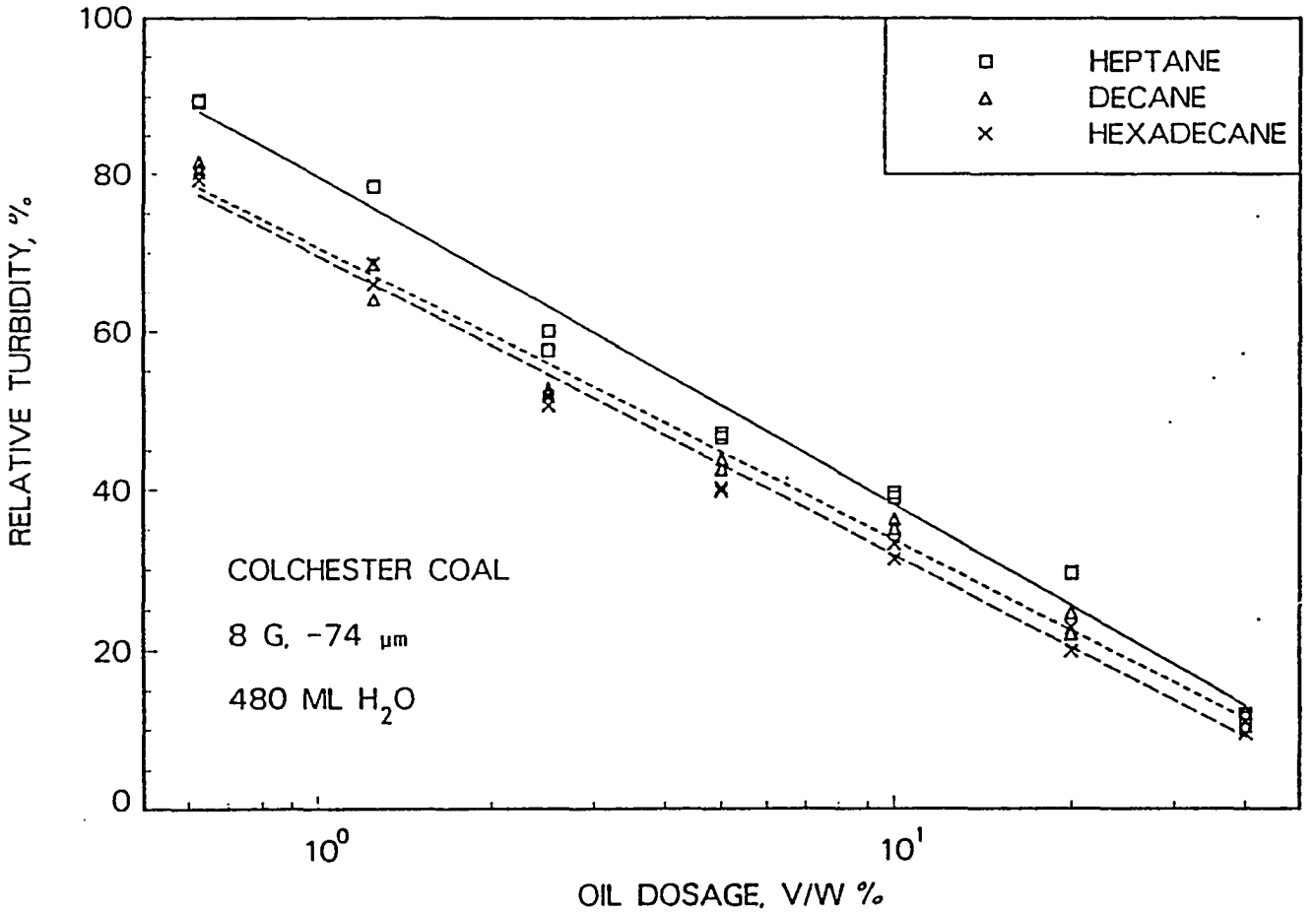

Figure 7.19: Results of agglomerating degassed and nondegassed Colchester coal with various hydrocarbons

changes observed for degassed coal than for nondegassed coal. However, except for pentane no differences in both the three-phase contact angle and the relative turbidity change were observed between different hydrocarbons.

CHAPTER 8. CONCLUSIONS AND RECOMMENDATIONS

Heat of Immersion

1. The heat of immersion can be used as an indicator for characterizing the surface of coal used in an oil agglomeration process.

2. The heat of immersion decreases with increasing coal moisture content, increases with decreasing coal rank, and varies with liquid type. The heat of immersion per unit mass (J/g) increases with decreasing particle size. Therefore, when comparing this surface property for different coal samples, the heat of immersion should be determined using coal samples having the same moisture content and particle size. The standard procedure described in Chapter 3 is recommended for equilibrating the coal moisture content. When comparing the heat of immersion of different coals or the interaction between a given coal and various liquid types, the comparison should be made for particles of the same size. Otherwise, the heat of immersion (J/g) must be measured for various size fractions and the comparison made based on the heat of immersion per unit of actual wetted surface area, h, which can be calculated by means of Equation 3.4.

Three-phase Contact Angle

1. The modified suction potential technique for three-phase contact angle measurement is more reliable and less time consuming than the original method.

2. The measured three-phase contact angle varies with coal rank, mineral matter content of coal, and oxygen functional group content on the coal surface.

The Effect of Coal Surface Oxidation

1. The concentration of hydrophobic functional groups on the coal surface decreases with increasing oxidation, while the concentration of hydrophilic groups increases. Consequently, the hydrophilicity index increases with increasing oxidation.

2. Both the heat of immersion in water and the three-phase contact angle depend on the oxygen functional group content and correlate with the hydrophilicity index. The heat of immersion of coal in water increases with increasing oxidation, and the three-phase contact angle measured through the water phase decreases.

3. The oil agglomeration response is degraded by oxidation of coal for a series of coal samples which have been oxidized to varying degrees. The oil agglomeration response of such a series correlates with the heat of immersion in water and also with the three-phase contact angle.

4. The relative turbidity change can be used as an alternative way to describe the agglomeration response. It can be determined more easily and more rapidly

than oil agglomeration recovery.

Involvement of Interfacial Phenomena in the Oil Agglomeration Process

1. Agglomerates are held together by oil bridges between coal particles. The oil-water interface of the bridge provides a force normal to the coal surface which holds the coal particles together. The magnitude of the force is $f = 2p \cdot \gamma_{ow} \cdot \sin\theta$. The more oleophilic/hydrophobic the coal surface, the smaller the three-phase contact angle, θ, measured through the oil phase and the larger the net force, f. An oil having a larger interfacial tension with water will provide a stronger force than an oil having a smaller interfacial tension with water.

2. The measured three-phase contact angle for the oil-water-pyrite system indicates that it is possible for oil to attach to pyrite particles, fresh or oxidized, and to agglomerate the pyrite particles. This explains the difficulty in completely separating pyrite from coal by the oil agglomeration process. It also suggests that to obtain a better separation between pyrite and coal, the three-phase contct angle of pyrite measured through the oil phase must be increased, and/or the three-phase contact angle of coal measured through the oil phase must be reduced.

3. The presence of air bubbles or an air film on a hydrophobic coal surface will favor the attachment of an oil droplet to the coal surface, and therefore will promote a higher initial agglomeration rate than would be experienced with degassed coal particles.

4. Water can completely replace air from a hydrophilic coal surface, and therefore,

degassing a hydrophilic coal suspension had no effect on the agglomeration process.

5. The surface tension and viscosity of the oil used for agglomeration may be important when air bubbles or an air film are present on a hydrophobic coal surface. The lower the surface tension of the oil, the more likely that some will be carried away by air bubbles, so less oil will be available for agglomerating coal particles. On the other hand, oils having a large surface tension will also tend to be more viscous and more difficult to disperse.

Recommendations

A mathematical model which includes the physical forces involved in the agglomeration process should be developed to describe the effects of coal surface properties, oil types, oil dosage, stirring speed and other agglomeration conditions on the agglomeration performance. The effect of viscosity of oils should be studied as well. The heat of immersion and the three-phase contact angle can be used to characterize the surface properties. The oil agglomeration response can be determined by measuring the oil agglomeration recovery or relative turbidity change. Coals representing a wide ranges of surface properties and oils having a broad range of interfacial tension with water, and oils having a broad range of viscosity should be used to test the model.

A new process which utilizes both oil droplets and air bubbles in the agglomeration process cna be developed to improve the oil agglomeration response of both hydrophobic and hydrophilic coal.

BIBLIOGRAPHY

[1] Diamond, S. "New Methods to Clean Coal," *New York Times,* 27 June 1985, 32.

[2] Mellish, M. L., *Mining Engineering* **1989**, 41(5), 334-336.

[3] Tsai, C. S. *Fundamentals of Coal Beneficiation and Utilization;* Elsevier Scientific Publishing Co.: New York, 1982.

[4] Fuerstenau, D. W.; Diao, J. "Surface Properties of Coal and Their Role in Coal Beneficiation"; Final Report, DOE/PC/90507-T13(DE90012250); University of California at Berkeley, March 1990.

[5] Aplan, F. F. In *Fine Coal Processing;* Mishra, S. K.; Klimpel, R. R. Ed.; Noyes Publications: New York, 1987, pp 19-53.

[6] Healy, T. W. *End of Grant Report Number 85;* The University of Melbourne, June 1982.

[7] Yang, G. C. C.; Drzymala, J. *Colloids and Surfaces* **1986**, 17, 313-315.

[8] Adamson, A. W. *Physical Chemistry of Surfaces,* 4th ed; John Wiley & Sons: New York, 1982.

[9] Zisman, W. A. In *Contact Angle, Wettability and Adhesion;* Advances in Chemistry Ser. 43; Gould, R. F. Ed.; ACS: Washington D. C., 1964, pp 1-51.

[10] Neumann, A. W.; Anner, W. J. *Colloid and Interface Sci.* **1970**, 34(1), 1-7.

[11] Drzymala, J., Ames Laboratory, private communication, 1989.

[12] Hollenbeck, R. G; Garnet E. P.; Kildsig, D. O. *J. Pharmaceutical Sci.* **1978**, 67(11), 1599-1606.

[13] Nordon, P. *Fuel* **1983**, 62, 619-621.

[14] Zettlemoyer, A. C.; Young, G. J.; Chessick, J. J. *J. Phys. Chem.* **1955**, 59, 962-966.

[15] Zettlemoyer, A. C.; Chessick, J. J. In *Contact Angle, Wettability and Adhesion;* Advances in Chemistry Ser. 43; Gould, R. F. Ed.; ACS: Washington D. C., 1964, pp 88-98.

[16] Everett, H. D. *Pure and Appl. Chem.* **1981**, 53, 2181-2198.

[17] Wierer, D. H.; Dobias, B. J. *Colloid and Interface Sci.;* **1988**, 122(1), 171-177.

[18] Griffith, M.; Hirst, W. *Proc. Conf. Ultrafine Struct. Coals Cokes,* BCURA: London, **1944**; p 80.

[19] Bond, R. L.; Magges, F. A. P. *Fuel* **1949**, 28, 172-175.

[20] Bangham, D. H.; Franklin, R. E.; Hirst, W.; Magges, F. A. P. *Fuel,* **1949**, 28, 231-238.

[21] Bond, R. L.; Spencer, D. H. T. *Soc. Chem. Ind. Proc. Conf. Ind. Carbon Graphite,* London, 1957, p 231.

[22] Berkowitz, N. *An introduction to coal technology,* Academic Press: New York, 1979, p 92.

[23] Fugassi, R.; Hudson, R.; Ostapchenko, G *Fuel,* **1958**, 37, 25-28.

[24] Robert, L.; Brusset, H. *Fuel,* **1965**, 44, 309-316.

[25] Robert, L.; Pregermain, S. *Fuel,* **1963**, 42, 389-393.

[26] Marsh, H. *Fuel,* **1965**, 44, 253-268.

[27] Spencer, D. H. T.; Bond, R. L. *Coal Science,* Advances in Chemistry, **55**, 724-733.

[28] Partyka, S.; Rouquerol, F.; Rouquerol, J. *J. of colloid and interface Sci.* **1979**, 68(1), 21-23.

[29] Harkins, W. D.; Jura, G. J. *J. Amer. Chem. Soc.,* **1944**, 66, 1362-1366.

[30] Harkins, W. D. *The physical chemistry of surface films,* Reinhold: New York, 1952, p 275.

[31] Glanville, J. O.; Hall, S. T; Messick, D. L.; Newcomb, K. L.; Phillips, K. M.; Webster, F; Wightman, J. P. *Fuel* **1986**, 65, 647-649.

[32] Starzewski, P.; Grillet, Y. *Calorim. anal. therm.* **1985**, 16, 84-91.

[33] Senkan, S. M.; Fuller, Jr., E. L. *Fuel,* **1979**, 58, 729-731.

[34] Hercules, D. M. " Characterization of Oxidized Coal Surfaces". *Fossil Final Report.* DOE/PC/90527-T8 (DE90002400), 1989.

[35] Duplessis, H. G.; Reinecke, C. F.; Van Nierop, J. G. *Proc. Int. Conf. on Coal Science.* Sidney, 1985, 521-524.

[36] Fuerstenau, D. W.; Williams, M. G.;Narayanan, K. S. Diao, J. L.; Urbina, R. H. "Assessing the Wettability and Degree of Oxidation of Coal by Film Flotation", *Energy and Fuel* **1988**, 2(3), 237-241.

[37] Sadowski, Z.; Venkatadri, R.; Druding, J. M.; Markuszewski, R.; Wheelock, T. D. *Coal Preparation* **1988**, 6, 17-34.

[38] Nandi, S. P.; Ramadass, V.; Walker, P. L. *Carbon* **1964**, 2, 199-210.

[39] Phillips, K. M.; Glanville, J. O.; Wightman, J. P. *Colloid and Surfaces* **1987**, 21, 1-8.

[40] Ye, Y.; Jin, R.; Miller, J. D. *Coal Preparation,* **1988**, 6, 1-16.

[41] Fuchs, W. *Brennstoff-Chem.* **1927**, 8, 337.

[42] Brooks, J. D.; Sternhell, S. *Aust. J. Appl. Sci.* **1957**, 8, 206-221.

[43] Schafer, H. N. *Fuel,* **1970**, 49, 197-213.

[44] Schafer, H. N. *Fuel,* **1970**, 49, 271-280.

[45] Gethner, J. S. *Applied Spectroscopy* **1987**, 41, 50-63.

[46] Bartell, F. E.; Osterhof, H. J. *Ind. Eng. Chem.* **1927**, 19, 1277-1280.

[47] Haines, W. B. *Jour. Agric. Sci.* **1927**, 7, **1930**, 20.

[48] Bailey, R.; Gray, V. R. *J. Appl. Chem.* **1958**, 8, 197-202.

[49] Gray, V. R. *J. Inst. Fuel* **1958**, 31, 96-108.

[50] Handfield-Jones, R. V. R. M. Ph. Thesis, University of Nottingham, 1973.

[51] Brookes, G. F.; Bethel, P. J. *Powder Technology* **1984**, 40, 207-214.

[52] Hanning, R. N.; Rutter, P. R. *Inter. J. Mineral Processing,* **1989**, 27, 133-146.

[53] Wei, D.; Chander, S.; Hogg, R. *Fine Coal Cleaning,* Palm Coast, Florida, USA, December 2-7, 1990.

[54] Ayat, M. G. *Powder Handling and Processing* **1989**, 1(1), 117-121.

[55] Vargha-Butler, E. I.; Absolom, D. R.; Neumann, A. W.; and Hamza, H. A. in *Interfacial Phenomena in Coal Technology,* Gregory D. Botsaris; Yuli M. Glazman, ed, Surfactant Sci. series, Vol 32, 1989, pp 33-84.

[56] Vargha-Butler, E. I.; Soulard, M. R.; Neumann, A. W.; Hamza, H. A. *CIM Bull.* **1981**, 74(836), 54-58.

[57] Soulard, M. R.; Vargha-Butler, E. I.; Hamza, H. A.; Neumann, A. W. *Chem. Eng. Commun.* **1983**, 21, 329-344.

[58] Johnson, R. E.; Dettre, R. H. In *Contact Angle, Wettability and Adhesion;* Advances in Chemistry Ser. 43; Gould, R. F. Ed.; ACS: Washington D. C., 1964, pp 112-135.

[59] Dettre, R. H.; Johnson, R. E. In *Contact Angle, Wettability and Adhesion;* Advances in Chemistry Ser. 43; Gould, R. F. Ed.; ACS: Washington D. C., 1964, pp 136-144.

[60] Drzymala, J., R. Markuszewski and T. D. Wheelock, *International Journal of Mineral Processing,* **1986**, 18, 277-286.

[61] Sharpe, L. H.; Schonhorn, H. In *Contact Angle, Wettability and Adhesion;* Advances in Chemistry Ser. 43; Gould, R. F. Ed.; ACS: Washington D. C., 1964, pp 189-201.

[62] Allen, R. W.; Wheelock, T. D. presented at *AIChE Annual Meeting,* Chicago, November, 1990.

[63] Brown, D. J.; Gray, V. R.; Jackson, A. W. *J. Appl. Chem.* **1958**, 8, 752-759.

[64] Moxon, N. T.; Bensley, C. N.; Keast-Jones, R.; Nicol, S. K. *International J. of Mineral Processing* **1987**, 21, 261-274.

[65] Agroskin, A. A.; Petrenko, I. G. *Zh. prikl. Khim.,* **1946**, 19, 737-746.

[66] Brady, G. A.; Gauger, A. W. *Industr. Engng. Chem.,* **1940**, 32, 1599.

[67] Jacques, M. T.; Hovarongkura, A. D.; Henry, J. D., Jr. *AIChE Journal* **1979**, 25(1), 160-170.

[68] Good, R. J.; Islam, M. *Langmuir* **1991**, 7, 3219-3221.

[69] Good, R.J.; Srivatsa, N. R.; Islam, M.; Huang, H. T. L.; Vanoss, C. J. *J. Adhesion Sci. Technol.* **1990**, 4(8), 607-617.

[70] Dunstan, D.; White, L. R. *J. Colloid and Interface Sci.*, **1986**, 111(1), 60-64.

APPENDIX A. AN ANALYSIS OF THE THREE-PHASE CONTACT ANGLE MEASUREMENT SYSTEM

Nomenclature

A	=	cross-sectional area of the sample holder, cm^2
A'	=	cross-sectional area of the bed voids, cm^2,
h_f	=	the height of water overflow, cm
h_w	=	the height of water from the base line to the top surface of the sintered plate, cm
Δh_1	=	the height of oil, cm
Δh_2	=	the height of water above the coal, cm
Δh_3	=	the maximum height of water in the coal bed, equivalent to the height of coal, cm
Δh_4	=	the height of water in the coal bed, when the oil-air interface just reaches the surface of the coal bed, cm
P_a	=	atmospheric pressure, cm H_2O
P_s	=	vacuum pressure of the system, cm H_2O

$\Delta P_{c/w/o}$ = suction pressure needed to overcome the surface tension of the water-oil interface on the coal surface, cm H_2O

$\Delta P_{c/o/a}$ = suction pressure needed to overcome the surface tension of the oil-air interface on the coal surface, cm H_2O

$\Delta P_{s/w/o}$ = suction pressure needed to overcome the surface tension of the water-oil interface on the surface of the sintered plate, cm H_2O

ΔP_m^i = pressure difference measured by manometer, cmH_2O, $i = 1, 2, 3...$

ε_b = void fraction of coal bed

ρ_o = density of oil, g/cm^3

ρ_w = density of water, g/cm^3

Hydraulic and Mechanical Analysis of the System

A hydraulic and mechanical analysis was made of the system illustrated by Figure A.1. A layer of coal particles is placed in the sample holder on the sintered plate. The coal bed is immersed in deionized water. At the beginning of the measurement, the water level is set above the top surface of the coal bed. A layer of oil which is immiscible with water is placed on top of the water.

At the start, the fluids are still and the following pressure balance applies:

$$P_s + h_f = P_a + h_w + \Delta h_3 + \Delta h_2 + \Delta h_1 \cdot \frac{\rho_o}{\rho_w} \qquad \text{(A.1)}$$

$$P_a - P_s = (h_f - h_w) - (\Delta h_3 + \Delta h_2 + \Delta h_1 \cdot \frac{\rho_o}{\rho_w})$$

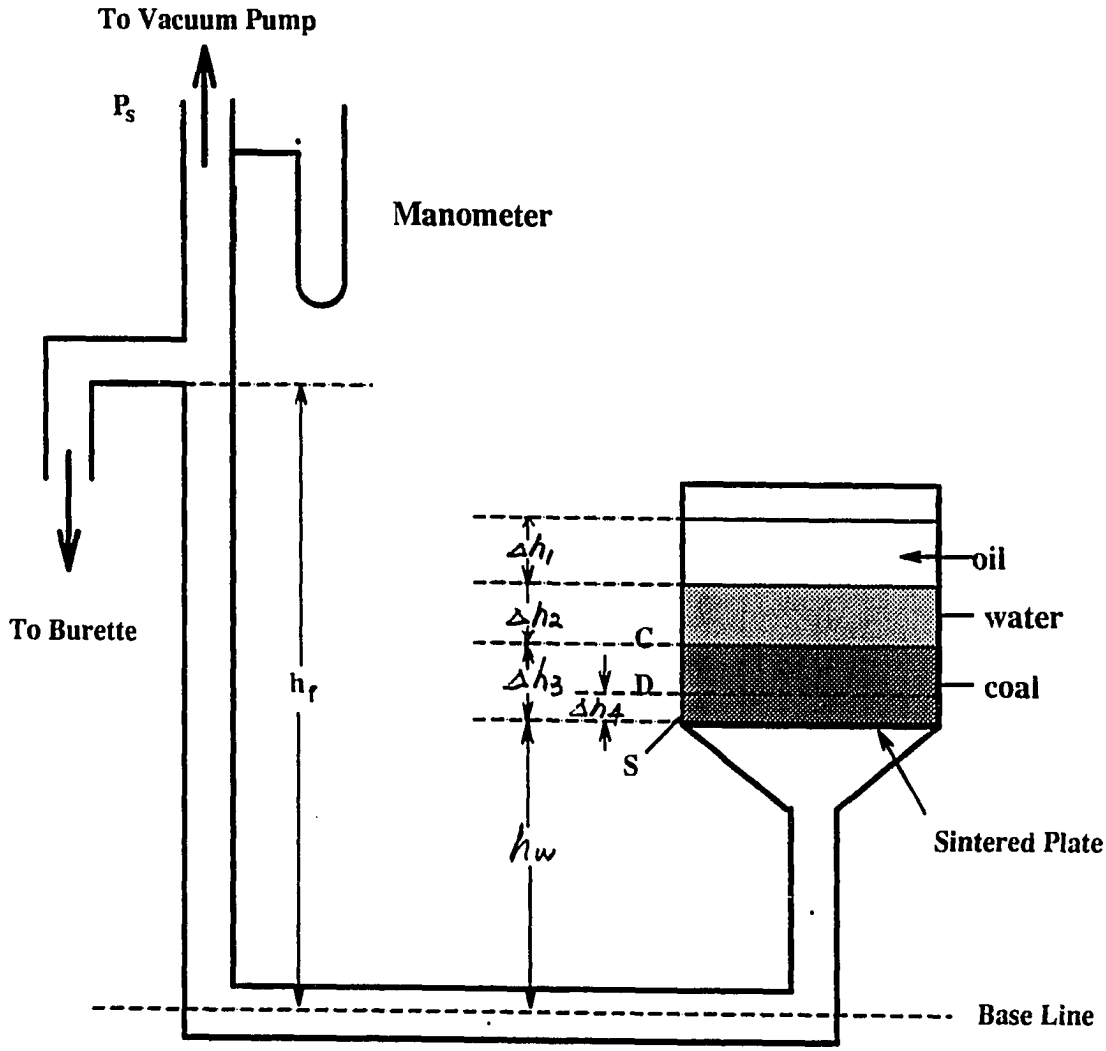

Figure A.1: A detailed illustration of the critical portion of the three-phase contact angle measurement apparatus

where $(P_a - P_s)$ is the pressure difference ΔP_m^i measured by the manometer. The initial manometer reading will be given by the expression,

$$\Delta P_m^1 = (h_f - h_w) - (\Delta h_3 + \Delta h_2 + \Delta h_1 \cdot \frac{\rho_o}{\rho_w}) \tag{A.2}$$

As the suction pressure is increased, water is drawn through the bed and Δh_2 decreases. When the water-oil interface reaches C, $\Delta h_2 \rightarrow 0$. At this point, Equation A.2 becomes

$$\Delta P_m^2 = (h_f - h_w) - (\Delta h_3 + \Delta h_1 \cdot \frac{\rho_o}{\rho_w}) \tag{A.3}$$

Since $(h_f - h_w)$ remains constant during the whole procedure, the incremental change in suction pressure for this step is given by subtracting Equation A.2 from Equation A.3:

$$\Delta P_m^2 - \Delta P_m^1 = \Delta h_2 \tag{A.4}$$

The preceding analysis assumes that the loss of oil is negligible, that is, Δh_1 is constant before oil is drawn into the coal bed.

A larger pressure is needed to overcome the surface tension and draw the water-oil interface into the coal bed. At the point that the water-oil interface just starts to enter the bed, the pressure balance becomes:

$$\Delta P_m^3 = (h_f - h_w) - (\Delta h_3 + \Delta h_1 \cdot \frac{\rho_o}{\rho_w}) + \Delta P_{c/w/o} \tag{A.5}$$

The incremental change in suction pressure required for drawing the water-oil interface into the bed is given by subtracting Equation A.3 from Equation A.5:

$$\Delta P_m^3 - \Delta P_m^2 = \Delta P_{c/w/o} \tag{A.6}$$

Assuming that $\Delta P_{c/w/o}$ remains constant, once the interface has started to move, only Δh_3 and Δh_1 in Equation A.5 will change as water is drawn through the bed. As the oil is drawn into the bed, however, the height of the oil layer will increase because A' is smaller than A. When the oil-air interface reaches the surface of the bed, at point C, the water-oil interface reaches point D. The height of water in the bed is Δh_4. Therefore, the height of the oil layer in the bed is

$$\Delta h_3 - \Delta h_4 = \frac{\Delta h_1 A}{A'} = \frac{\Delta h_1 A}{A\varepsilon_b} \tag{A.7}$$

hence,

$$\Delta h_4 = \Delta h_3 - \frac{\Delta h_1}{\varepsilon_b} \tag{A.8}$$

At this point the pressure difference measured by the manometer is given by the expression,

$$\Delta P_m^4 = (h_f - h_w) - \Delta h_3 - \frac{\Delta h_1}{\varepsilon_b} + \frac{\Delta h_1}{\varepsilon_b} \cdot \frac{\rho_o}{\rho_w} + \Delta P_{c/w/o} \tag{A.9}$$

Subtracting Equation A.5 from Equation A.9 gives the incremental change in suction pressure for the step in which the oil layer is drawn into the bed.

$$\Delta P_m^4 - \Delta P_m^3 = \frac{\Delta h_1}{\varepsilon_b} - (\frac{\Delta h_1}{\varepsilon_b} - \Delta h_1)\frac{\rho_o}{\rho_w} \tag{A.10}$$

A higher pressure is needed to draw the oil-air interface into the coal bed. When the oil-air interface is just about to enter the bed, the manometer reading will be

$$\Delta P_m^5 = (h_f - h_w) - \Delta h_3 - \frac{\Delta h_1}{\varepsilon_b} + \frac{\Delta h_1}{\varepsilon_b} \cdot \frac{\rho_o}{\rho_w} + \Delta P_{c/w/o} + \Delta P_{c/o/a} \tag{A.11}$$

The incremental change in suction pressure required to draw the air-oil inteface into the bed is given by subtracting Equation A.9 from Equation A.11.

$$\Delta P_m^5 - \Delta P_m^4 = \Delta P_{c/o/a} \tag{A.12}$$

As the oil-air interface moves down through the bed, the water-oil interface will eventually touch the top surface of the sintered plate. Since the resistance of the sintered plate to the water-oil interface is very large, the interface will not be drawn into the sintered plate within the pressure range of this measurement. At this point, $\Delta h_4 = 0$ and $\Delta h_3 = 0$, and the height of the oil in the bed is $\frac{\Delta h_1}{\varepsilon_b}$, hence,

$$\Delta P_m^6 = (h_f - h_w) + \frac{\Delta h_1}{\varepsilon_b} \cdot \frac{\rho_o}{\rho_w} + \Delta P_{c/w/o} + \Delta P_{c/o/a} \tag{A.13}$$

Subtracting Equation A.11 from Equation A.13 gives

$$\Delta P_m^6 - \Delta P_m^5 = \frac{\Delta h_1}{\varepsilon_b} \tag{A.14}$$

According to the above analysis, the following relationships exist between ΔP and ΔV which are shown in Figure A.2.

1. Stage I: draining water:

$$\Delta P_1 = \Delta P_m^2 - \Delta P_m^1 = \Delta h_2$$

$$\Delta V_1 = \Delta h_2 A = \Delta P_1 A \tag{A.15}$$

2. Stage II: water-oil interface touches the top surface of coal bed:

$$\Delta P_2 = \Delta P_m^3 - \Delta P_m^2 = \Delta P_{c/w/o}$$

$$\Delta V = 0 \tag{A.16}$$

3. Stage III: drawing oil into the coal bed:

$$\Delta P_3 = \Delta P_m^4 - \Delta P_m^3 = \frac{\Delta h_1}{\varepsilon_b} - (\frac{\Delta h_1}{\varepsilon_b} - \Delta h_1)\frac{\rho_o}{\rho_w}$$

$$\Delta V_3 = A\Delta h_1 = \frac{A\varepsilon_b}{1 - (1 - \varepsilon_b)\frac{\rho_o}{\rho_w}} \cdot \Delta P_3 \tag{A.17}$$

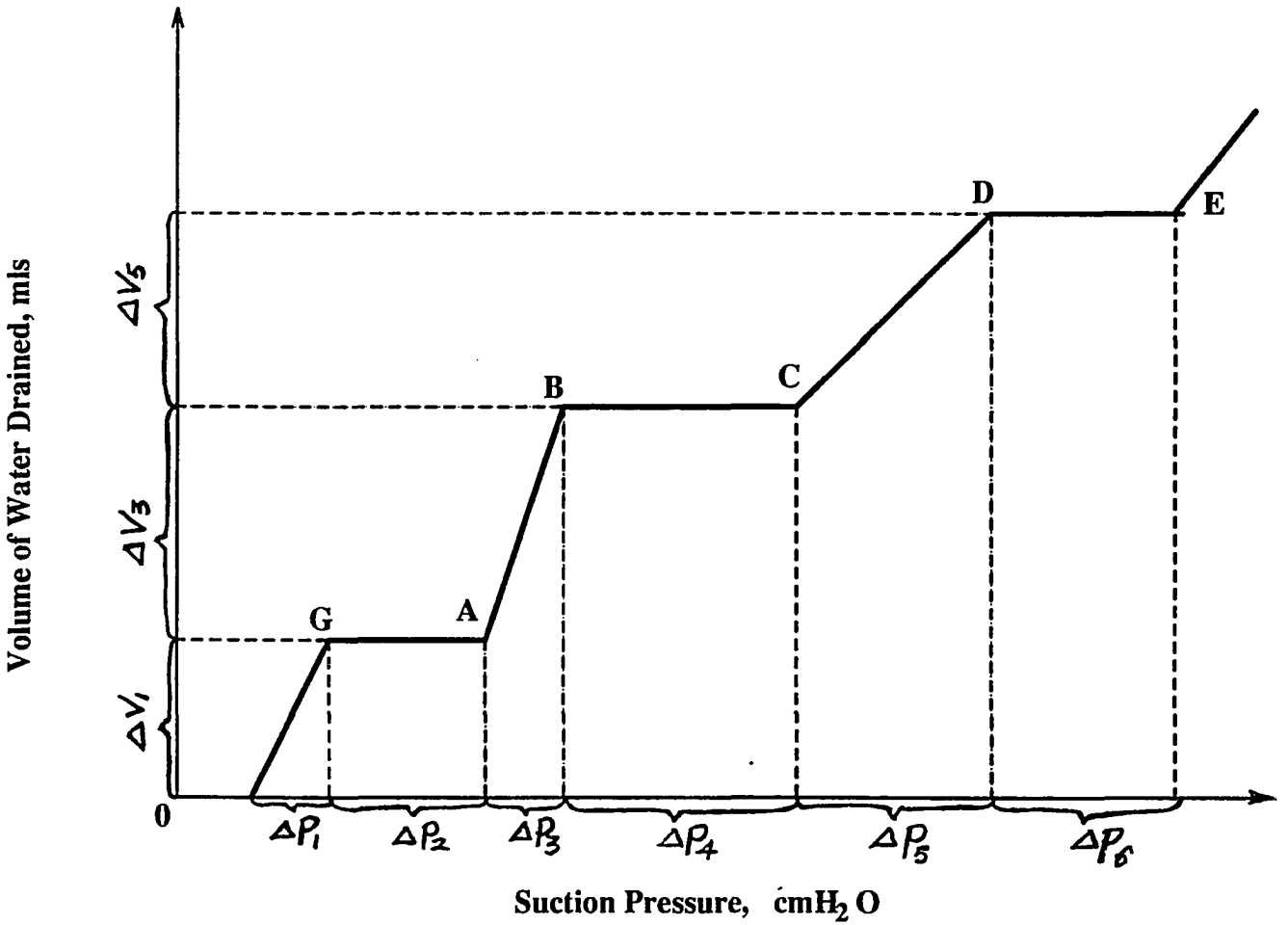

Figure A.2: An ideal typical suction potential curve

4. Stage IV: oil-air interface touches the top surface of the coal bed:

$$\Delta P_4 = \Delta P_m^5 - \Delta P_m^4 = \Delta P_{c/o/a}$$

$$\Delta V_4 = 0 \tag{A.18}$$

5. Stage V: drawing oil-air interface into the coal bed:

$$\Delta P_5 = \Delta P_m^6 - \Delta P_m^5 = \Delta h_3 - \frac{\Delta h_1}{\varepsilon_b}$$

$$\Delta V_5 = (\Delta h_3 - \frac{\Delta h_1}{\varepsilon_b}) A\varepsilon_b = A\varepsilon_b \cdot \Delta P_5 \tag{A.19}$$

6. Stage VI: water-oil interface touches the sintered pate:

$$\Delta P_6 = \Delta P_{s/w/o}$$

$$\Delta V_6 = 0 \tag{A.20}$$

Analysis of the relationship between ΔP and three-phase contact angle

Basic Assumptions:

1. Particles are uniform spheres with diameter d_p.

2. There are n particles in the cross-sectional area of the sample holder at the interface.

3. The cross-sectional area of every particle at the interface is the same, and is given by

$$S = \frac{\pi d_p^2}{4}$$

Since assumptions 1 and 2 may not apply to an actual bed of coal particles, a correction factor, k, is introduced into the preceding equation to obtain

$$\bar{S} = k\pi\frac{d_p^2}{4} \tag{A.21}$$

Hence, the number of particles occupying the sample holder cross section will be

$$n = \frac{A(1-\varepsilon_b)}{\bar{S}} = \frac{4A(1-\varepsilon_b)}{k\pi d_p^2} \tag{A.22}$$

Since the surface tension on a coal surface due to the interface between phase i and phase j is

$$\gamma_{ij}\cos\theta, \quad dyne/cm$$

the force needed to overcome the surface tension and to move the interface through each particle is

$$\pi d_p \gamma_{ij}\cos\theta, \quad dyne$$

For the n particles at the interface, the force needed to move the interface through the bed of particles is given by

$$\pi d_p n\gamma_{ij}\cos\theta, \quad dyne$$

and the correspondig pressure is

$$\Delta P = \frac{Force}{Area\ of\ liquid}$$

Therefore, the suction pressure needed to move the interface is

$$\Delta P = \pi d_p n\frac{\gamma_{ij}\cos\theta}{A\varepsilon_b}, \quad dynes/cm^2 \tag{A.23}$$

Substituting Equation A.22 into Equation A.23 gives

$$\Delta P = \frac{4\gamma_{ij}\cos\theta}{d_p} \cdot \frac{1-\varepsilon_b}{k\varepsilon_b}, \quad dynes/cm^2 \tag{A.24}$$

If ΔP is expressed directly in $\mathrm{cm}H_2O$,

$$\Delta P = \frac{4\gamma_{ij}\cos\theta}{d_p} \cdot \frac{1-\varepsilon_b}{k\varepsilon_b} \cdot \frac{1}{\rho_w g}, \quad dynes/cm^2 \tag{A.25}$$

Hence, for the water-oil interface the preceding expression will become,

$$\Delta P_{c/w/o} = \frac{4\gamma_{w/o}\cos\theta_{w/o}}{d_p} \cdot \frac{1-\varepsilon_b}{k\varepsilon_b} \cdot \frac{1}{\rho_w g}, \quad dynes/cm^2 \tag{A.26}$$

and for the oil-air interface the expression will become

$$\Delta P_{c/o/a} = \frac{4\gamma_{o/a}\cos\theta_{o/a}}{d_p} \cdot \frac{1-\varepsilon_b}{k\varepsilon_b} \cdot \frac{1}{\rho_w g}, \quad dynes/cm^2 \tag{A.27}$$

Assuming that ε_b remains constant during the measurement, the correction constant k should also remain constant as it is related to bed packing and particle size. Therefore, dividing Equation A.26 by Equation A.27 gives:

$$\frac{\Delta P_{c/w/o}}{\Delta P_{c/o/a}} = \frac{\gamma_{w/o}\cos\theta_{w/o}}{\gamma_{o/a}\cos\theta_{o/a}} \tag{A.28}$$

If $\cos\theta_{o/a} = 1$, this reduces to the following:

$$\cos\theta_{w/o} = \frac{\Delta P_{c/w/o}}{\Delta P_{c/o/a}} \cdot \frac{\gamma_{o/a}}{\gamma_{w/o}} \tag{A.29}$$

Equations A.28 and A.29 are the same as equations reported in the literature [50][51][54].

Discussion

According to Equation A.15, the slope of $the\Delta V - \Delta P$ curve for Stage I is A, a constant. Equation A.17 shows that the slope of the $\Delta V - \Delta P$ curve for Stage III is

$\frac{A\varepsilon_b}{1-(1-\varepsilon_b)\frac{\rho_o}{\rho_w}}$, and A.19 shows that the slope of $\Delta V - \Delta P$ curve for Stage V is $A\varepsilon_b$. Therefore, the slopes for stage III and Stage V will be affected by the void fraction of the coal bed, ε_b, which is related to the packing and particle size distribution of the coal particles. Also because

$$1-(1-\varepsilon_b)\frac{\rho_o}{\rho_w} < 1$$

it follows that

$$\frac{A\varepsilon_b}{1-(1-\varepsilon_b)\frac{\rho_o}{\rho_w}} > A\varepsilon_b$$

Therefore, the slope for Stage III is always steeper than the slope for Stage V. The slopes for Stage III and V will both decrease with decreasing void fraction, ε_b; that is, if the bed is packed tighter, both lines will become flatter. The slope of the line for Stage I is also related to the ratio of densities of oil and water, but this ratio is constant for a given oil.

According to the previous analysis, the $\Delta V - \Delta P$ curve for each stage should be a straight line. However, the experiment curve is not always so. Some experimental points in Stages III and V are not on straight lines as they should be, especially those near Stages II and IV. This can be explained by the non-uniformity of the capillaries formed between coal particles.

Equations A.26 and A.27 show that the particle size, d_p, and the bed void fraction, ε_b, will affect the suction pressure required to draw both the water-oil and oil-air interfaces into the bed. The suction pressure will increase with decreasing particle size, d_p, and with decreasing bed void fraction, ε_b.

Equation A.23 is similar to the following equation derived by Dunstan and White [70]:

$$\Delta P = (1 - \varepsilon_b)\rho_s \bar{A} \frac{\gamma \cos\theta}{\varepsilon_b} \tag{A.30}$$

where

ρ_s = density of particle, g/cm^3,

$\bar{A}$ = specific surface area per gram of solid.

Since for a sphere,

$$\rho_s \bar{A} = \frac{6}{d_p}$$

and by taking $k = 2/3$, Equation A.24 becomes identical to Equation A.30.

APPENDIX B. COMPARISON OF TIME REQUIRED TO REACH EQUILIBRIUM BY THE ORIGINAL AND MODIFIED TECHNIQUES FOR MEASURING THE THREE-PHASE CONTACT ANGLE

The flow rate of liquids in the sample holder is given by the expression

$$Q(vol/time) = \frac{dV}{dt} = A_s \frac{dh_s}{dt} \tag{B.1}$$

According to the modified Darcy equation, the rate of fluid flowing through a packed bed of solids, in laminar flow is

$$Q = \frac{KA_s\Delta P}{\eta L} \tag{B.2}$$

where

A_s = cross-sectional area of liquid in the sample holder

h_s = height of the liquid in the sample holder

A_t = cross-sectional area of liquid in the adjustable tube

h_t = height of liquid in the adjustable tube

ΔP = the pressure difference across the bed of solids

η = viscosity of liquid

L = thickness of the solid bed

K = "permeability" constant

For the original suction potential method, a pressure increment ΔP_i is set to move the interfaces in order to reach an equilibrium point. ΔP_i is measured in cm

H_2O. To reach a pressure equilibrium point, a certain volume of water must be drawn from the coal bed and conducted to the burette to balance the pressure change. This volume can be calculated by Equations A.15, A.17 and A.19 for Stage I, III, and V, respectively. For Stage I

$$\Delta V = A_s \Delta h_s = A_s \Delta P$$

$$dP = -dh_s \tag{B.3}$$

Combining Equations B.1 and B.3 gives the following:

$$Q = A_s \frac{dh_s}{dt} = -A_s \frac{d\Delta P}{dt} = -\frac{K A_s \Delta P}{\eta L}$$

$$dt = -\frac{\eta L}{K} \frac{d\Delta P}{\Delta P} = -\frac{\eta L}{K} d(ln\Delta P)$$

The time required to reach the equilibrium state is the time required for the pressure difference across the coal bed to become zero, that is, for $\Delta P_f = 0$, so

$$t = \lim_{\Delta P_f \to 0} \int_{\Delta P_f}^{\Delta P_i} \frac{\eta L}{K} d(ln\Delta P) = \frac{\eta L}{K} [\lim_{\Delta P_f \to 0} (ln\Delta P_i - ln\Delta P_f)] \tag{B.4}$$

Since it would take forever for $\Delta P_f \to 0$, it must be assumed that equilibrium is achieved when ΔP_f reaches a predetermined value. Then, the time required will be

$$t = \frac{\eta L}{K} (ln \frac{\Delta P_i}{\Delta P_f}) \tag{B.5}$$

For the modified suction potential technique, the mechanism for balancing the pressure is different. No water is drained out to the burette. Instead, the pressure difference across the coal bed drives a small amount of water up in the adjustable tube, the increase of water level in the adjustable tube balances the pressure difference across the coal bed. For Stage I in Figure A.2, Equations B.1 and B.2 still hold, but Equation B.3 is different.

An infinitessmal change in the water level in the adjustable tube becomes an infinitesmal change in the water level in the sample holder.

$$dV = A_s dh_s = -A_t dh_t$$

$$-dh_t = \frac{A_s}{A_t} dh_s$$

$$d\Delta P = -(\mid dh_s \mid + \mid dh_t \mid)$$

$$d\Delta P = -(1 + \frac{A_s}{A_t}) dh_s \tag{B.6}$$

$$Then \qquad Q = A_s \frac{dh_s}{dt} = -A_s \frac{1}{1 + \frac{A_s}{A_t}} \frac{d\Delta P}{dt} = -\frac{K A_s \Delta P}{\eta L}$$

For the same initial and final pressure differences across the coal bed, ΔP_i and ΔP_f, we have

$$t = \frac{1}{1 + \frac{A_s}{A_t}} \frac{\eta L}{K} (ln \frac{\Delta P_i}{\Delta P_f}) \tag{B.7}$$

For the system we used, $\frac{A_s}{A_t} = 20.25$, so the time required to reach the equilibrium in Stage I by the modified technique is only 1/20 of the time required by the old technique. Similar results can be obtained also for Stage II and Stage V.

APPENDIX C. THERMODYNAMIC RELATIONSHIP BETWEEN THE HEAT OF IMMERSION AND THE CONTACT ANGLE

By definition, the Gibbs free energy is

$$G = H - TS \tag{C.1}$$

The following is another basic thermodynamic expression for a closed system:

$$dG = V\ dP - S\ dT \tag{C.2}$$

When pressure is held constant, the preceding equation reduces to

$$\left(\frac{\partial G}{\partial T}\right)_p = -S \tag{C.3}$$

Substituting this expression for S in Equation C.1 gives

$$G = H + T\left(\frac{\partial G}{\partial T}\right)_p$$

Differentiating this equation yields

$$dG = dH + \left(\frac{\partial G}{\partial T}\right)_p dT + T\ d\left(\frac{\partial G}{\partial T}\right)_p \tag{C.4}$$

When temperature is held constant, $dT = 0$, and Equation C.4 reduces to

$$dG_T = dH_T + T\ d\left(\frac{\partial G}{\partial T}\right)_{p,T}$$

Integration at constant temperature yields

$$\Delta G_T = \Delta H_T + T\Delta \left(\frac{\partial G}{\partial T}\right)_{p,T}$$

which is equivalent to

$$\Delta G_T = \Delta H_T + T \left(\frac{\partial \Delta G}{\partial T}\right)_{p,T} \tag{C.5}$$

Therefore, rearranging this expression gives

$$-\Delta H_T = -\Delta G_T + T \left(\frac{\partial \Delta G}{\partial T}\right)_{p,T} \tag{C.6}$$

1. Liquid-Vapor-Solid System

For a three-phase system in which a given solid is saturated initially with a given liquid vapor, the immersion process can be represented schematically by Figure C.1:

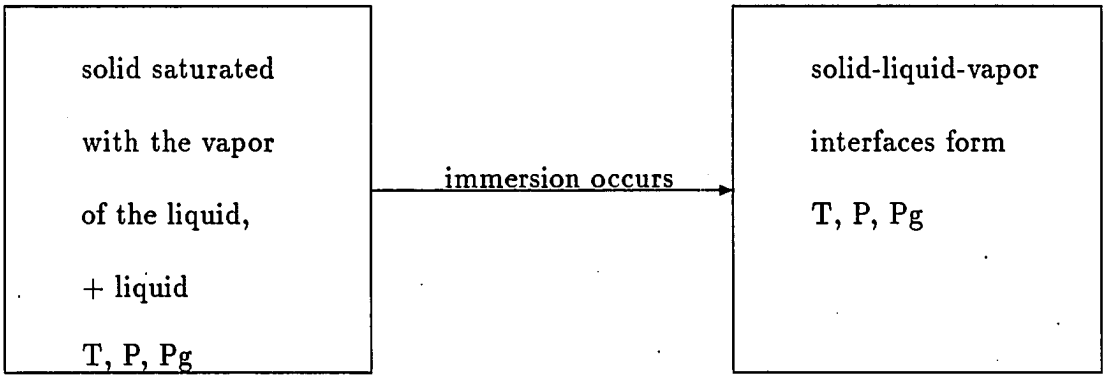

Figure C.1: Schematic representation of the immersion process

where

P = total system pressure,

T = temperature of system,

Pg = partial pressure of the liquid.

For a solid-liquid-vapor system at equilibrium, the well known Young's Equation is:

$$-\Delta G = \gamma_{sv} - \gamma_{sl} = \gamma_{lv} cos\ \theta_{slv}. \tag{C.7}$$

Substituting Equation C.7 into Equation C.6 gives:

$$-\Delta H = \left[\gamma_{lv} - T\left(\frac{\partial \gamma_{lv}}{\partial T}\right)_p\right] cos\ \theta_{slv} - \gamma_{lv} T \left(\frac{\partial cos\ \theta_{slv}}{\partial T}\right)_p. \tag{C.8}$$

When a powder with a clean surface is immersed into a liquid, heat is released. The heat is usually denoted as the integral heat of wetting or heat of immersion if there are no unusual interactions. Equation C.8 provides a theoretical basis for relating the heat of immersion to the surface hydrophobicity as represented by the contact angle.

Thermodynamically speaking, the preceding relationship holds when the process is conducted reversibly at constant temperature and pressure. The heat of immersion is defined by the following expression:

$$Q_w = E_{sv} - E_{sl}$$

where

Q_w = generated heat of wetting, erg/g solid,

E_{sv} = total surface energy of solid saturated with vapor, erg/g solid,

E_{sl} = total surface energy of solid immersed in liquid, erg/g solid

For the immersion process, the heat of immersion is equal to the enthalpy change because no work is done by the system and other forms of energy should be negligible.

$$-\Delta H = H_{sv} - H_{sl} = E_{sv} - E_{sl} \tag{C.9}$$

Usually , $-\Delta H$ is expressed as ergs per square centimeter of surface so the relationship between the enthalpy change and the heat of wetting becomes

$$-\Delta H = H_{sv} - H_{sl} = \frac{Q_w}{A} \tag{C.10}$$

where A is the specific surface area of the solid, cm^2/g. Therefore, the experimental heat of wetting can be correlated theoretically with the contact angle by Equations C.8 and C.10. However, the relationship is complicated. The parenthetical term is constant under given T and P. It is the last term in Equation C.8 which makes the contact angle difficult to calculate using Equation C.8. However, one study [10] showed that the change in contact angle with temperature is small; therefore, the last term may be negligible compared with the first term. For some systems, the following truncated forms of Equation C.8 may be sufficiently accurate:

$$-\Delta H = \left[\gamma_{lv} - T\left(\frac{\partial \gamma_{lv}}{\partial T}\right)_p\right] cos\ \theta_{slv} \tag{C.11}$$

This equation shows that the heat of wetting is inversely proportional to the contact angle, and, therefore, to hydrophobicity.

However, for some systems, the last term in Equation C.8 may not be negligible, and, therefore, Equation C.11 may not be suitable for all systems.

2. Liquid-Liquid-Solid System

For a solid-liquid-liquid system, Young's Equation is:

$$-\Delta G = \gamma_{sl_1} - \gamma_{sl_2} = \gamma_{l_1 l_2} cos\ \theta_{sl_1 l_2}. \tag{C.12}$$

Combing this equation with Equation C.6 in the same way as for a solid-liquid-vapor system, the following expression is obtained:

$$-\Delta H = \left[\gamma_{l_1 l_2} - T\left(\frac{\partial \gamma_{l_1 l_2}}{\partial T}\right)_p\right] cos\ \theta_{sl_1 l_2} - \gamma_{l_1 l_2} T\left(\frac{\partial cos\ \theta_{sl_1 l_2}}{\partial T}\right)_p . \quad \text{(C.13)}$$

The most difficult problem in this case is the determination of ΔH. To relate ΔH to the three-phase contact angle, the ΔH measured must be the heat released in the process of transferring the solid from liquid 1 to liquid 2. The process can be schematically illustrated by Figure C.2 This process is difficult to conduct in

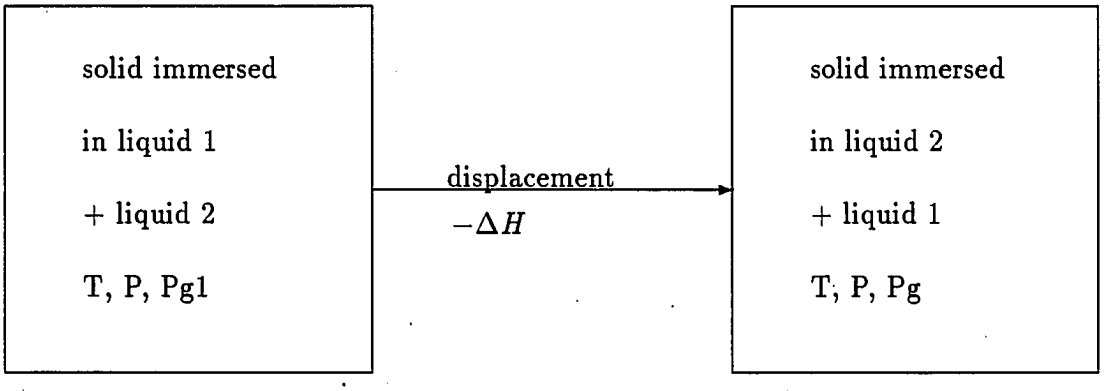

Figure C.2: Schematic representation of the process of transferring a solid from one liquid to another liquid

practice. However, an alternative process can be proposed as shown in Figure C.3. For process III, the enthalpy change is

$$-\Delta H = H_{sl_2} - H_{sl_1}. \quad \text{(C.14)}$$

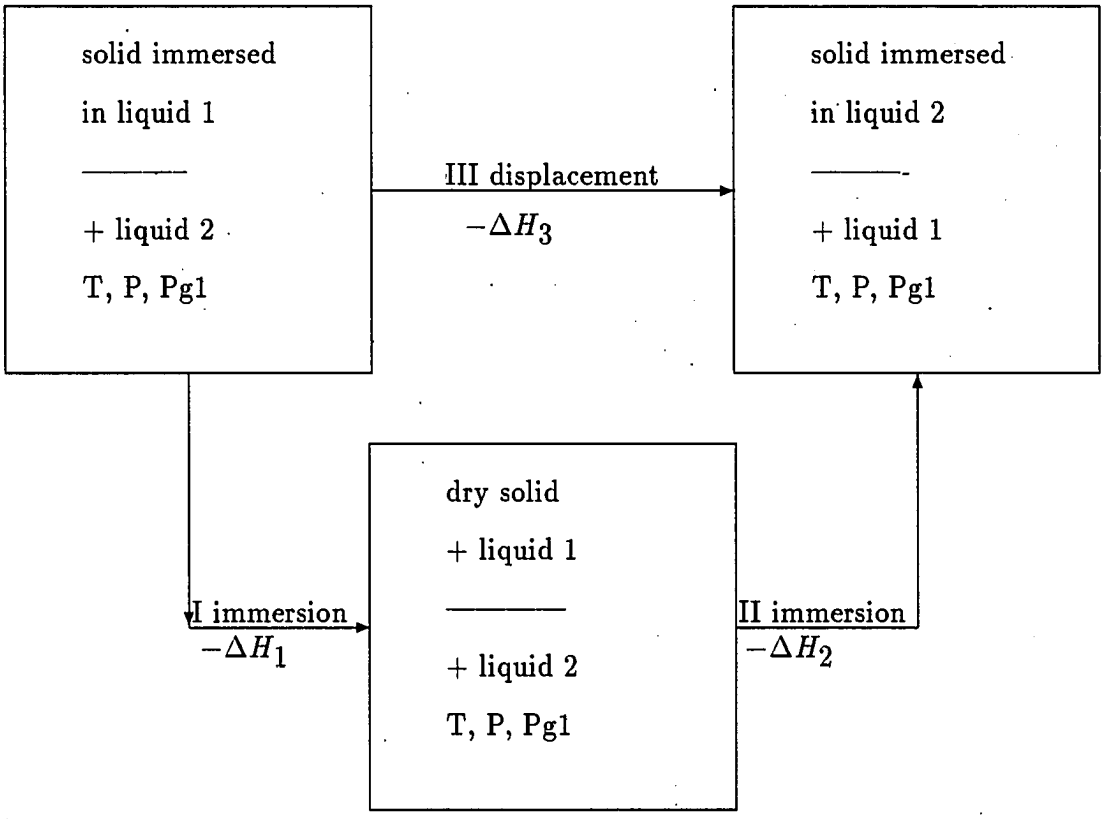

Figure C.3: Schematic representation of an alternative process

For processes I and II, the enthalpy changes are, respectively,

$$-\Delta H_1 = H_s - H_{sl_1} \tag{C.15}$$

$$-\Delta H_2 = H_s - H_{sl_2} \tag{C.16}$$

By combining the preceding equations, the following equation is obtained:

$$-\Delta H_3 = H_{sl_2} - H_{sl_1} = -\Delta H_1 - (-\Delta H_2) \tag{C.17}$$

However, in process III, the displacement of one liquid by another may not be complete, some molecules of liquid 1 may remain on the solid surface. An alternative thermodynamic process is shown in Figure C.4 which assumes that the number of molecules remaining on the solid surface is equal to the number of molecules isothermally adsorbed by the dry solid.

For this process, Equation C.17 still applies. When Equation C.8 is applied to the liquid 1/solid and liquid 2/solid systems the following two equations are obtained, respectively:

$$-\Delta H_1 = \left[\gamma_{l_1 v} - T\left(\frac{\partial \gamma_{l_1 v}}{\partial T}\right)_p\right] cos\ \theta_{sl_1 v} - \gamma_{l_1 v} T \left(\frac{\partial cos\ \theta_{sl_1 v}}{\partial T}\right)_p \tag{C.18}$$

$$-\Delta H_2 = \left[\gamma_{l_2 v} - T\left(\frac{\partial \gamma_{l_2 v}}{\partial T}\right)_p\right] cos\ \theta_{sl_2 v} - \gamma_{l_2 v} T \left(\frac{\partial cos\ \theta_{sl_2 v}}{\partial T}\right)_p \tag{C.19}$$

Substituting Equations C.19 and C.13 into Equation C.17 provides a relationship between the contact angle for a solid-liquid-vapor system and the three-phase contact angle for a solid-liquid-liquid system:

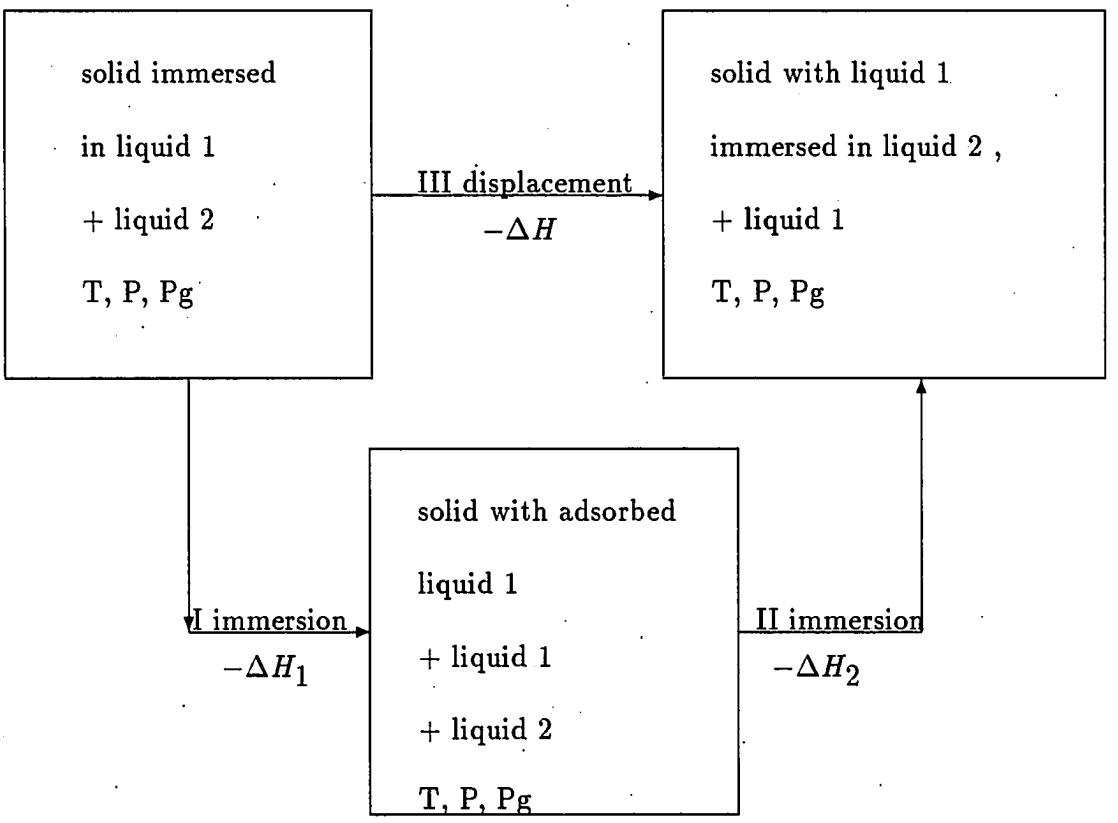

Figure C.4: Schematic representation of the alternative process

$$\left[\gamma_{l_1 l_2} - T\left(\frac{\partial \gamma_{l_1 l_2}}{\partial T}\right)_p\right] cos\ \theta_{sl_1 l_2} - \gamma_{l_1 l_2} T\left(\frac{\partial cos\ \theta_{sl_1 l_2}}{\partial T}\right)_p$$

$$= \left[\gamma_{l_1 v} - T\left(\frac{\partial \gamma_{l_1 v}}{\partial T}\right)_p\right] cos\ \theta_{sl_1 v} - \gamma_{l_1 v} T\left(\frac{\partial cos\ \theta_{sl_1 v}}{\partial T}\right)_p$$

$$- \left(\left[\gamma_{l_2 v} - T\left(\frac{\partial \gamma_{l_2 v}}{\partial T}\right)_p\right] cos\ \theta_{sl_2 v} - \gamma_{l_2 v} T\left(\frac{\partial cos\ \theta_{sl_2 v}}{\partial T}\right)_p\right) \qquad \text{(C.20)}$$

This equation provides the possibility for calculating the three-phase contact angle $\theta_{sl_1 l_2}$ from contact angles $\theta_{sl_1 v}$ and $\theta_{sl_2 v}$. However, the calculation will become practical only when the terms, $\gamma_{l_1 l_2} T\left(\frac{\partial cos\ \theta_{sl_1 l_2}}{\partial T}\right)_p$, $\gamma_{l_1 v} T\left(\frac{\partial cos\ \theta_{sl_1 v}}{\partial T}\right)_p$, and $\gamma_{l_2 v} T\left(\frac{\partial cos\ \theta_{sl_2 v}}{\partial T}\right)_p$, are negligible. For this case, Equation C.20 becomes

$$\left[\gamma_{l_1 l_2} - T\left(\frac{\partial \gamma_{l_1 l_2}}{\partial T}\right)_p\right] cos\ \theta_{sl_1 l_2}$$

$$= \left[\gamma_{l_1 v} - T\left(\frac{\partial \gamma_{l_1 v}}{\partial T}\right)_p\right] cos\ \theta_{sl_1 v} - \left[\gamma_{l_2 v} - T\left(\frac{\partial \gamma_{l_2 v}}{\partial T}\right)_p\right] cos\ \theta_{sl_2 v}. \qquad \text{(C.21)}$$

This equation suggests that the three-phase contact angle for a solid-liquid-liquid system can be obtained from the contact angles for a solid-liquid 1-vapor and a solid-liquid 2-vapor systems. However, as mentioned in the preceding section, further work is needed to show whether Equation C.21 is sufficiently accurate.